



Permafrost in Switzerland

2002/2003 and 2003/2004

Glaciological Report (Permafrost) No. 4/5

2007

Permafrost in Switzerland

2002/2003 and 2003/2004

Glaciological Report (Permafrost) No. 4/5

Permafrost Monitoring Switzerland

Edited by

Daniel Vonder Mühll^{1,2}, Jeannette Noetzi², Isabelle Roer²,

Knut Makowski³, and Reynald Delaloye⁴

With contributions from

S. Gruber², C. Hauck⁵, M. Hoelzle², A. Kääb⁶, M. Luetscher⁷,

M. Phillips⁸, N. Salzmann², T. Stucki⁸, and W. Haeberli²

¹ SystemsX.ch, ETH Zurich

² Glaciology, Geomorphodynamics & Geochronology, Dept. of Geography, University of Zurich

³ Institute for Atmospheric and Climate Science, ETH Zurich

⁴ Geography Institute, Dept. of Geosciences, University of Fribourg

⁵ Institute for Meteorology and Climate Research, University of Karlsruhe (D)

⁶ Department of Geosciences, University of Oslo (N)

⁷ School of Geographical Sciences, University of Bristol (UK)

⁸ Swiss Federal Institute for Snow and Avalanche Research, Davos

2007

Publication of the Cryospheric Commission (former Glaciological Commission) of the Swiss Academy of Sciences (SCNAT).

c/o Department of Geography, University of Zurich-Irchel
Winterthurerstrasse 190, CH-8057 Zurich, Switzerland

© Cryospheric Commission 2007

Printed by

Ebnoether Joos AG
print & publishing
Sihltalstrasse 82
Postfach 134
CH-8135 Langnau am Albis
Switzerland

Cover Page: Visible ice in a rock fall starting zone at ca. 3560 m a.s.l. just below the Marco e Rosa hut in the Bernina massif. The event occurred in August 2003.

Photo: European Tourism Institute (ETI) at the Academia Engiadina.

Preface

Permafrost science in cold mountain regions is still very young. Systematic studies started well after World War II and first networks for long-term monitoring were only established around the year 2000. Switzerland and several other European countries thereby played a leading role. With the chain of deep boreholes from Svalbard through Scandinavia and the Alps to the Sierra Nevada, installed within the framework of the EU-funded PACE project (Permafrost and Climate in Europe), the Terrestrial Network for Permafrost (GTN-P) as part of the climate-related Global Terrestrial Observing System (GTOS) received an important longitudinal transect. The Alps – and especially the Swiss Alps – represent a focal point of these European and global networks.

The present report is the second of its kind and covers the extreme summer of 2003. In comparison with long series of air temperatures measured in the past, this summer is beyond all reasonable statistics. Viewed in retrospect, however, from climate-change scenarios computed with high-resolution regional climate models for the second half of our century, it could just be average. The darkening mountain peaks of this summer with their water dripping out of snow-free rock walls and the noise and dust from the many rockfalls originating from them for the first time showed to a large public that there is ice inside mountains and that the warming and melting of this subsurface ice relates to slope stability. The steadily rising probability of large rockfall events in the most densely populated high-mountain region of the world has since been a growing concern. As a logical consequence, integrated monitoring of mountain permafrost became an important national task. Accordingly, pressure increases for public information and easily accessible assessments on current developments and newly evolving conditions far beyond historically known variability ranges.

Young science also means young scientists. In a new research field such as mountain permafrost, young scientists have a wide-open field for innovative research. Helping and encouraging each other is easy and to the benefit of all parties involved. Fruitful collaboration is indeed a remarkable characteristic of research on mountain permafrost in Switzerland and abroad. A whole number of university institutions together have helped to build up the now existing Swiss permafrost monitoring network PERMOS as a brilliant example of future-oriented environmental monitoring concepts and networks supported by the Academy of Sciences (scnat), the Federal Office for the Environment (FOEN) and MeteoSwiss. They all deserve our admiration and gratitude for their continued and most successful efforts. Special thanks go to Daniel Vonder Mühll who successfully guided PERMOS through its early childhood by combining excellent science with a determined will, a diplomatic attitude and a good amount of strategic wisdom.

The child PERMOS is now in its adolescent phase. It must become, and will most hopefully be, strong and safe in order to meet the great challenges of a near future with a rapidly warming world and deeply heated icy peaks.

May 2007, Wilfried Haeberli

Published reports

The PERMOS-concept and annex were approved by the permafrost-coordination group on November 18, 1999 and by the Cryospheric Commission (former Glaciological Commission) on January 14, 2000 and were published in 2000.

Annual reports on "Permafrost in Switzerland" started in the year of 1999:

Years	Nr.	Source
1999/2000	1	www.permos.ch
2000/2001 and 2001/2002	2/3	www.permos.ch
2002/2003 and 2003/2004	4/5	www.permos.ch

Summary

The Permafrost Monitoring Switzerland (PERMOS) enlarged its number of stations during the reported period between October 2002 and September 2004, and passed from its pilot phase to its consolidation phase. It consists of (a) 15 drill sites with one or more boreholes, (b) 10 areas where ground surface temperatures (GST) are obtained, and which are complemented with rock temperatures and BTS measurements (bottom temperature of the snow cover), and (c) aerial photographs taken by Swisstopo.

The first of the two reported years started with an early and snow-rich winter 2002/2003, followed by extreme summer 2003, the warmest and sunniest summer ever recorded since records began in 1864. Intense snow fall in October 2003 and high air temperatures in the first months of the second reported year 2003/2004 continued a warming phase of permafrost, until it was interrupted by the cold April 2004.

The extreme summer 2003 caused record thicknesses of active layer at all drill sites. At Schilthorn, for example, the active layer was almost twice as thick as usual. The relatively warm summer 2004 again caused active layer thicknesses with above average values. Temperatures measured in boreholes between the permafrost table and the depth of the ZAA (zero annual amplitude) at about 20 m continued to increase and were slightly higher than before the cold winter 2001/2002. Similarly, ground surface temperatures (GST) increased by about 2-3 °C, exceeding the warmest values measured so far by more than 1 °C. Some GST sites were complemented by additional temperature loggers installed in rock surfaces of different steepness (flat and near-vertical), whereas the number of BTS sites was reduced. Quantification of the creep velocity of a number of rockglaciers indicates that the creep velocity varies considerably both between rock glaciers and observation periods, and generally has increased during the past years.

In addition to the three key elements, special items like the occurrence of ice caves in western Switzerland, first applications of geophysical monitoring on Schilthorn, and rock fall events from permafrost slopes in the hot summer 2003 are compiled in this report.

In general, near-surface permafrost in the Swiss Alps was even warmer in 2003 and 2004 than in the already warm summer 2001 and, hence, was warmest since the beginning of the measurements.

Zusammenfassung

Das Messnetz PERMOS (Permafrost Monitoring Schweiz) hat in den Berichtsjahren 2002/2003 und 2003/2004 die Anzahl der Beobachtungs-Standorte ausgebaut und ist von der Aufbauphase in die Konsolidierungsphase übergegangen. In dieser Zeit besteht das Messnetz aus (a) 15 Bohrlochstandorten (einige davon mit mehreren Bohrlöchern), (b) 10 Gebieten mit kontinuierlichen Messungen der Oberflächentemperaturen, die durch BTS-Messungen (Basis-Temperatur der Schneedecke) sowie neu von Felstemperaturen ergänzt werden und (c) Luftbilddaufnahmen, die von Swisstopo aufgenommen werden.

Das Jahr 2002/2003 lässt sich charakterisieren durch einen frühen und schneereichen Winter, gefolgt vom ausserordentlich heissen Sommer 2003, der als der wärmste und sonnigste Sommer seit Beginn der Messungen im Jahr 1864 in die Statistik einging. Starke Schneefälle prägten den Beginn des Berichtsjahres 2003/2004, und hohe Lufttemperaturen Anfang des Jahres 2004 verlängerten die Erwärmungsphase für den Permafrost bis der kalte April 2004 diese Entwicklung unterbrach.

Alle PERMOS Standorte reagierten auf den ausserordentlichen Sommer 2003 mit den mächtigsten Auftauschichten seit Beginn der Messungen. So war zum Beispiel die Auftauschicht am Schilthorn mit über 9 m doppelt so mächtig wie der bisherige Durchschnittswert. Auch im relativ warmen Sommer 2004 waren die Auftautiefen überdurchschnittlich. Die Bohrlochtemperaturen zwischen dem Permafrostspiegel und der Tiefe der ZAA (zero annual amplitude) bei ca. 20 m stiegen weiter an und waren leicht höher als vor dem kalten Winter 2001/2002. Gleichzeitig stiegen die Oberflächentemperaturen im Mittel um 2-3 °C an und überschritten die bisherigen Höchstwerte um mehr als ein Grad. In der Berichtsperiode wurden einige Standorte mit Oberflächentemperaturmessungen durch Felstemperaturlogger erweitert, die in unterschiedlich geneigtem Gelände installiert wurden. Parallel dazu wurde die Anzahl der Gebiete mit wiederholten BTS-Messungen reduziert. Die Quantifizierung des Permafrost-Kriechens anhand von Luftbildvergleichen zeigte starke räumliche und zeitliche Unterschiede der Geschwindigkeiten, mit generell erhöhten Raten in den letzten Jahren.

Neben den Hauptelementen des Messnetzes wurden auch sogenannte «special events» dokumentiert. Dazu gehört das Vorkommen von Eishöhlen in der Westschweiz, der Aufbau eines geophysikalischen Monitorings am Schilthorn sowie eine Zusammenstellung der Felssturzereignisse des Sommers 2003 aus den Permafrostbereichen in den Alpen.

Insgesamt erreichte der oberflächennahe Permafrost in den Schweizer Alpen in der Berichtsperiode 2003/2004 höhere Temperaturen als der warme Sommer 2001 und damit die höchsten seit Beginn der Messungen.

Résumé

Durant les deux années couvertes par le rapport, soit d'octobre 2002 à septembre 2004, le réseau PERMOS (Permafrost Monitoring Switzerland) a vu le nombre de ses stations augmenté. Durant cette période, il comprenait (a) 15 sites de forage, dont la plupart équipés plusieurs forages, (b) 10 sites d'observation de la température de la surface du sol (GST), lesquels sont complétés régionalement par un suivi de la température de la roche et, sur cinq sites, par des mesures BTS (température à la base de la couche de neige), (c) des photographies aériennes prises par l'Office fédéral de topographie (swisstopo).

La période reportée a débuté par un hiver 2002/2003 précoce et enneigé, suivi d'un été 2003 qui a été le plus chaud et le plus ensoleillé depuis le début de mesures en 1864. D'intenses chutes de neige en octobre 2003 et des températures de l'air élevées durant les premiers mois 2004 ont prolongé une phase de réchauffement du pergélisol qui ne s'est interrompue qu'à partir d'avril 2004.

L'été extrême de 2003 a provoqué un dégel superficiel estival record sur tous les sites de forage PERMOS. Au Schilthorn, la profondeur du dégel (couche active) fut presque deux fois plus grande qu'habituellement. Les épaisseurs de couche active durant l'été 2004 relativement chaud ont à nouveau été supérieures aux moyennes. Les températures mesurées dans les forages entre le toit du permafrost et la profondeur de 20 m environ (amplitude thermique annuelle nulle) ont continué d'augmenter et furent légèrement plus chaudes qu'avant l'hiver froid 2001/2002. Similairement, les températures moyennes annuelles de surface (MAGST) ont augmenté d'environ 2-3 °C, dépassant les valeurs précédentes les plus chaudes de plus de 1 °C. Les sites GST ont été complétés par des capteurs thermiques additionnels installés à la surface de pans de roche en place d'inclinaisons diverses. Dans le même temps, le nombre de sites BTS a été réduit. L'analyse des déformations d'un certain nombre de glaciers rocheux a montré que leur vitesse varie considérablement que ce soit d'un glacier rocheux à l'autre ou d'une période d'observation à la suivante.

En complément aux trois éléments clés de PERMOS, ce rapport comprend également des chapitres spéciaux consacrés aux glaciers de Suisse occidentale, aux premières applications de monitoring géophysique et à des éboulements qui se sont produits durant l'été 2003 à partir de zones de permafrost.

En général, la température du permafrost de faible profondeur dans les Alpes Suisses fut plus élevée en 2003 et 2004 que durant la phase chaude de l'été 2001. Ce dernier avait été suivi d'un hiver 2001/2002 froid et peu enneigé qui avait permis un refroidissement temporaire du permafrost.

Riassunto

L'ufficio per il monitoraggio del Permafrost in Svizzera (PERMOS) ha aumentato il numero delle sue stazioni nel periodo compreso tra ottobre 2002 e settembre 2004. Attualmente consiste di (a) 15 siti di perforamento con uno o più fori di trivellazione, (b) 10 aree dove vengono rivelate le temperature di superficie (GST), implementate dalle temperature delle rocce e del fondo della copertura nevosa (BTS) in siti selezionati, e (c) fotografie aeree prese da Swisstopo.

I due anni sopra riportati sono iniziati con l'inverno 2002/2003, precoce e ricco di neve, seguito dall'estate 2003, la più calda e assolata mai riportata dall'inizio dei rilevamenti, cominciati nel 1864. Un'intensa caduta di neve nell'ottobre del 2003 e alte temperature dell'aria nei primi mesi del 2004 hanno continuato una fase di riscaldamento del permafrost fino all'interruzione avvenuta nel gelido aprile del 2004.

L'estate estrema del 2003 ha causato un record di spessore dello strato attivo in tutti i siti di perforazione. A Schilthorn, lo strato attivo era spesso circa il doppio rispetto al solito. In seguito, gli spessori degli strati attivi, successivi alla relativamente calda estate 2004, hanno mostrato nuovamente valori inferiori alla media. Le temperature misurate nei siti di trivellazione tra il livello del permafrost e il livello neutro (zero annual amplitude, ZAA) a circa 20 metri hanno continuato ad incrementare e hanno mostrato valori leggermente più alti di quelli registrati nel freddo inverno 2001/2002. Allo stesso modo, le temperature di superficie (GST) sono aumentate di circa 2-3 °C, superando così i valori più alti misurati fino a quel momento di oltre 1 °C. I siti per il rilevamento delle temperature di superficie (GST) sono stati implementati da ulteriori strumenti di registrazioni della temperatura installati sulle superfici rocciose a differenti pendenze (orizzontali e quasi verticali), mentre il numero dei siti BTS (temperature di fondo della copertura nevosa) sono stati ridotti. L'analisi della velocità di scorrimento di un numero di pietraie semoventi (ghiacciaio roccioso) indica che la suddetta velocità varia considerevolmente sia tra pietraie semoventi stessi, che tra i periodi di osservazione.

In questo report, in aggiunta ai 3 elementi chiave, sono stati aggiunti anche notizie su l'occorrenza di cave di ghiaccio nella Svizzera Ovest, prime applicazioni di monitoraggio geofisico, ed eventi di caduta roccia da pendici con permafrost nella calda estate 2003.

In linea generale, il permafrost vicino alla superficie nelle Alpi Svizzere è stato più caldo nel 2003 e 2004 che nella già calda estate del 2001. Quest'ultima è stata seguita da un freddo inverno 2001/2002, caratterizzato da poca neve, che ha temporaneamente raffreddato il permafrost nei primi decimetri.

Resumaziun

Durant ils onns da rapport 2002/2003 e 2003/2004 ha la reit da mesiraziun PERMOS (Permafrost Monitoring Schweiz) engrondiu il diember da posts da mesiraziun. Cun quellas installaziuns novas ei la fasa d'engrondaziun serrada giu e la reit sesanfla usas en la fasa da consolidaziun. La reit consista ord (a) 15 posts da mesiraziun, entgins cun pliras foras da sondagi; (b) 10 regions nua che la temperatura dalla surfatscha vegn mesirada continuanadamein e cumpletada cun mesiraziun dalla BTS (temperatura alla basa dalla cozza da neiv) sco era daniev cun la temperatura dil grep, e finalmein (c) regions nua che la Swisstopo fa fotografias ord l'aria.

Igl emprem dils dus onns da rapport ei staus characterisau entras in baul unviern cun bia neiv suandaus dad ina extraordinari caulda stad, la quala ei reportada en las statisticas sco la pli caulda dapi l'entschatta da las mesiraziuns da temperatures egl on 1864. Il secund onn da rapport ha entschiet cun nevaglia el meins d'October 2003 suandada dad aultas temperatures dall'aria all'entschatta digl onn 2004, las quallas han prolungiu la fasa da scaldament dalla schelira permanente entochen il fraid Avrel 2004.

La calira extrema dalla stad 2003 ha caschuna la pli pussonta rasada da sdregliada dapi l'entschatta dallas mesiraziuns. Aschia era per exempel la rasada da sdregliada al Schilthorn cun 9 meters dubel schi gronda sco la media entochen da cheu. Era la stad 2004, la quala ei stada relativamein caulda ha purtau mesiraziuns sur la media. La temperaturas dallas foras da sondagi denter il nivel da schelira permanente e la profunditad ZAA (zero annual amplitude) en ina profunditad da ca. 20 meters ein carschidas vinavon ed ein stadas levamain pli aultas che quellas avon il fraid unviern 2001/2002. Ella medema perioda ein las temperaturas dalla surfatscha carschidas ella media per 2-3 °C ed han aschia surpassau la valur maximala per dapli che in grad Celsius. En la perioda da rapport ein entgins posts da mesiraziun da temperatura dalla surfatscha vegni extendi cun instruments per mesirar la temperatura dil grep, ils quals ein vegni plazai en territoris cun inclinaziun variabla. El medem temps ei il diember da regions per mesiraziun periodica BTS vegnius reducuis. La quantificaziun dil moviment dils glatschers da schelira permanente entras cumparegliaziuns dallas fotografias dall'aria muossa grondas variaziuns spazialas e temporalas dalla spertadad cun ratas generalmein pli aultas ils davos onns.

Sper ils elements principals dalla reit da mesiraziun ein era aschinumnai «special events» vegni documentai. Tier quels saudan l'existenza da cuvels da glatsch ella Svizra occidentala, la construcziun d'in monitoring geofisical al Schilthorn, sco era ina survesta dallas boas el spazi da schelira permanente dallas Alps durant la stad 2003.

En general ha la schelira permanente en las Alps Svizras durant la perioda da rapport 2003/2004 cuntunschiu temperatura pli aultas che la caulda stad 2001 e cunquai er las pli aultas temperaturas dapi l'entschatta dallas mesiraziuns.

Contents

Preface	III
Published reports	IV
Summary	V
Zusammenfassung	VI
Résumé	VII
Riassunto	VIII
Resumazium	IX
1 Introduction	1
2 Weather and climate	3
2.1 Weather and climate in 2002/2003	3
2.2 Weather and climate in 2003/2004	4
2.3 Climate deviation from the mean value 1961–1990	8
2.4 Duration of the snow cover	10
3 Borehole measurements	11
3.1 Active layer thickness	13
3.2 Permafrost temperatures	17
3.3 Borehole deformation	20
3.4 Conclusions	20

4	Surface temperatures	21
4.1	Surface temperature measurements in 2002/2003 and in 2003/2004	22
4.2	Evaluation of the BTS method within PERMOS	28
4.3	Conclusions	30
5	Air photos	31
5.1	Air photos in 2002/2003 and in 2003/2004	31
5.2	Recent acceleration of rockglaciers in the Swiss Alps	33
6	Conclusions	37
7	Selected aspects of permafrost monitoring and special events	39
7.1	Ice caves	39
7.2	Pilot study for the use of geophysical monitoring systems within PERMOS	43
7.3	Rock fall from permafrost areas in summer 2003	51
	Acknowledgements	56
	References	57
	Appendix	61

1 Introduction

PERMOS – from the pilot phase to consolidation

During the reporting period, the Permafrost Monitoring Switzerland (PERMOS) has taken root and passed from its pilot phase (2000–2003) to its consolidation phase (2003–2006). That is, the three key elements (boreholes, ground surface temperatures, and aerial photographs) proved to be suitable for long term permafrost monitoring and the methodology used is well adapted and established.

The boreholes in various terrain provide the basis of the monitoring network. The number of monitoring sites was extended by two additional boreholes in the Valais during the reporting period (Gentianes and Tsaté, cf. Appendix). In order to better understand subsurface characteristics and to monitor changes in ground ice content at the borehole sites, a monitoring strategy using a surface-based geophysical monitoring system was developed and installed at a test site (Schilthorn, BE).

An adaptation was conducted concerning the ground surface temperatures: here, more sites were equipped with single channel temperature data loggers, which allow a continuous recording. The number of BTS (Bottom Temperature of the Snow cover) campaigns will be reduced in the future. In addition, rock surfaces of different slope steepness and aspect were instrumented with near-surface temperature loggers during the summers 2003 and 2004. The measured data can be used to monitor and investigate the influence of snow on the near-surface thermal regime.

Exceptional rock fall occurred throughout the Alps during the unusually hot summer of 2003. This is mainly related to the rapid and direct thermal reaction of steep and snow-free rock walls to changes in atmospheric temperatures, especially thaw penetration that exceeded that of the preceding already warm years, and caused unprecedented thickening of the active layer.

Within the international community of permafrost monitoring and research, PERMOS is well known and highly regarded. For instance, several contributions from the PERMOS office as well as from the participating institutes were given at the 8th International Conference on Permafrost, taken place in Zurich in July 2003. In addition, close cooperation with colleagues from abroad exists and is encouraged by PERMOS.

The measurements for the present report have been realised by the following institutes (in alphabetical order, except for the coordinating institute, which is listed first):

- University of Zurich: Department of Geography, Glaciology, Geomorphodynamics and Geochronology (GIUZ)
- ETH Zurich: Institute for Geotechnical Engineering (IGT-ETH)
- ETH Zurich: Laboratory of Hydraulics, Hydrology and Glaciology (VAW-ETH)
- Swiss Federal Institute for Snow and Avalanche Research Davos (SLF)

- University of Berne: Department of Geography (GIUB)
- University of Fribourg: Department of Geosciences, Geography Institute (IGUF)
- University of Lausanne: Faculty of Earth Science and Environment, Geography Institute (IGUL)

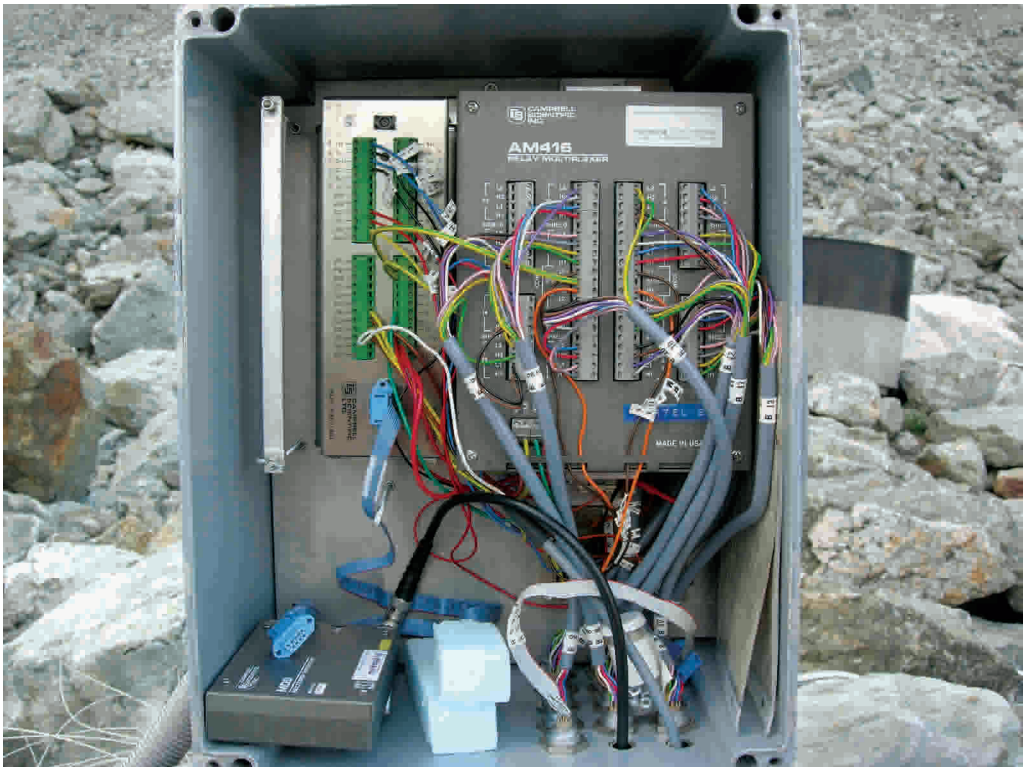


Photo 1: Logger box of the permafrost borehole on the rock glacier Murtèl. Photo: A. Hasler.

2 Weather and climate

2.1 Weather and climate in 2002/2003

Both the weather and the climate data are taken from reports by the “MeteoSwiss” (MeteoSwiss, 2002, 2003). The snow data originate from SLF.

Weather and climate conditions in the hydrological year 2002/2003

The global mean surface temperature in 2003 was 0.46 °C above the 1961–1990 annual average, which makes 2003 the third warmest year in the instrumental temperature record since 1861, just after 2002. The warmest year remains 1998 (+0.55 °C; WMO, 2002, 2003).

In Switzerland, the year 2002 continues a series of warm years since 1997. In the reporting period, the month October was affected by a quick change between cold and warm air. November was very wet, especially in the southern parts of Grison, where at several places the normal monthly sum was exceeded by 600%. The year 2003 was 1.5–1.8 °C warmer than average, resulting mainly from the exceptionally warm months June and August of an unprecedented heat wave. In the warmest areas a temperature mean of 23–25 °C was recorded, which is comparable to climate conditions of Rio de Janeiro. Also the months March, May, and July had considerably higher temperatures than normal, especially in mountain regions. The year 2003 was one of 10 most dry years since 1901.

Snow

From September 2002 snow fall began on the central and eastern Alpine north slope above approx. 2400 m a.s.l. In the middle and end of November in the south above 2400 m a.s.l. intensive rainfalls led to an increase in fresh snow of over two meters. At the end of January in the west and alpine north slope three heavy snow falls occurred. As from mid February until the end of March a period of fine weather arose. At the beginning of April winter returned, with snow down to low altitudes. Throughout the winter, the snow thickness was above average in high altitudes, but below average in low altitudes. In all reaches the slopes became snow free earlier in spring than average. The combination of a snowy winter with an early snow free period is unfavourable for permafrost and contributed to the high ground temperatures of the summer 2003.

Summer temperatures May – September 2003

The year 2003 was extremely warm and sunny. In many regions of Switzerland it was the warmest and sunniest year since the beginning of measurements in 1864. The prevailing high-pressure influence was the main cause for the record summer, which was on average 5 °C above average temperatures. From June to August, 74 to 83 summer days (i.e., temperature values >25 °C) were counted in Switzerland. The average temperature from April to September almost reached the average mean temperature of a normal July. Due to these exceptional summer temperatures the 0 °C isotherm rose to over 4000 m a.s.l. during the day for several weeks. Temperatures constantly stayed above the freezing point even during the night at the gauging station Jungfrauoch, 3580 m a.s.l., from August

Table 2.1: Key climatic features from the “Monthly weather reports of MeteoSwiss” (Meteo Swiss, 2002, 2003).

2002

October	Storm disasters in Valais, highest water levels in Lago Maggiore since 1868
November	Unsettled in the north, mild with foehn winds, extremely wet in the south
December	North of the Alps and in Valais: extremely mild and very little precipitation
Year overall	Unusually warm, extreme autumn rain in the south and in Valais

2003

January	Mild with foehn winds. Little snow north of the Alps, little sun in the south
February	Very mild in the first half of the month; not much fog in the lowlands
March	Rainy and mild; record amounts of precipitation north of the Alps
April	Changeable in the south, cold and wet in the north; return of delayed winter
May	Sunny, dry and extremely warm
June	First wet and cool, then sunny and warm in the last third of the month
July	Cool and rainy at mid-month, midsummer conditions in the last third of the month
August	Very warm, abundant sunshine on the north side of the Alps, generally too dry
September	Very cool, unusually dull on the north side of the Alps
Year overall	Warm and quite sunny in the lowlands, wet on the north side of the Alps

1 to August 14 and during 12 successive days, minimum temperatures ranged between 3.5 and 5.0 °C. Such a long lasting high level of minimum temperatures in high altitude during nearly two weeks is probably the most outstanding feature of the heat wave in the first half of August 2003. At the same time, rainfall was extremely little in almost all regions of the country.

2.2 Weather and climate in 2003/2004

Both the weather and the climate data are taken from reports by the “MeteoSwiss” (MeteoSwiss, 2003, 2004). The snow data originate from SLF.

Weather and climate conditions in the hydrological year 2003/2004

The global mean surface temperature in 2004 was 0.44 °C above the 1961–1990 annual average (14 °C) making 2004 the fourth warmest year since 1861, just behind 2003. The last 10 years (1995–2004), with the exception of 1996, are among the warmest on record, and the five warmest years in decreasing order are 1998, 2002, 2003, 2004, and 2001. During the past century the increase in global surface temperature was between 0.6 and 0.7 °C. The rate of change since 1976 is roughly three times that for the total past 100 years. In the northern hemisphere, the 1990s was the warmest

Table 2.2: Key climatic features from the “Monthly weather reports of MeteoSwiss” (Meteo Swiss, 2003, 2004).

2003

October	Cold spell, snow down to the lowlands on the north of the Alps
November	Mild with foehn winds, wet in the south
December	Foehn winds, sunny in the lowlands, much snow in the south
Year overall	Extremely warm, sunny, and little precipitation – record summer

2004

January	Rainy with strong west winds and storm activity, much snow after mid-month
February	First mild and sunny, then increasingly wintery towards the end of the month.
March	First wintery, warm at mid-month, then heavy snowfall on the foothills of the Alps
April	Wet in the south, dry with foehn in the north; wet and cool at Easter
May	Unsettled, winter conditions in the mountains, midsummer conditions at Ascension
June	Unsettled – intense rain in Central Switzerland, extremely dry in the south
July	Average conditions, widespread hail storm on July 8 north of the Alps
August	Hot and sticky, heavy thunderstorms in the west, unsettled at the end of the month
September	Late summer conditions first, dry in the south and in the west
Year overall	Warmer than usual and unsettled – hail storm in the midlands

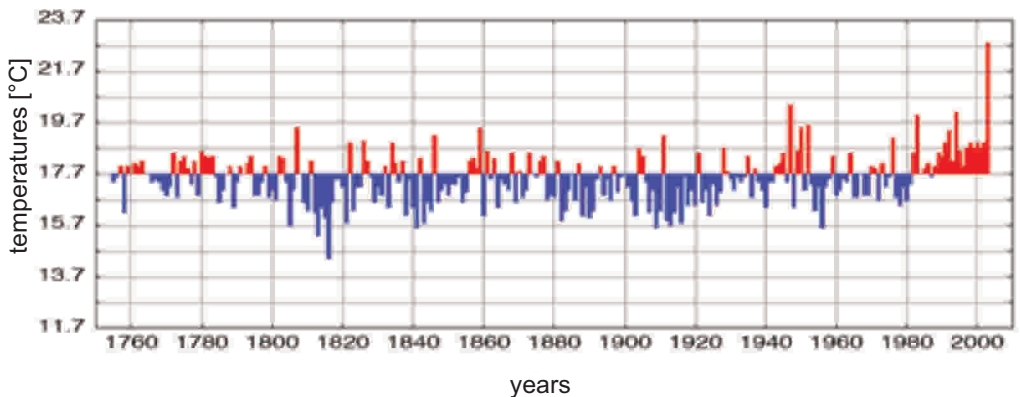


Figure 2.1: Summer temperatures (June–August) in Basel from 1755–2003. The temperature of 17.7 °C corresponds to the mean summer temperature of the climatic norm period from 1961–1990 (MeteoSchweiz, 2003).

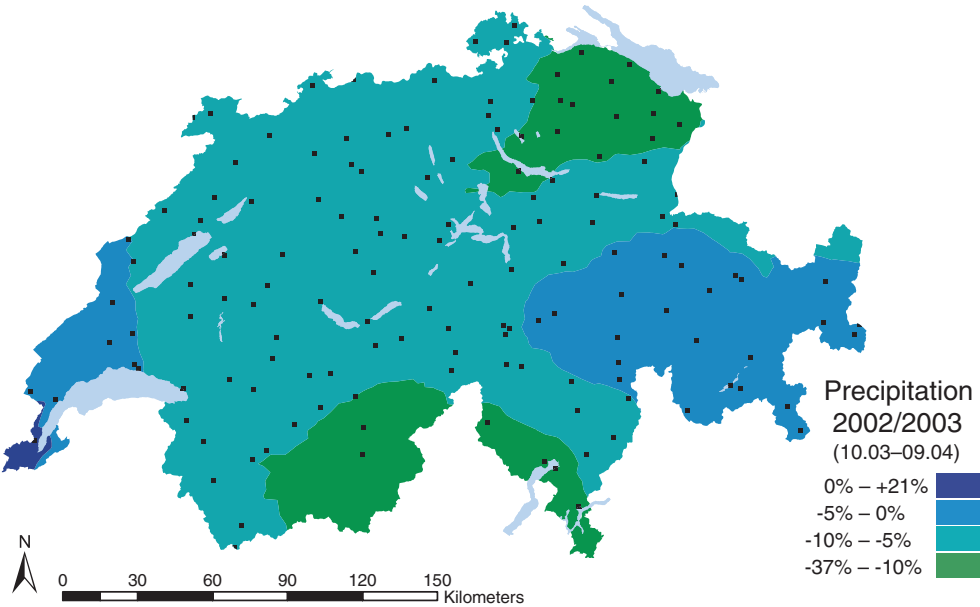


Figure 2.2a: Annual precipitation 2002/2003, deviation from the mean value 1961–1990. Deviation in percentage.

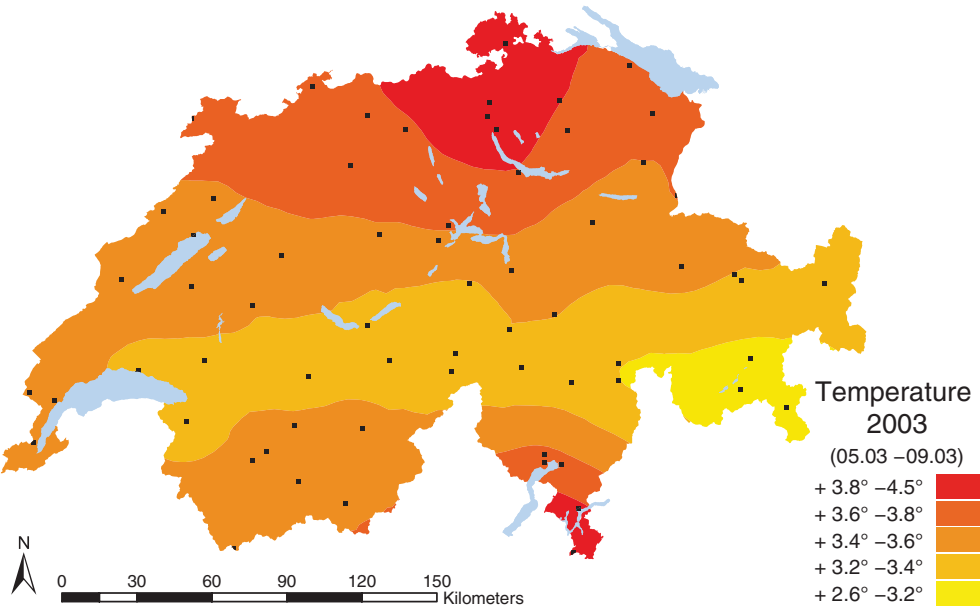


Figure 2.2b: Mean summer air temperatures 2003, deviation from the mean value 1961–1990. Deviation in degree Celsius.

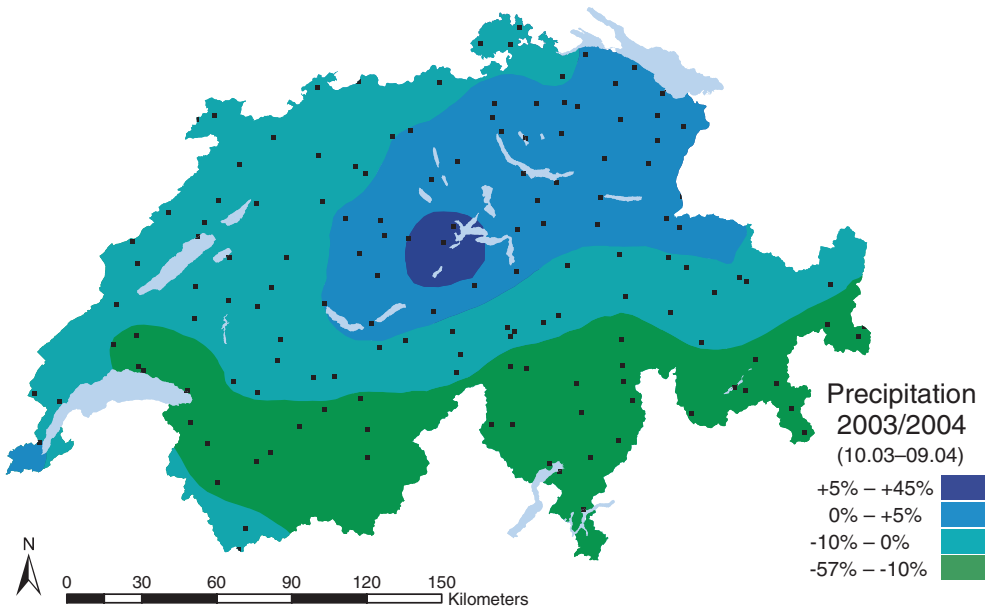


Figure 2.3a: Annual precipitation 2003/2004, deviation from the mean value 1961–1990. Deviation in percentage.

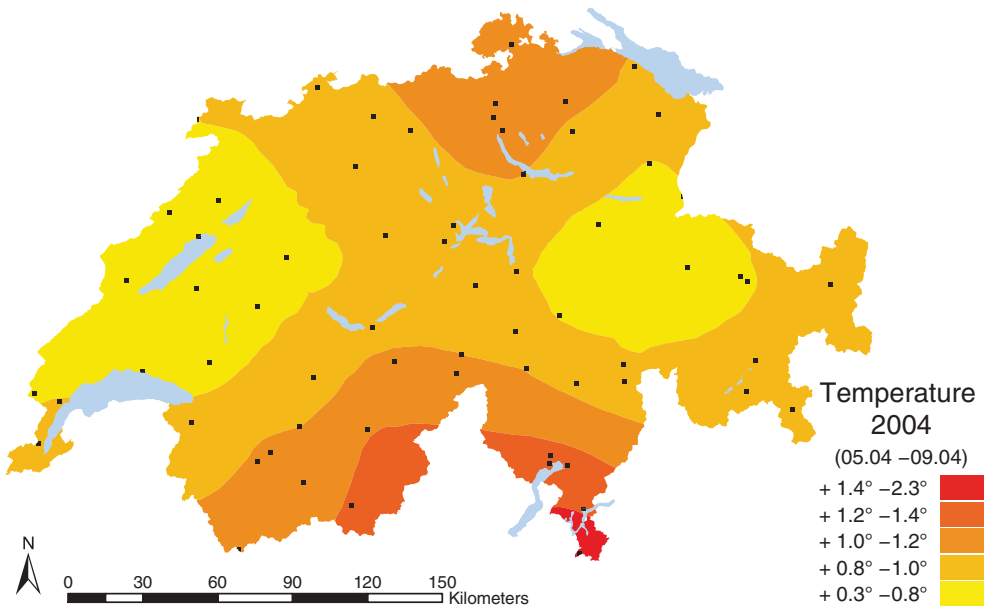


Figure 2.3b: Mean summer air temperatures 2004, deviation from the mean value 1961–1990. Deviation in degree Celsius.

decade with an average of 0.38 °C. The surface temperatures averaged over the recent five years (2000–2004) were, however, much higher with 0.58 °C (WMO, 2003, 2004).

In Switzerland, the weather in 2004 was rather uneventful compared to 2003. The temperatures in the lowlands on the northern side of the Alps as well as in the high mountain areas were ca. 1 °C above the mean values for 1961–1990. Precipitation fell in usual amounts, except for Valais showing large precipitation amounts for January and August. However, they were compensated by February–April and September, with mostly less than half of the normal precipitation.

Snow

The winter 2003/2004 started at the beginning of October with intensive snow falls in the north and east, following an unusual hot summer. In the south flank numerous build-up layers led to an above-average thickness of snow cover. In January the snow line varied strongly, it partly rose up to altitudes of over 2000 m a.s.l. In February and March, variations in temperatures with amplitudes up to 20 °C occurred. Warm phases were registered in January, February, and March with a 0 °C isotherm above 3500 m a.s.l. It snowed several times down to low altitudes with strongest snow falls around the middle and end of March. At the beginning of April it snowed down to low altitudes again in the north and very intensely at the beginning of May. The snow depth was slightly above average in the east, slightly below average in the south and clearly below average in the west. After many cold periods in the north in April and May the snowmelt was delayed for several weeks, favouring cold ground temperatures by inhibiting warm air from seeping into the ground.

Summer temperatures May – September 2004

The summer 2004 was – at least in the lowlands – warmer than the thirty year average. The month of July started moderately warm, and in midmonth the snow line even fell once below 2000 m a.s.l. However, the cold spell was short-lived. By the end of July air temperatures were again over 30 °C, and on August 2, the highest temperature was recorded. The month of August was influenced by humid and warm weather with heavy rain. The month of September started with a distinctive heat surplus. Then, a rapid change occurred, and the rest of the month was mostly cool to cold. The rainfall reached normal values in many places.

2.3 Climate deviation from the mean value 1961-1990

The regional differences in the important climatic elements for permafrost conditions are illustrated in the Figures 2.1 and 2.2. Mean values 1961–1990 for both summer air temperatures and annual precipitation are based on the standard values that have been determined within the projects KLIMA90 (Aschwanden et al., 1996) and NORM90 (Begert et al., 2003). In cases where the standard values of the two projects disagree, the values of NORM90 are considered. Temperature values from 2002–2003 are taken from the automatic measurement stations (ANETZ), precipitation values 2002–2004 from the observational network NIME.

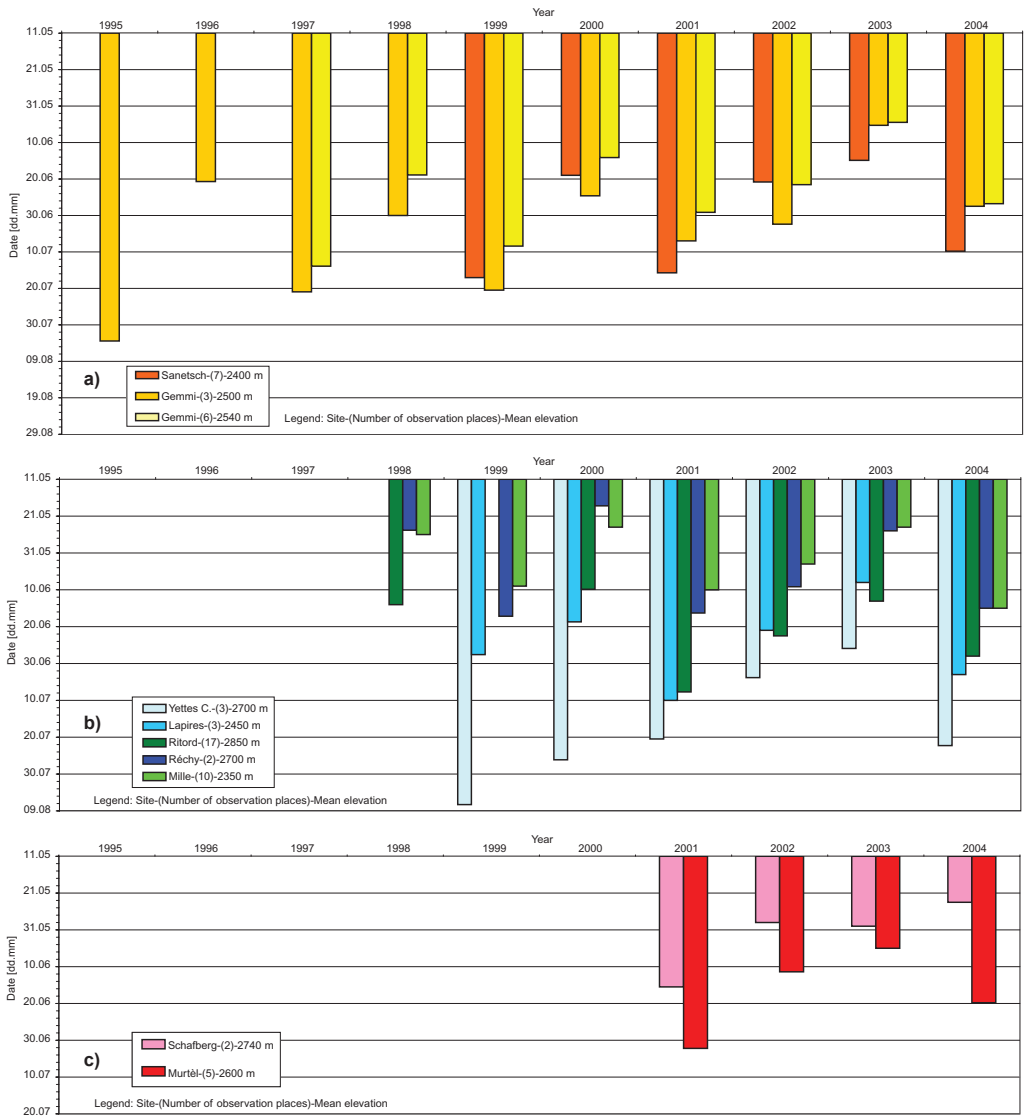


Figure 2.4: Date of snow melt (1995–2004) on PERMOS GST-sites (cf. Chapter 4): a) Bernese Alps, b) Valais Alps, and c) Engadine. If several series are available, the mean value per site was calculated.

2.4 Duration of the snow cover

Continuous recording of ground surface temperature (GST; cf. Chapter 4.1) allows to determine the date when the snow disappears (the first day with temperatures above 0 °C). Figure 2.4 shows the results for all PERMOS-sites where GST observations are available.

The two reported years were quite different. Depending on the location, the snow disappeared between 15 and 26 days earlier in 2003 than in 2004. Due to the heat wave in June 2003, the snow disappeared very early in 2003. At Furggentälti/Gemmi, in the Bernese Alps, the 2003 snowmelt was the earliest for at least one decade. In contrast, in the Valais Alps and in Grisons, at some locations snow disappeared later than in 2000 and 1998. In 2004, the snow cover melted relatively late. Significant differences occurred between the sites. For instance, Mille in the Valais Alps 2004 experienced the latest snowmelt since the beginning of the measurement in 1997/1998.



Photo 2: The Schilthorn crest in the Bernese Alps: the three boreholes are located on the northern (snow covered) slope. Photo: J. Noetzli.

3 Borehole measurements

Borehole measurements were continued at the PERMOS borehole sites. These data are used for observing (a) the thermal state of permafrost in general, (b) the evolution, maximum thickness (including corresponding date) and refreezing of the annual active layer, and – in boreholes that are equipped accordingly – (c) deformation of the permafrost body.

The thickness of the permafrost only changes slowly, i.e., over decades to centuries. Therefore, all PERMOS sites show the same depth of the permafrost base as in the previous report. Figures 3.5a-c show temperature-depth plots for all boreholes, from which a permafrost thickness of 10 m up to more than 100 m can be concluded.

During the reporting period (October 2002 to September 2004) two new permafrost boreholes, both located in the Valais, joined the PERMOS network: (1) Gentianes was equipped with 10 thermistors that are registered by a data logger in November 2002, and (2) Tsaté, drilled in summer 2004, equipped with a string of UTL single channel temperature loggers.



Figure 3.1: Locations of the PERMOS boreholes for the reporting period 2002–2004.

Table 3.1: *Borehole study sites. Data in PERMOS: L: Logger-measurements, M: Manual measurements; L. sensor: Lowest sensor.*

Borehole	Abbrev.	Data	Region	Depth [m]	L.sensor [m]	Since [year]
Jungfrauoch	N/95	L	Berner Oberland, BE	11.0	11.0	1995
Jungfrauoch	S/95	L	Berner Oberland, BE	10.0	10.0	1995
Schilthorn	51/98	L	Berner Oberland, BE	14.0	13.7	1998
Schilthorn	50/00	L	Berner Oberland, BE	101.0	100.0	2000
Schilthorn	52/00	L	Berner Oberland, BE	100.0	92.0	2000
Flüela	1/02	L	Flüelapass, GR	23.0	20.0	2002
Muot da Barba Peider	B1/96	L	Upper Engadine, GR	18.0	17.5	1996
Muot da Barba Peider	B2/96	L	Upper Engadine, GR	18.0	17.5	1996
Muragl	1/99	L	Upper Engadine, GR	70.2	69.7	1999
Muragl	2/99	L	Upper Engadine, GR	64.0	59.7	1999
Muragl	3/99	L	Upper Engadine, GR	72.0	69.6	1999
Muragl	4/99	L	Upper Engadine, GR	71.0	69.6	1999
Murtèl-Corvatsch	1/87	M	Upper Engadine, GR	39.0	21.0	1987
Murtèl-Corvatsch	2/87	L	Upper Engadine, GR	62.0	58.0	1987
Murtèl-Corvatsch	1/00	–	Upper Engadine, GR	51.9	–	2000
Murtèl-Corvatsch	2/00	L	Upper Engadine, GR	63.2	62.0	2000
Schafberg-Pontresina	1/90	–	Upper Engadine, GR	67.0	–	1990
Schafberg-Pontresina	2/90	L	Upper Engadine, GR	37.0	25.2	1990
Arolla, Mt. Dolin	B1/96	L	Val d'Herens, VS	10.0	5.5	1996
Arolla, Mt. Dolin	B2/96	L	Val d'Herens, VS	10.0	5.5	1996
Emshorn	4/96	M	Central Valais, VS	8.0	6.4	1996
Emshorn	5/96	M	Central Valais, VS	8.0	6.4	1996
Emshorn	6/96	M	Central Valais, VS	8.0	6.4	1996
Gentianes	1/02	L	Val d'Entremont, VS	20.0	20.0	2002
Grächen	1/02	L	Matter Valley, VS	25.0	24.0	2002
Grächen	2/02	L	Matter Valley, VS	25.0	24.0	2002
Lapires	1/98	L	Val de Nendaz, VS	19.6	19.6	1998
Randa Wisse-Schijen	1/98	L	Matter Valley, VS	4.0	2.8	1998
Randa Wisse-Schijen	2/98	L	Matter Valley, VS	4.0	2.8	1998
Randa Wisse Schijen	3/98	L	Matter Valley, VS	4.0	2.8	1998
Stockhorn	60/00	L	Matter Valley, VS	100.0	98.3	2000
Stockhorn	61/00	L	Matter Valley, VS	31.0	20.0	2000
Tsaté	1/04	M	Val d'Herens, VS	20.0	19.5	2004

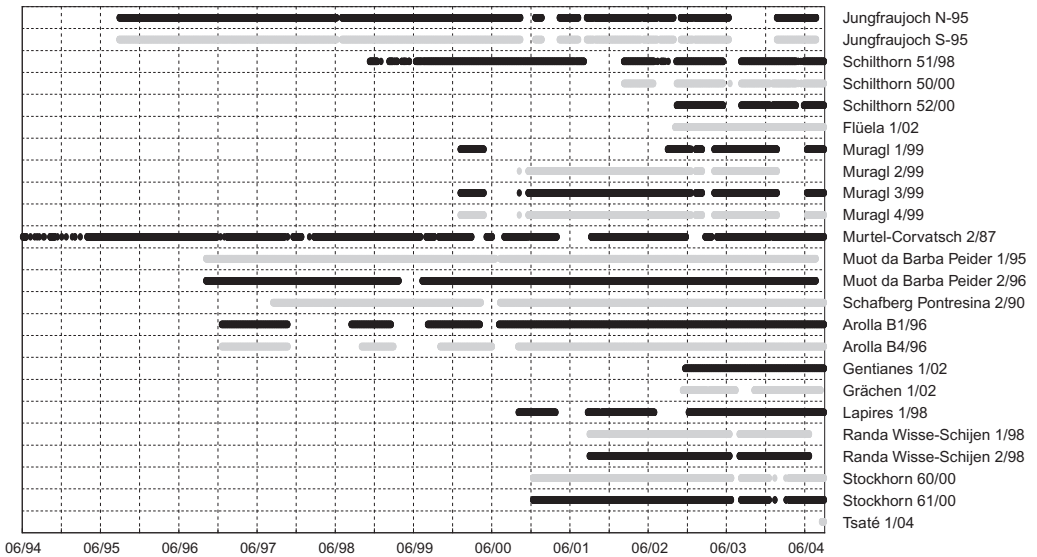


Figure 3.2: Available data for the PERMOS boreholes until 2004. Details for each borehole can be found in the appendix.

3.1 Active-layer thickness

The thickness of the active layer is of special interest, as it represents the atmospheric conditions of the observed year. The heat supply from the surface to the ground is used both, temperature increase or melting ice. Two extreme examples are (a) the ice-rich rockglacier Murtèl-Corvatsch and (b) the constantly frozen but nearly ice free rock on Schilthorn. At both locations the thickest active layers ever were measured in 2003. While the previous records of Murtèl-Corvatsch with 3.51 m was exceeded only by about 5 cm, the active layer at the Schilthorn increased from ca. 5 m to almost 9 m. In the following year the active layer again reached a depth of 4.8 m.

Similar, extraordinary thick active layers in 2003 were observed at Lapires (7.7 m instead of 4.8 m), Stockhorn (4.3 instead of 3.5 m), and Muot da Barba Peider (1.6 m instead of 0.8 m, and 2.5 m instead of 1.9 m). Interestingly, at the sites Arolla, Randa, Flüela, Muragl, and Pontresina-Schafberg no marked increase in active layer thickness was recorded in 2003. The date of maximal active layer thickness is site specific and varies between mid of August (Randa, 2003) and mid of November (Schilthorn, 2003). An overview of the active layer thickness of the reporting period at all PERMOS drill sites is given in Table 3.2 and Figures 3.3a-d and 3.4. For the data series only starts in 2004, Tsaté is not included in the figures.

Table 3.2: *Maximum thickness of the active layer and corresponding date for the PERMOS boreholes in the years 2002 and 2003.*

Borehole	2002 zmax [m]	date	2003 zmax [m]	date
Jungfrauoch S/95	2.24	07.07.2002	–	no data
Jungfrauoch N/95	–	no a.l. recorded	–	no a.l. recorded
Schilthorn 51/98	4.46	08.10.2002	8.55	05.11.2003
Schilthorn 50/00	–	no data	7.43	15.11.2003
Schilthorn 52/00	–	no data	6.86	16.09.2003
Flüela 01/02	–	no data	2.96	13.08.2003
Muot da Barba Peider 1/96	0.78	08.09.2002	1.63	01.09.2003
Muot da Barba Peider 2/96	1.86	04.09.2002	2.47	04.09.2003
Muragl 1/96	–	no a.l. recorded	–	no a.l. recorded
Muragl 2/99	5.08	24.10.2002	6.13	29.08.2003
Muragl 3/99	3.88	18.09.2002	4.25	17.09.2002
Muragl 4/99	3.31	08.09.2002	3.46	31.08.2003
Murtèl-Corvatsch 2/87	3.44	05.09.2002	3.51	10.08.2003
Schafberg-Pontresina 2/90	4.87	08.09.2002	5.10	30.08.2003
Arolla B1/96	2.47	03.09.2002	2.49	09.08.2003
Arolla B2/96	–	no a.l. recorded	–	no a.l. recorded
Gentianes 1/02	–	no data	1.42	29.08.2003
Graechen 1/02	–	no data	7.68	09.11.2003
Lapires 1/98	–	no data	4.13	13.11.2003
Randa Wisse-Schijen 1/98	1.66	21.08.2002	1.74	11.08.2003
Randa Wisse-Schijen 2/98	1.81	21.08.2002	1.93	11.08.2003
Stockhorn 60/00	2.88	22.09.2002	4.27	03.10.2003
Stockhorn 61/00	3.39	26.09.2002	4.07	11.10.2003
Tsaté	–	no data	–	no a.l. recorded

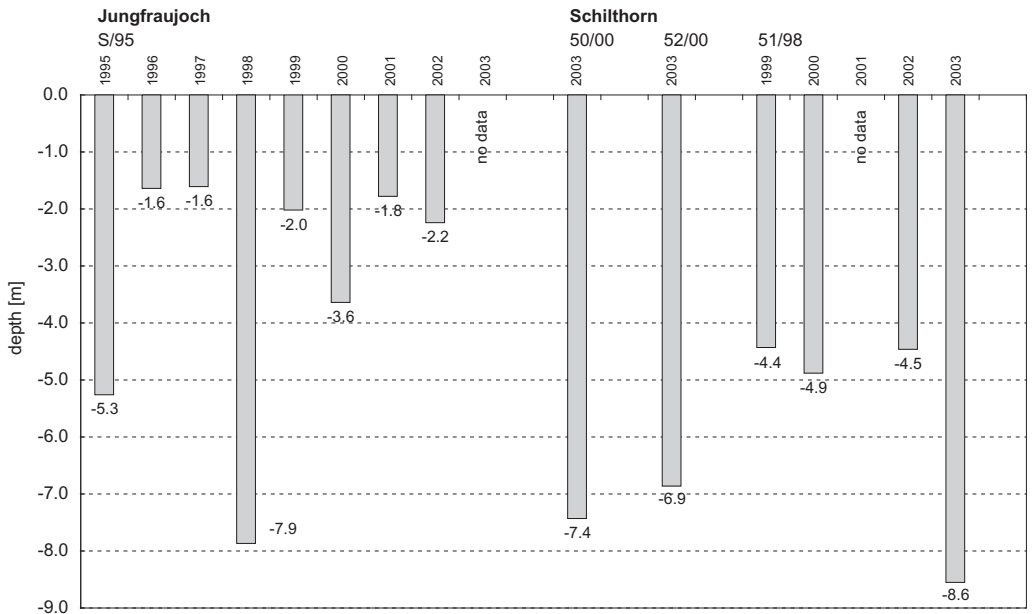


Figure 3.3a: Maximum active layer thickness for the boreholes in the Bernese Alps, until 2003.

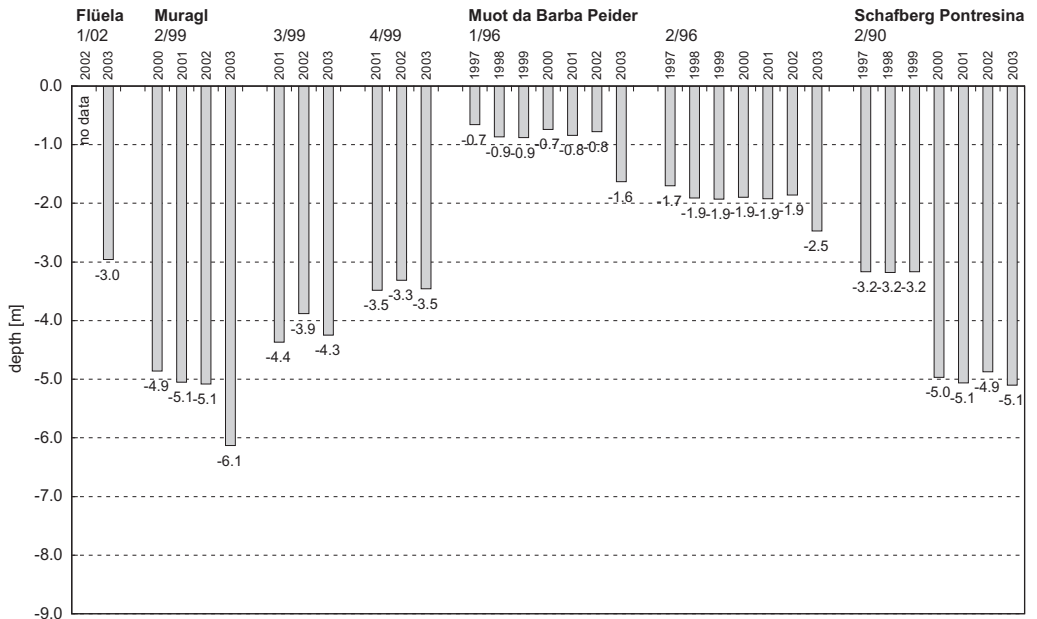


Figure 3.3b: Maximum active layer thickness for the boreholes in Grisons, until 2003.

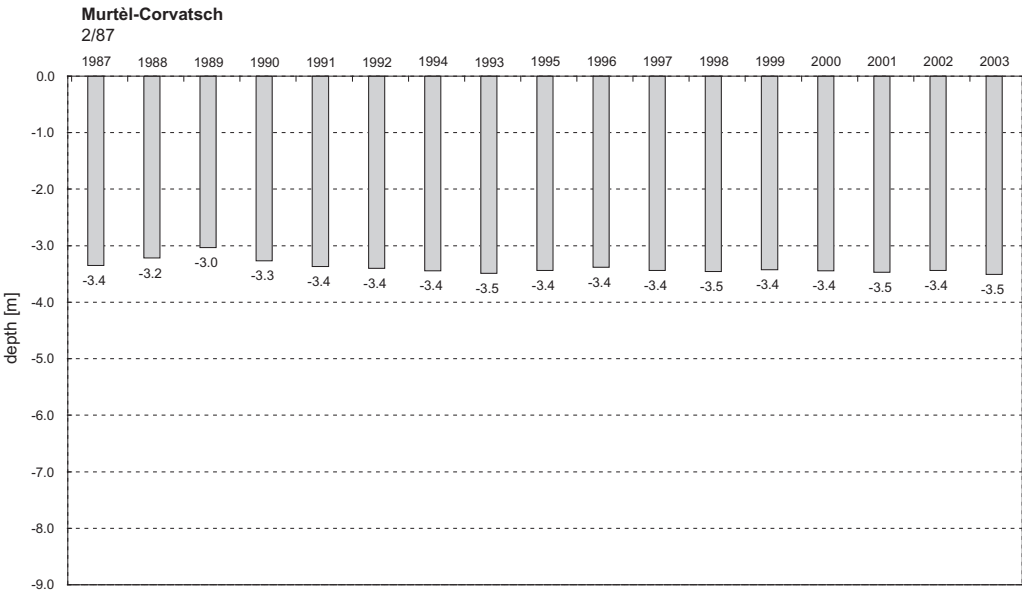


Figure 3.3c: Maximum active layer thickness for the Murtèl-Corvatsch borehole 2/87, until 2003.

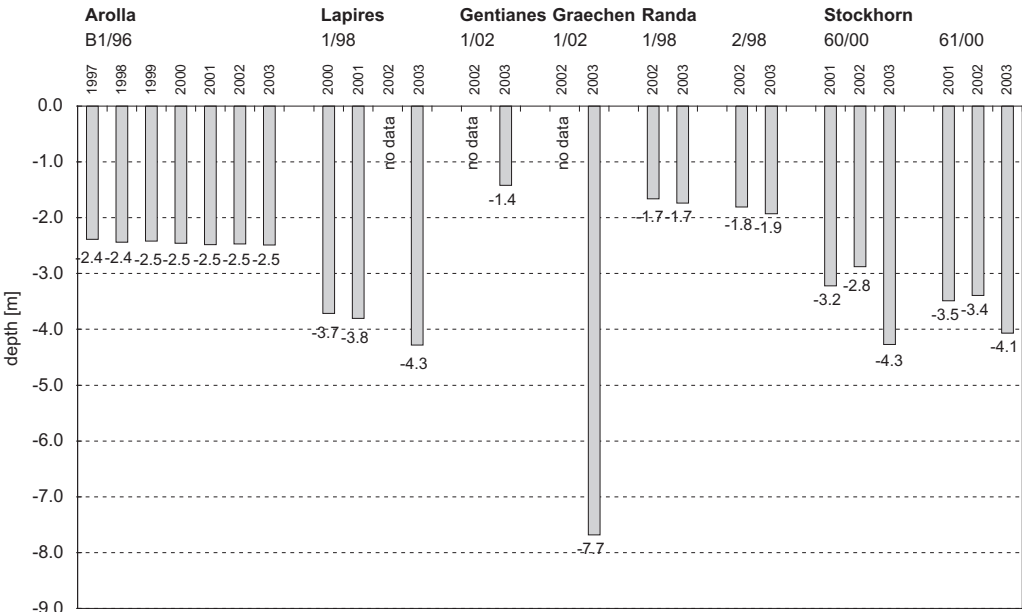


Figure 3.3d: Maximum active layer thickness for the boreholes in Valais, until 2003.

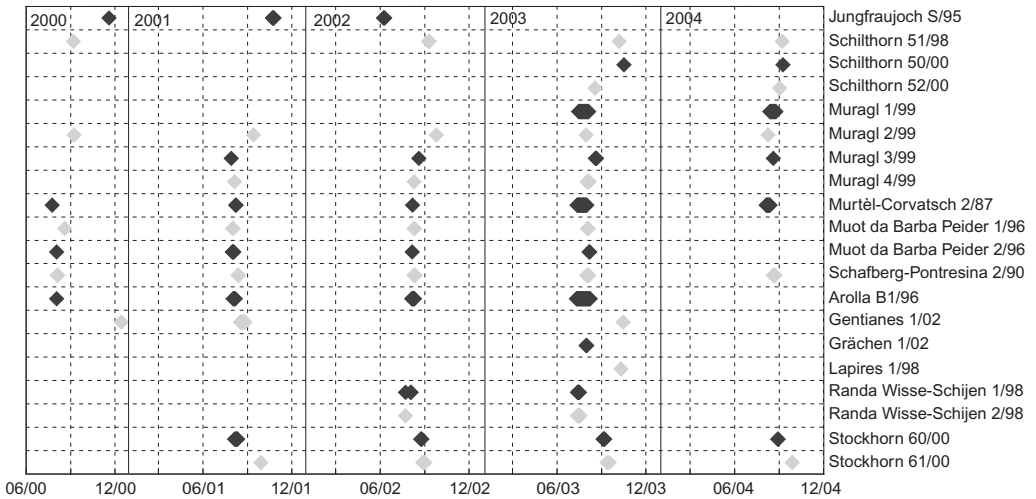


Figure 3.4: Date of maximum active-layer thickness, 2000–2004.

3.2 Permafrost temperatures

Due to the marked topography and low latitude, subsurface temperatures in high mountains vary within short distances compared to circumpolar permafrost areas. Moreover, permafrost temperatures are strongly influenced by surface characteristics (e.g., albedo, available moisture, surface cover) and snow accumulation during winter. In order to allow comparison between the various sites, temperatures over time just above and below the permafrost table, and at the depth of about 10 m, 20 m, and the deepest thermistor are plotted for each borehole in the appendix. In Figure 3.6, the temperature values for the borehole Schilthorn 50/00 are plotted as an example.

Temperatures at the permafrost table

Temperature values are close to 0 °C at all sites, but the depth of the permafrost table varies considerably (cf. Chapter 3.1). Maximum temperatures in the boreholes area are 0 °C due to phase change and zero-curtain. Minimum temperatures, in contrast, depend on site characteristics and on snow thickness in fall and early winter. In addition, comparison between sites is difficult, because the distance of the permafrost table to the thermistors is somewhat arbitrary.

Temperatures at 10 m depth

It takes about half a year until a temperature signal reaches a depth of 10 m. In contrast to surface temperatures, diurnal variations are filtered out and are not identifiable at this depth. Hence, the influence of the seasonal variations is much clearer. In general, the winter 2001/2002 with only

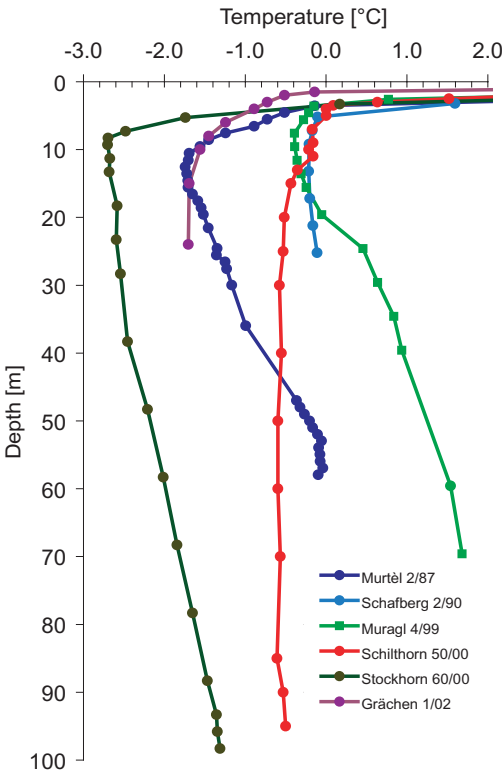


Figure 3.5a: Permafrost-temperature distribution with depth at six PERMOS drill sites. The T-z profiles are plotted for August 2003 (except Grächen for July 2003).

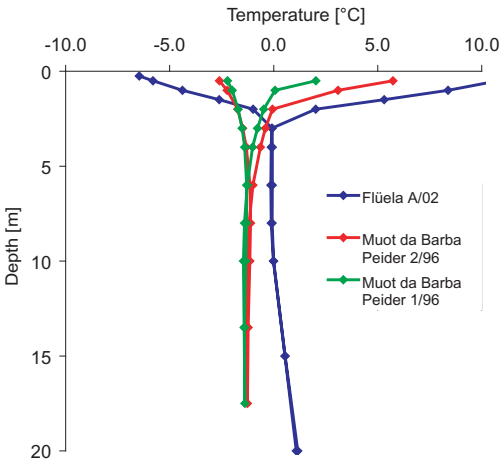


Figure 3.5b: Permafrost-temperature distribution with depth at three PERMOS drill sites. The T-z profiles are plotted for February and August 2003 for Muot da Barba Peider, and for March and August 2003 for Flüela, respectively.

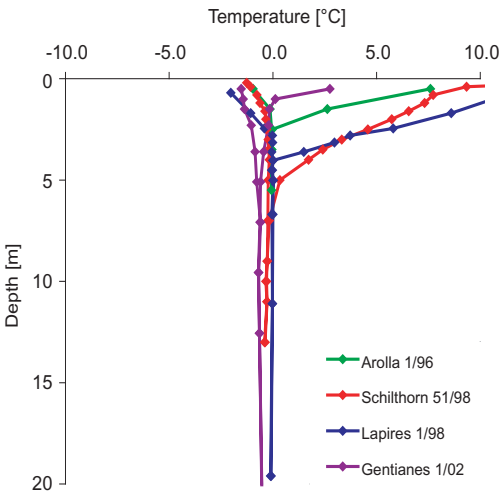


Figure 3.5c: Permafrost-temperature distribution with depth at four PERMOS drill sites. The T-z profiles are plotted for April and August 2003.

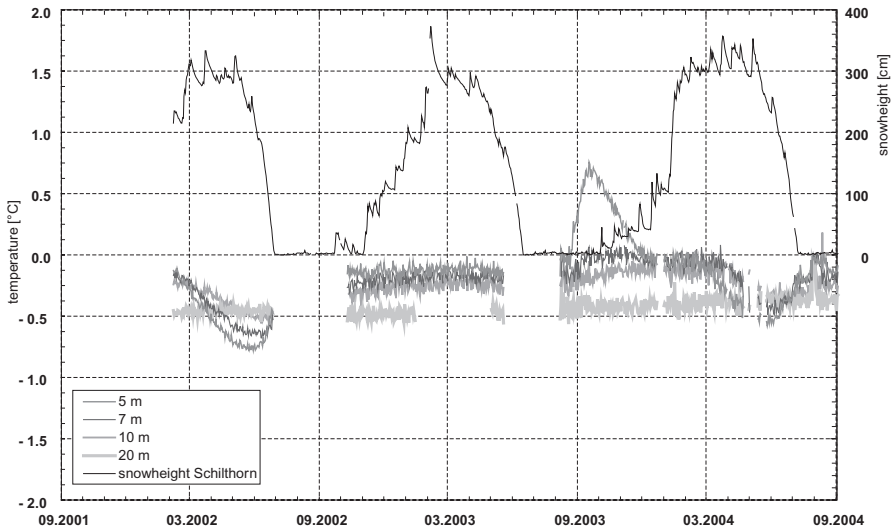


Figure 3.6: Temperature-time-plot of the borehole Schilthorn 50/00 for the thermistors at 5.0, 7.0, 10.0, and 20.0 m depth. Additionally, the snow height is depicted.

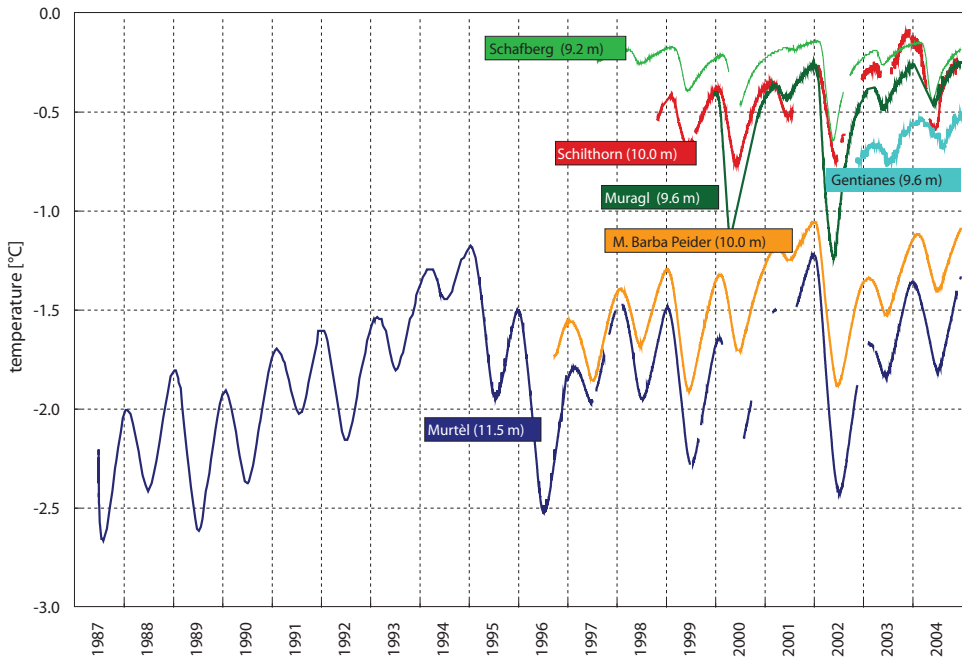


Figure 3.7: The longest time series at Murtèl-Corvatsch allows to relate the reporting period to the past 15 years. Temperatures between 2002 and 2004 are above average.

little snow brought the 10 m-temperatures back to an average level after a continuous warming trend since 1997. The early snow fall at the beginning of the winter 2002/2003, the extremely warm summer 2003, and the following snow-rich winter warmed the subsurface again. Consequently, the 10 m-temperatures clearly increased between October 2002 and September 2004. In fact, they reached values, that are the warmest or at least among the warmest since the beginning of the measurements, depending on the length of the observation period. The observed heating trend since 1997, which was interrupted by the almost snow free and cold winter 2001/2002, continued in the two reporting years. The temperature trend is the more pronounced the colder the permafrost temperature is. At temperatures close to the melting point, a larger part of the energy was used to produce unfrozen water.

In Figure 3.7, the discussed trends are depicted. At Murtèl and Muot da Barbra Peider the temperature curves are mainly sinusoidal with annual amplitudes of ca. 0.2 °C. Schafberg, Gentianes, and Schilthorn, where temperatures are close to -0.5 °C, amplitudes are only about half of those of the colder sites.

3.3 Borehole deformation

No borehole deformation data are available for the period 2002–2004 as the slope inclinometers at Muragl, Schafberg, Murtèl-Corvatsch, and Jungfrauoch are no longer accessible. The pilot project using Time Domain Reflectometry (TDR) at Murtèl-Corvatsch still shows inclusive results. Active layer deformation measurements were installed at Muot da Barbra Peider. Results will be published individually.

3.4 Conclusions

Weather conditions during the reporting period from October 2002 to September 2004 were characterized by early snow fall in both winters and very warm summers. Consequently, active layer thicknesses reached similar amounts as in previous years, but were far thicker than ever since beginning of the monitoring in 2003 at several sites. At Schilthorn, active layer thickness reached almost twice the maximum value observed so far. Permafrost temperatures at about 10 m depth (and also at 20 m depth) increased at all sites during the reporting period.

4 Surface temperatures

The variations in near-surface temperatures are a key parameter influencing the thermal regime of the subsurface. The most important factors that determine near-surface temperatures are air temperature, solar irradiation, snow cover characteristics, and active-layer heat transfer. Temperatures measured several meters deep in boreholes reflect the signals of all these components. Surface temperatures are measured on different types of terrain using different techniques. That is, in

- a) loose sedimentary material (e.g., talus, moraine)
 - continuous recording of ground surface temperatures (GST),
 - mapping of the bottom temperature of snow cover (BTS) in late winter, and in
- b) bedrock
 - continuous recording of rock surface temperature (RST), both on gently inclined slopes and in near-vertical rock walls.

Within PERMOS, the year-round recording of GST on loose sedimentary terrain is carried out by means of >100 single-channel temperature data logger (UTL) at 9 sites (Figure 4.1). Most of the

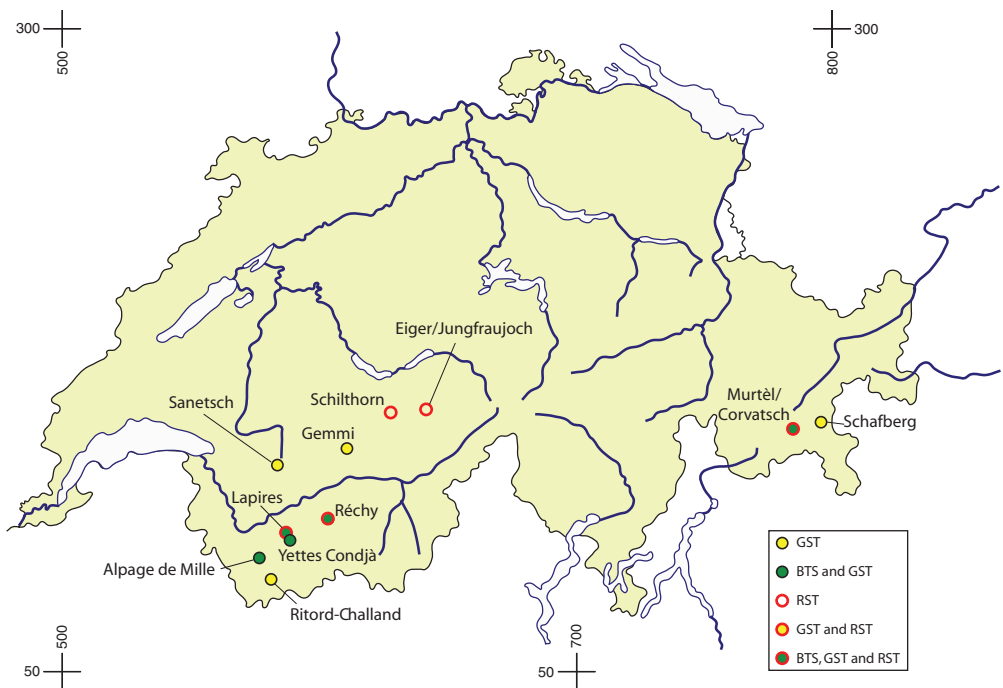


Figure 4.1: Locations of BTS- and GST-sites.

loggers are located on rock glaciers, talus slopes, and moraines with slope angles ranging from 0 to about 40°. Except for a few wind-exposed sites, a relatively thick snow pack (i.e., between 0.5 and 3 m) is expected during winter.

The main observed parameters are (a) the duration of the snow cover (see Chapter 2.4), which indicates how long the ground is protected from summer heating, (b) the Ground Freezing Index (GFI), which is the sum of all daily negative ground temperatures measured during the winter and indicates how cold a winter is at the ground surface, and (c) the Mean Annual Ground Surface Temperature (MAGST), which is mainly the resulting effect of (a), (b), and summer temperatures.

4.1 Surface-temperature measurements in 2002/2003 and in 2003/2004

4.1.1 Bottom temperature of the snow cover (BTS)

BTS measurements were performed only on 4 sites in 2003 and on 3 sites 2004. All sites are located in the Valais Alps (Table 4.1).

Mean BTS values and snow heights are depicted in Figure 4.2. At Yettes Condjà, Réchy and Lapires (only in 2003), mean BTS values in 2003 and 2004 were significantly warmer than in 2002. At Mille, the two years were close to the value of 2002, and to the average BTS 1996-2002. Despite much "warmer" GFIs in winter 2002/2003 than in winter 2003/2004, mean BTS values were only ca. 0.2 °C warmer on all sites, which indicates a general cooling of the ground surface during the second part of the winter 2002/2003 and is probably in relation to the cold air temperatures in February and the cooling of the snow cover at that time.

Worth mentioning is that the snow cover was particularly thick in 2003 at the time of the BTS (end of February, early March). At Mille it reached the second highest value since 1996 (after 1999). This contributed to a prolonged snow period and, consequently, to warmer MAGST in 2003.

Table 4.1: BTS sites and available data, BH=Borehole linkage.

Site	Region	Available BTS	BTS 2003	2004	Mean 2000 ¹	BH
Alpage de Mille	Val de Bagnes, VS	1996– ...	07.03	09.03	yes	no
Lapires	Val de Nendaz, VS	2001– ...	11.03	n.a. ²	yes	yes
Réchy	Val de Réchy, VS	2000–2004	12.03	04.03	yes	no
Yettes Condja	Val de Nendaz, VS	2001–2004	24.02	19.02	yes	no

¹3- to 5-year average BTS map available

²very dense snow that did not allow penetration of the probe to the ground surface

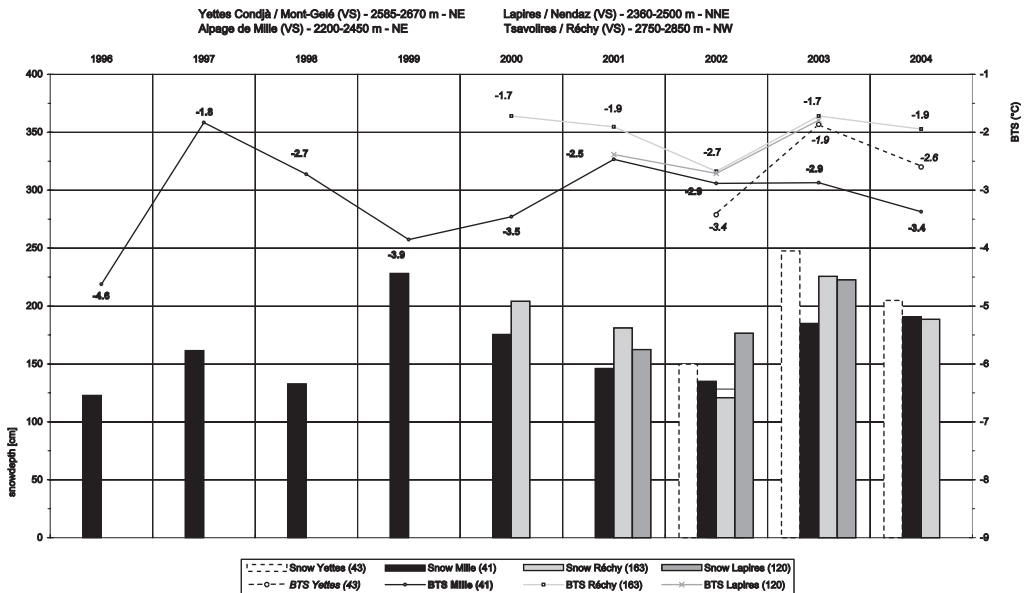


Figure 4.2: Mean BTS and snow depth values since 1996 on three sites in the Valais Alps. In brackets the annual number of BTS measurements is given.

The last campaign at Yettes Condjà and Réchy took place in 2004, of which 3 and 5 annual BTS maps are available. They will be compared to future measurements in a decade or more. However, data acquisition continues at Alpage de Mille as a "control" series, and likely in Lapires (for reasons of accessibility).

BTS at Yettes Condjà

BTS measurements in the Yettes Condjà valley were performed on a small north-east facing talus slope at about 2600 m a.s.l. A vertical electrical sounding carried out in summer 1998 indicates that the talus is ca. 15 m thick and that permafrost is likely present in the entire slope. The resistivity values – and thus the probability that permafrost is present – are slightly higher in the lower part of the slope (Reynard et al., 1999). The absence of surface movements points to a low ice-content.

BTS mapping revealed lower temperatures at the base of the talus (Figure 4.3). The mean BTS was the coldest in 2002 (Figure 4.2). However, a stronger temperature difference between the lower and upper part of the slope was measured in 2003 and 2004, with significantly warmer temperatures in the upper part than in 2002. The accentuation of these differences is typical for low elevation talus slopes (e.g., Creux du Van, Jura mountains, 1200 m a.s.l.; Delaloye et al., 2003) after periods of cold weather. The large temperature difference between the air in the interior of the scree and outside not only generates but intensifies an ascending air circulation within the debris (chimney effect). This effect causes the aspiration of cold air in the lower part of the talus and the expulsion

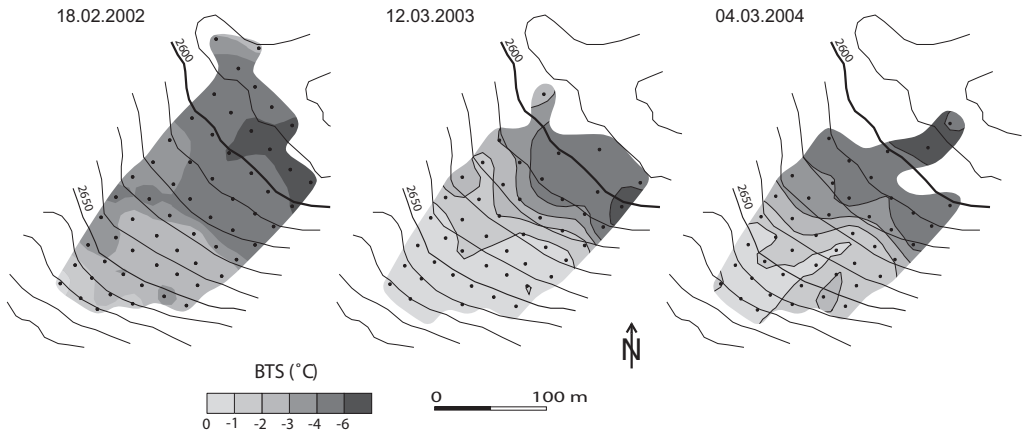


Figure 4.3: Yearly repeated BTS measurements on a talus slope in the Yettes Condjà valley (Mont-Gelé area). Mean air temperature during the 30 days before the measurements: -1.9°C in 2002, -7.6°C in 2003, and -6.4°C in 2004.

of warmer air in the upper part. A similar phenomenon was detected on an inactive rockglacier at Alpage de Mille by means of BTS measurements (Delaloye and Lambiel, 2005).

4.1.2 Ground surface temperature

GST was measured at 9 sites in 2002/2003 and 2003/2004 (Figure 4.1) instrumented with 7-39 loggers (Table 4.2). Data was successfully acquired on most sites in the Valais Alps and Upper Engadine. Unfortunately, frequent loss of data occurred at Gemmi/Furggentälti in the Bernese Alps due to water infiltration into the sensors or due to strong movement of the rockglacier (some sensors were "gubbled up" and new positions were defined in 2003/2004).

The longest GST-serie available since October 1994 for a single place at Gemmi/Furggentälti was interrupted in 2003. To fill the gap in the recordings data from the Creux de la Lé (Sanetsch pass area) was integrated.

Ground freezing index (GFI)

After the low temperature values reported in winter 2001/2002, GFI values were high again on all sites in winter 2002/2003 (Figure 4.4). Early snowfall in autumn 2002 and rather warm air temperatures in December prevented the ground from strong cooling. In the Bernese and Valais Alps, GFIs were the highest since the beginning of the measurements (1994/1995 at Gemmi; 1997/1998 at Mille, Ritord, and Réchy). In the Upper Engadine, the winter 2002/2003 was significantly milder than the winter 2001/2002.

The winter 2003/2004 was colder due to the late arrival of first significant snowfalls in autumn, and probably also due to lower air temperatures in early winter, which contributed the cooling of the ground surface. However, GFIs were not lower than in 2001/2002, except for Schafberg-Pontresina. In the Valais Alps, the values were close to the average of the period 1998–2003. In the Bernese Alps, GFIs were significantly lower.

Mean annual ground surface temperature (MAGST)

At most sites, the mean annual ground surface temperature (MAGST) rose significantly between October 2002 and September 2003, by some 2-3 °C in average (Figure 4.5). Most of the warming (about 2/3) already occurred during the winter 2002/2003. In May 2003, MAGST values were high and close to or even above the maximum of the last decade. The extreme summer 2003 then "only" lead to an increase in MAGST of 0.7 to 1.2 °C. The immediate succession of a warm winter and an exceptionally hot summer induced MAGST values about 0.5 to 1.5 °C above the record values registered since the beginning of the measurements.

Winter 2003/2004 then provoked a slight decrease in MAGST, which was more pronounced during the summer 2004 – warm, but without heat wave. At the end of the hydrological year 2003/2004, MAGST were again close to the mean value of the last decade.

Since 2000 consistent variations in MAGST were monitored at all sites, except for Schafberg, which points to similar climatic conditions in all geographic regions during the period 2000–2004. This was not the case in the period 1998–2000, when MAGST variations differed between regions.

Table 4.2: GST-sites and available data. GST-measurements: c/n + (i), n = total number of measurements places ; c = complete series ; i = incomplete series. BH = Borehole linkage.

Site	Region	Available data	GST 2003	GST 2004	BTS	BH
Gemmi	Berner Oberland, BE	1994– ...	2/38	7/38 + (1)	yes	no
Schilthorn	Berner Oberland, BE	1999– ...	2/10	8/10	no	yes
Creux d.la Lé-Sanetsch	Berner Oberland, BE	199–...	7/7	6/7 + (1)	no	no
Murtèl-Corvatsch	Upper Engadine, GR	2000–...	5/9	7/9	no	yes
Schafberg-Pontresina	Upper Engadine, GR	2000–...	5/9	5/9	no	yes
Ritord-Challand	Grand-Combin, VS	1997–...	22/22	22/22	no	no
Alpage de Mille	Val de Bagnes, VS	1997–...	18/18	18/18	yes	no
Lapires	Val de Nendaz, VS	1998–...	14/16+(1)	15/18+(1)	yes	yes
Yettes Condjà	Val de Nendaz, VS	1998–...	19/27+(3)	22/27+(1)	yes	no
Réchy	Val de Réchy, VS	1997–...	10/10	10/10	yes	no

PERMAFROST IN SWITZERLAND 2002/2003 AND 2003/2004

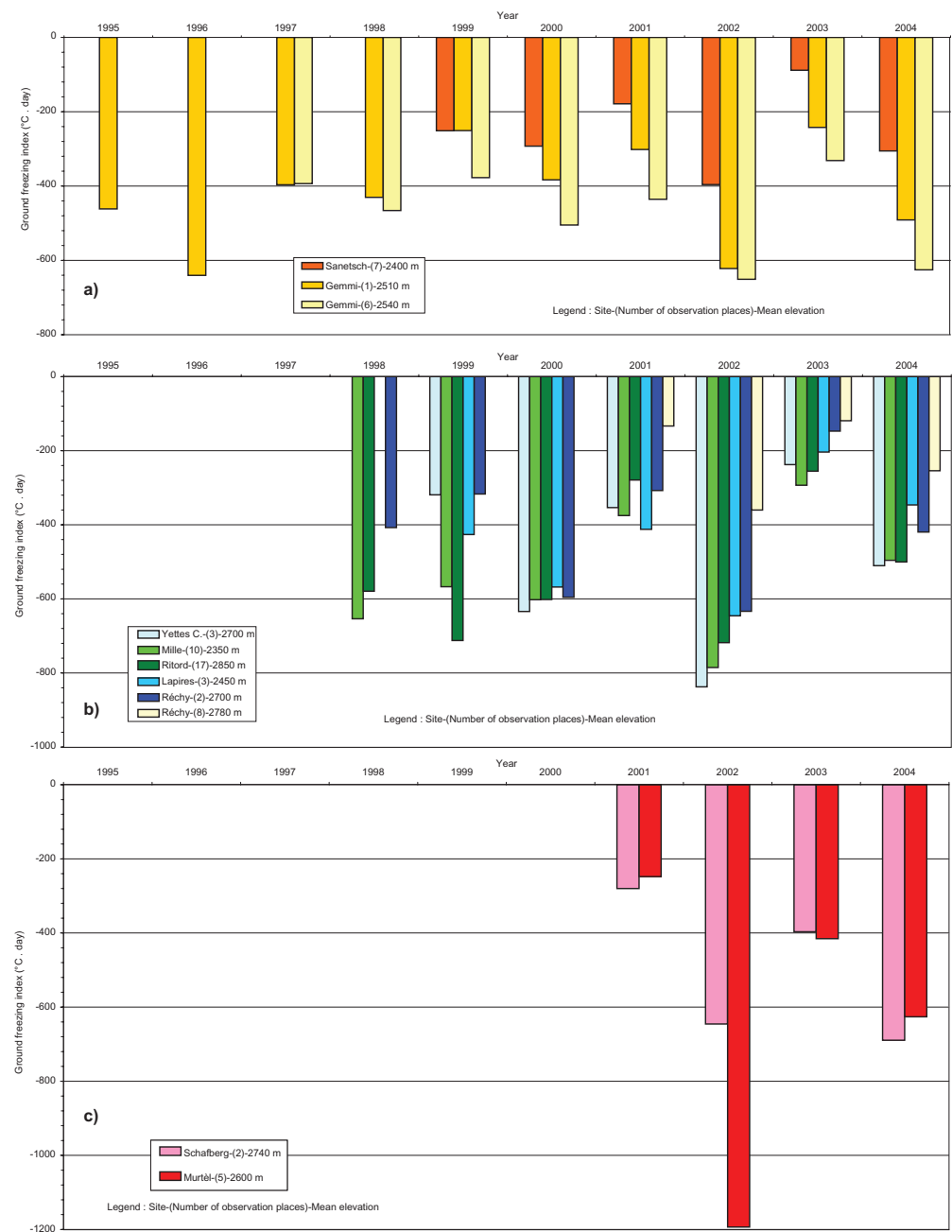


Figure 4.4: Ground freezing index (GFI) at the PERMOS GST-sites; a) Bernese Alps; b) Valais Alps; c) Upper Engadine.

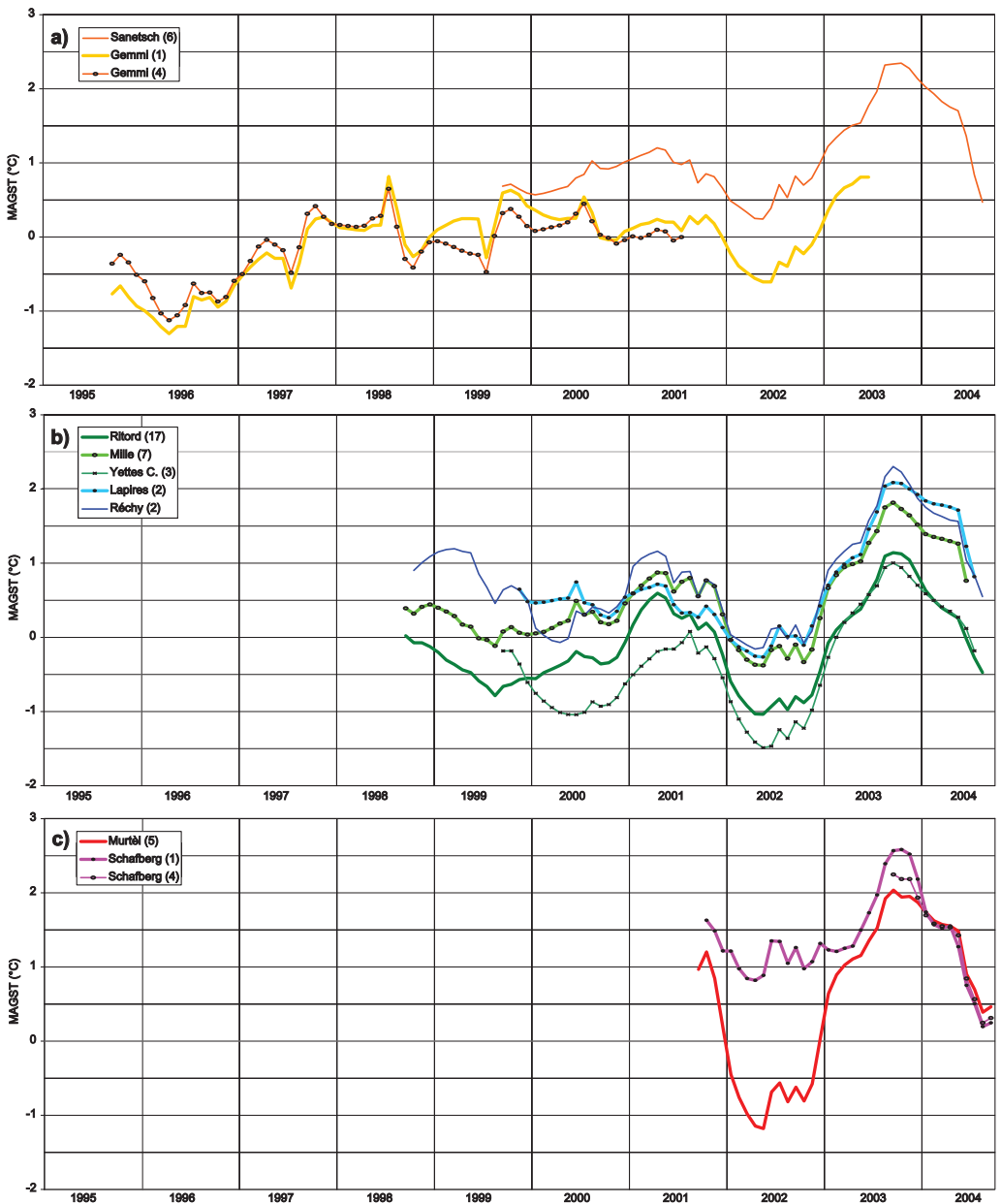


Figure 4.5: Evolution of the mean annual ground surface temperature (MAGST) on PERMOS GST-sites; a) Bernese Alps; b) Valais Alps; c) Upper Engadine. MAGST is computed each month. Dates correspond to the end of the annual period used for the calculation. Legend: site-(total number of sensors).

4.1.3 Rock surface temperature

Ground surface temperature measurements – if performed in coarse blocks – are subject to considerable influence of all governing factors. Measuring near-surface temperatures in rock helps to disentangle the individual factors: in near-vertical rock walls the effects of air temperature and solar radiation dominate (relative influence changes with slope aspect), whereas in gently inclined rock surfaces the additional effect of the snow cover can be observed (Figure 4.6). In addition to the improved monitoring of individual factors, which is important for the reaction of permafrost to climate change, this data provides a base for the validation of numerical simulation models.

During the summers of 2003 and 2004 most of the targeted 36 sites have been selected, described and instrumented. Since summer 2005 the full range of sites is monitored.

By 2004, the following areas were instrumented:

- | | |
|--------------|--|
| 1. Jungfrau: | Schilthorn, Birg, Eiger, Mönch, and Jungfrau
6 data loggers in steep rock, 5 in gently sloping rock |
| 2. Engadine: | Corvatsch, Murtèl, and Fuorcla Surlej
5 data loggers in steep rock, 6 in gently sloping rock |
| 3. Valais: | Réchy and Lapires
10 data loggers in steep rock, 2 in gently sloping rock |

4.2 Evaluation of the BTS method within PERMOS

The aim of BTS monitoring within PERMOS was to document the spatial variations of the permafrost lower limit. To achieve this, it is indispensable to perform measurements on areas of restricted dimensions where a transition permafrost – no permafrost occurs and does not correspond to a geomorphic limit (for instance the border of a rock glacier). The experience gained during the pilot-phase of PERMOS, however, showed that

- such terrains (moreover accessible and avalanche safe) are difficult to find,
- permafrost is often restricted to the lower part of the slope (detecting the lower limit of a permafrost area is thus obsolete),
- thermal processes within the talus slopes are complex (see 4.1.2), and
- long term changes are difficult to observe due to significant interannual variability in winter ground surface temperature (see 4.1.2).

For these reasons, it was decided

- to limit the number of BTS-sites,
- to end the already initiated series in order to obtain the so-called "Mean 2000" maps (see Report 2000–2002), that are the average of 3-5 annual BTS campaigns, and
- to continue only with a limited number of sites, and Alpage de Mille as a control series.

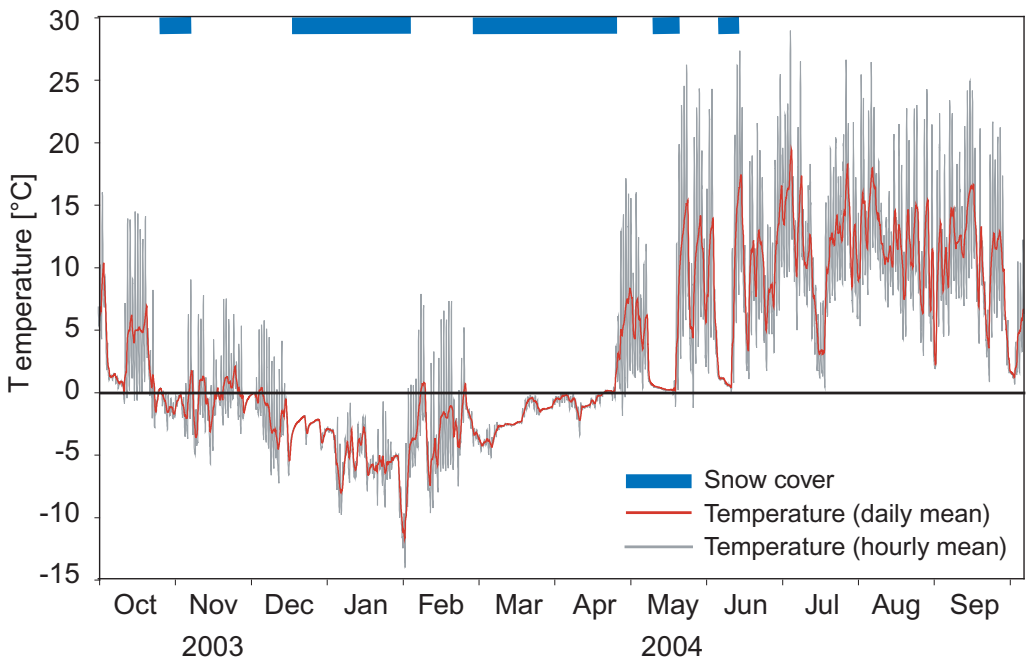


Figure 4.6: Example of year-round rock surface temperatures from the Schilthorn area (elevation: 2670 m a.s.l.; aspect: 130°; slope: 22°). Annual and diurnal temperature cycles are clearly visible as well as times of snow cover with low temperature variability.



Photo 3: Rock temperature logger at Mönch/Jungfrauoch. Photo: A. Hasler.

4.3 Conclusions

Ground surface temperatures were unusually high in 2003. The sequence of a warm winter 2002/2003, an early snow melt, and an extremely warm summer lead to an increase in MAGST by about 2-3 °C. At the end of the hydrological year 2003/2004, MAGST rose again close to the mean value of the past decade.

BTS measurements have shown that permafrost is often restricted to the lower part of the slope and that processes related to air circulation influence the thermal regime of the slope in a complex but dominating manner. This emphasises the difficulty of both mapping and surveying the lower permafrost limit.

In order to disentangle the influences of various factors, GST sites were complemented with a number of near-surface temperature loggers in both near-vertical and rather flat bedrock.

5 Air photos

5.1 Air photos in 2002/2003 and 2003/2004

Aerial photographs are collected for documentation purposes and photogrammetric analyses. Several areas have been flown over regularly since the 1980s (Table 5.1 and Figure 5.1).

For photogrammetrical interpretation and analysis, aerial photos have to be taken in a regular cycle. Information about surface phenomena at a certain time is abundant on aerial photos, which allows quantification of different parameters using photogrammetry.



Figure 5.1: Areas where air photos are taken regularly.

Table 5.1: Rockglacier areas where airphotos are acquired regularly since 1980 for systematic monitoring of creep (low flying height (low f. h.), black and white (b-w)).

Region	Type	Max. speed	Available years
Murtèl	low f. h., b-w	15 cm/a	1987, 1988, 1991, 1995, 1996, 2002
Muragl	low f. h., b-w	50 cm/a	1981, 1985, 1990, 1994, 1998, 1999, 2000, 2002
Schafberg	low f. h., b-w	10 cm/a	1991, 1994, 1998, 1999, 2000
Réchy	low f. h., b-w		1986, 1991, 1995, 1999, 2004
Gruben	low f. h., b-w	100 cm/a	1967, 1975, 1983, 1985, 1988, 1989, 1990, 1991, 1992, 1994, 1995, 1996, 1997, 1999, 2000, 2001, 2002, 2003
Suvretta	low f. h., b-w	200 cm/a	1992, 1997, 2002
Gross Gufer	low f. h., b-w	250 cm/a	1987, 1994, 2000
Furggentälti	low f. h., b-w	70 cm/a	1990, 1995, 1999, 2000

Table 5.2: Available infrared air photos.

Region	IR-air photos
Morteratsch	1981
Goms North	1983
Goms South	1983
Goms-Gerental	1983
Goms-Münsterbach	1983
Upper Engadine – Julier	1988
Upper Engadine – Val Roseg	1988
Piz Quattervals	1984
Piz Vadret – Piz Fora	1984
Vals da Camp	1984
Val Maroz – Julier – Piz Ot	1984
Roseggletscher	1985, 2004
Val Réchy – Moiry	1986
Simplon	1987
Turtmann – Zinal	1987
Mattertal	1991
Saastal	1991
Simplon – Almagell	1991
Flüelapass	1997

5.2 Recent acceleration of rockglaciers in the Swiss Alps

Recently, questions arose as to whether and how the atmospheric warming, which is currently observed in many mountain regions (McCarthy et al., 2001), e.g., in the European Alps (Böhm et al., 2001), influences the creep of perennially frozen debris. On the one hand, this is of large scientific interest, for instance, in view of climate change projections or landscape evolution. On the other hand, geotechnical changes of frozen debris slopes have notable impact on slope stability, and are thus of interest related to applied problems such as construction stability, debris flow hazards, or rock fall hazards (Haeberli, 1992; Haeberli et al., 1997; Arenson, 2002; Kääb et al., 2005a; Kääb et al., 2005b).

In Figure 5.2 speeds of rockglaciers since the 1970s are compiled according to different measurement periods. The rockglaciers analysed are part of the PERMOS photogrammetric network. All data represent average speeds from the central parts of the rockglaciers. By that procedure, slow or even inactive lateral rockglacier sections were excluded. For each rockglacier, exactly the same sample of points was taken for each period in order to avoid biases due to sample differences. However, since the delimitation of the «central parts» was defined manually, the absolute numbers for the average speeds are somewhat arbitrary and will change with a different definition of the area where rockglacier speed is tracked over time. Thus, the proportional change in speed should be interpreted rather than the absolute speed of the rockglaciers investigated. Furthermore, the time periods compared to each other are in parts different. It should, therefore, be kept in mind that potential speed variations within a longer measurement period are not captured by the comparison. Caution is also needed when short periods are analysed, because the measurements then just depict a «snapshot» of speed, which is not necessarily representative for the long-term behaviour of a rockglacier. (For the photogrammetric technique applied for all rockglaciers see Kääb and Vollmer, 2000).

The data for Gufer rockglacier (Eggishorn, Aletsch region, Valais) stem from photogrammetric analyses based on air photos of 1976, 1995 and 2000 (Kääb, 2005). An increase in average speed of about 40% can be observed.

The data for Gruben rockglacier (Saas valley, Valais) were compiled from air photos of 1970, 1975, 1979, 1985, 1991, 1994, 1995, and 1999 (Kääb et al., 1997; Strozzi et al. 2004). The sample analysed is for the fast-creeping lower part of the rockglacier only, not for the entire section (cf. Kääb et al., 1997). Between 1970 and 1995 speed variations in a range of 10% can be found. An increase of about 20% or more seems to have occurred after 1995.

Air photos from 1981, 1985, 1990, and 1994 were compiled for the central part of Muragl rockglacier (Upper Engadine, Grisons) revealing a drop in average speed from 1981–1985 to 1985–1990 by over 30%, and then again a rise for 1990–1995 by 70% to approximately the same speed as 1981–1985 (Kääb, 1998; Frauenfelder and Kääb, 2000). The data are also compared to terrestrial measurements at the same location from 1998–2001, revealing another rise of about 80%. However, the fact that Muragl rockglacier shows drastic changes in speed within very short time intervals (Kääb et al., 2003; Kääb, 2005) calls for special care when interpreting the speed variations for this

rockglacier. A small shift in the measurement period, e.g., by some weeks, is potentially able to significantly alter the speed variations obtained photogrammetrically (and geodetically).

For Becs-de-Bosson rockglacier (Val Réchy, Valais) air photos of 1986, 1991, and 1999 were analysed. An increase in speed of about 70% was found (Kääb, 2005). The Réchy measurements were made in a collaborative effort between the University of Zürich (A. Kääb) and the University of Fribourg (J.-P. Dousse, R. Delaloye).

Air photos of 1971, 1992, 1997, and 1998 were analysed for Suvretta rockglacier (Piz Julier, Upper Engadine, Grisons; Kääb, 2000; Frauenfelder et al., 2004; Kääb, 2005). The photogrammetric measurements reveal an increase in speed by about 20–30% between the periods 1971–1992 and 1992–1997.

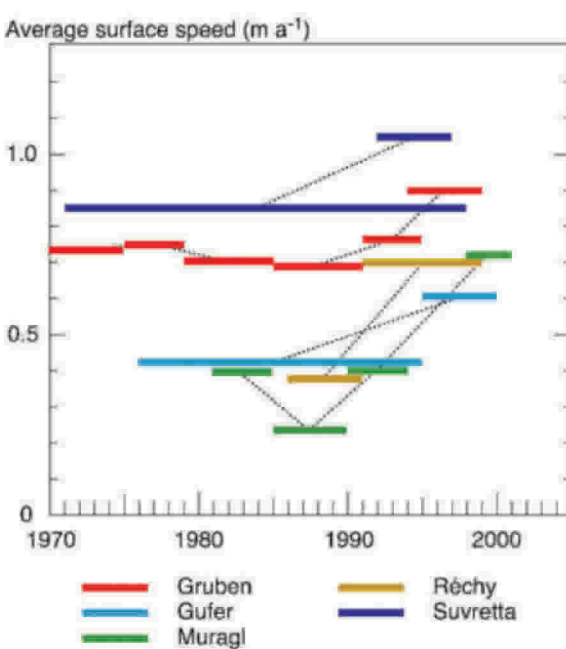


Figure 5.2: Average rockglacier surface speed in the Swiss Alps measured for different periods since 1970. Most of the data are from photogrammetry, some from geodesy. The Macun data are from Zick (1996), all other from the authors of this contribution.

Further time series of rockglacier speed, most of them also showing a recent increase in speed, are available for the Swiss, French, Italian, and Austrian Alps (Turtmann valley: Roer, 2005; Roer et al., 2005b; Roer et al., 2005c, Macun, Engadine: Barsch and Zick, 1991; Zick, 1996, Lower Valais: Lambiel and Delaloye, 2004; Lambiel, 2005; Perruchoud and Delaloye, 2005, Austrian Alps: Kaufmann, 1998; Schneider and Schneider, 2001; Kaufmann and Ladstädter, 2002). A more detailed compilation of rockglacier acceleration data and a general discussion about the response of rockglacier creep to atmospheric warming are underway (Kääb et al., 2007.; Roer et al., 2005a).

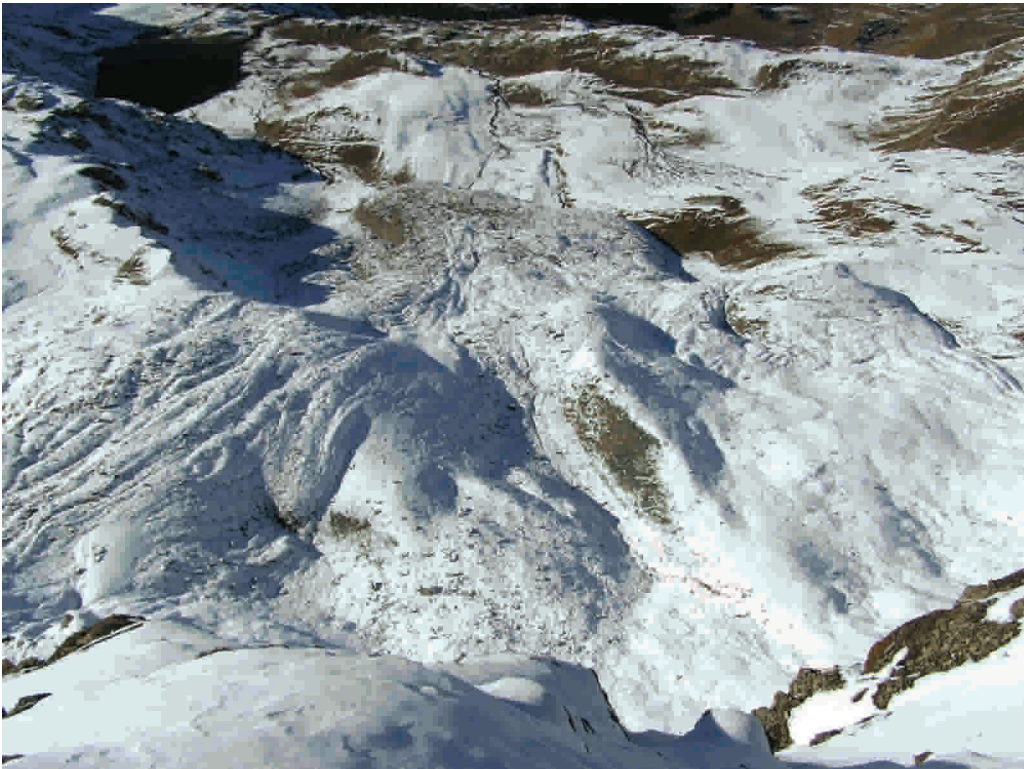


Photo 4: Little Ice Age push-moraine structures in the morphological rooting zone of the active Becs-de-Bosson rockglacier in the Val de Réchy. There is no more glacier since decades at that place, but permafrost is still mostly lacking in the former glacierized area. Permafrost creep occurs nevertheless in the lower part of the rockglacier and has even accelerated significantly since the 1980s. Photo: R. Delaloye.

6 Conclusions

The present report for the period 2002/2003 and 2003/2004 documents measurements of the three key elements established in PERMOS: (1) Borehole measurements including active layer thickness, permafrost temperatures, but no borehole deformations during the reporting period, (2) ground surface temperature measurements in loose debris and the newly set up monitoring of rock surface temperatures, and (3) data from aerial photographs, especially for the quantification of rockglacier movements.

Since permafrost is defined by temperature, weather conditions of the period under report are described first. The year 2002/2003 is characterised by a mild and wet autumn, a snowy winter with an early snow free period and the extraordinary hot and dry summer. The following year 2003/2004 shows a snowy winter with late snowmelt and a warm and partially humid summer. Due to the extreme temperature conditions in 2003, active layer thickness exceeded previous measurements in the PERMOS boreholes. In the following year, the active layer thickness was again in the range of the previous years. The permafrost temperatures at about 10 m depth increased at all sites due to the given weather conditions.

The ground surface temperatures indicated extremely high values in 2002/2003 to MAGST values of about 0.5 to 1.5° C warmer than the former maxima registered during the last 5-10 years. But, at the end of the following year, the MAGST was again close to the mean value of the last decade. The newly installed monitoring of surface temperatures in rock walls is now ready to operate. In this period, aerial photographs were compiled for the following rockglacier sites: Murtèl, Muragl, Suvretta, Réchy, and Gruben. In combination with other studies at non-PERMOS sites, a general acceleration of rockglaciers in the Swiss Alps is documented.

7 Selected aspects of permafrost monitoring and special events

7.1 Ice caves

7.1.1 Introduction

Perennial cave ice occurrences have been described for most karst regions in Switzerland and are often located at altitudes where the mean annual air temperature is far above 0 °C. Since low-altitude cave ice accumulations are assumed to be sensitive to climate changes, fluctuations of subsurface ice volumes are considered good indicators of environmental conditions. However, the monitoring of ice caves requires special techniques and is a logistical challenge as they are usually not easy to access. The absence of energy supply (power or solar) and the presence of freezing conditions in a humidity saturated atmosphere increases the difficulty of a proper instrumentation.

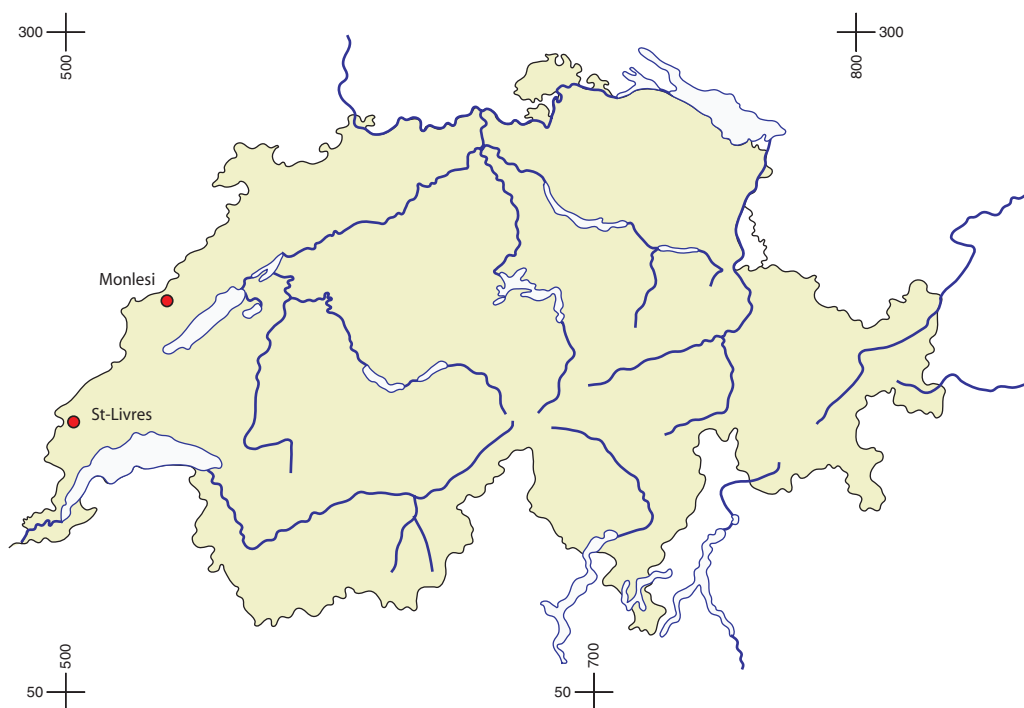


Figure 7.1: Location of the two ice caves monitored during the PERMOS pilot phase.

The monitoring of ice caves in Switzerland started in 2001 at two selected study sites in the Jura Mountains which were later integrated into the pilot phase of the PERMOS program (Figure 7.1). The Glacière de St-Livres (Bière, Vaud, 6°17'50"/46°33'47", 1359 m a.s.l.) and the Glacière de Monlési (Boveresse, Neuchâtel, 6°35'4"/46°56'18", 1135 m a.s.l.) were both selected for their distinguishing cave ice accumulation processes. A large collapsed doline (Ø ~20 m) constitutes the entrance of St-Livres ice cave and leads to the deepest part of the cavity at -45 m. The ice filling, with an estimated volume of 1200 m³, occupies the base of the entrance shaft. It is formed from the diagenesis of snow accumulated during winter, but local refreezing processes of infiltration water also contribute to the actual ice mass. In contrast to the St-Livres ice cave, the filling of Monlési ice cave results mainly from the accumulation of annual deposits of congelation ice. The cave opens with three entrance shafts and is subject to significant air circulation during winter (forced convection), but acts as a thermal trap during summer. The ice volume was estimated at 6000 m³ in 2002, based on morphological evidence suggesting a maximal ice thickness of 12-15 m.

The selection of further monitoring sites is under way. Selection criteria, concept of monitoring as well as detailed instrumentation descriptions are presented in the general concept. This report aims at presenting preliminary data from the pilot phase.

7.1.2 Air temperature records

Cave air temperatures provide valuable data on the thermal state of the cave system, especially when compared to external air temperature. Temperatures are measured at two hour intervals using single channel miniature temperature loggers (UTL-1). Within the cave, a logger is placed at the bottom of the main room. Outside the cave, a logger is located at a ventilated place in the shadow of direct solar radiation.

The temperature records do not vary significantly from one year to the next (Figure 7.2). Both caves display a characteristic thermal response characterized by 1) a first period mostly during winter (i.e., November to April), that shows a good correlation between the cave air temperature and the negative external air temperature, and 2) a second period, from May to October, which shows stable temperatures close to 0 °C. During this period, when the external temperature is higher than the cave temperature, no significant air circulation can be observed and both caves act as a thermal trap.

Inter-annual comparison is provided by the number of "freezing hours" (i.e., the number of hours where the mean air temperature is below 0 °C) and the "freezing index" (i.e., integer of mean air temperature below 0 °C; Table 7.1).

7.1.3 Cave ice fluctuation

Cave ice fluctuations were measured at Monlési between April 2001 and November 2004, by manually measuring the distance between the rock and the ice surface at a station located at the top of the ice filling. The marked seasonal variation of the cave ice volume underlines a still active crystallization process. Freezing of cave ice is favoured by mid-winter warm spells or by the thawing of the external snow cover in early spring. Although a negative trend of the annual mass balance

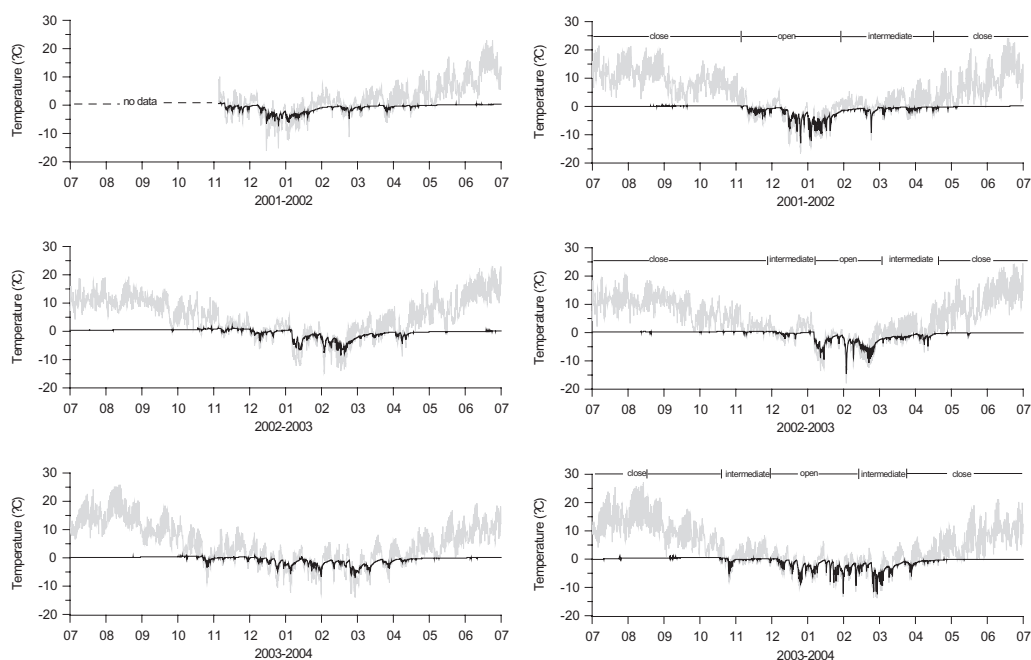


Figure 7.2: Cave air (black) and external atmosphere (grey) temperature recorded at St-Livres (left) and Monlési (right) ice cave.

Table 7.1: Inter-annual comparison (2001–2004) of temperature records at Monlési and St-Livres ice cave.

Site Year	Mean temp. [°C]		Minimum temp. [°C]		Freezing hours [h]		Freezing Index [°C*h]	
	external	cave	external	cave	external	cave	external	cave
Monlési								
2001-2002	4.5	-0.9	-16.7	-13.0	2496	4238	-8911	-8140
2002-2003	4.9	-0.7	-17.9	-14.7	2340	3212	-8150	-8916
2003-2004	4.4	-0.9	-13.8	-12.4	2896	3660	-9259	-8916
St. Livres								
2001-2002	n.a.	n.a.	-16.2	-7.4	2172	4284	-7694	-5583
2002-2003	4.9	-0.5	-15.0	-8.5	2190	4514	-8461	-6374
2003-2004	4.7	-0.6	-14.0	-7.0	2522	4772	-8787	-6280

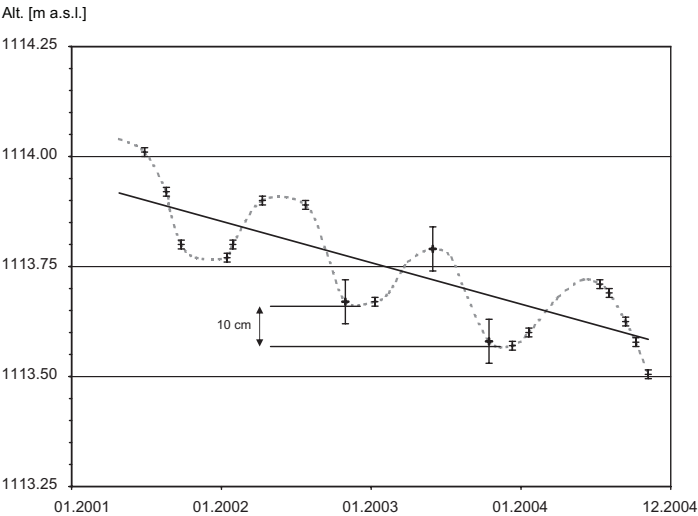


Figure 7.3:
Cave ice fluctuation measured in Monlési ice cave between 2001 and 2004. Vertical bars reflect the accuracy of measurements. The thickness of the ice body decreased of about 10 cm during the 2002–2003 annual cycle. Although a negative trend of the ice mass balance can be observed, the exceptionally hot period in the summer of 2003 had no significant impact on the cave ice volume.



Photo 5: Comparison of two pictures from St-Livres ice cave taken in 1978 (left) and 2002 (right). Photos: R. Wenger-ISSKA.

is observed, no significant increase of melting rates was observed during summer 2003, which was characterized by exceptionally high temperatures in Europe (Figure 7.3).

7.1.4 Conclusions

Observations performed during 2002–2004 at Monlési ice cave suggest a general melting of the subsurface ice accumulation. However, because of a reduced heat exchange during summer due to thermal trapping, the 2003 heat wave did not have a significant impact on the overall cave ice mass balance. Since winter climate conditions varied only little during the observation period (FI: $\pm 7\%$), significant changes in the ice cave volumes cannot be observed.

Historical documentation from both study sites suggested that cave ice mass balance remained almost in equilibrium until the 1980s. However, a noticeable decrease of the cave ice volume can be observed for the last fifteen years, which is in good agreement with measurements performed during the 2002–2004 monitoring period.

7.2 Pilot study for the use of geophysical monitoring systems within PERMOS

7.2.1 Introduction

Monitoring the amount of permafrost degradation in mountain regions is one of the foremost tasks in current permafrost research, especially in the context of climate change and the increased rock-fall activity in the European Alps during the anomalously warm summer 2003. For this reason, the PERMOS borehole network supplies information about changes in ground temperature at several monitoring sites in the Swiss Alps. However, to assess the amount of permafrost degradation, two additional aspects have to be included: (1) the spatial information around the single-point borehole temperatures and (2) the monitoring of changes in ground ice content, which is a dominant factor regarding the possible instability of partly frozen mountain slopes.

As a result, a monitoring strategy fulfilling the above requirements was initiated within a pilot study for PERMOS using a surface-based geophysical monitoring system. The system is based on the Electrical Resistivity Tomography (ERT) method, which has been increasingly applied to detect mountain permafrost in the last years (e.g., Hauck et al., 2003; Marescot et al., 2003). A permanently installed ERT system has been initiated in 1999 to monitor the long-term change in electrical resistivity along a 60 m long and 10 m deep profile line at the PACE21 (Permafrost and Climate in the 21st century) monitoring station Schilthorn, Swiss Alps (Hauck, 2002). Monitoring the electrical resistivity allows determination of the amount of freezing and thawing within the subsurface on a regular basis. Additional information is provided through three boreholes and an energy balance station, which observes meteorological parameters like radiation, air temperature, and snow cover thickness (see chapter 2).

The pilot study was conducted for an initial 5-year period from 1999–2004, including the exceptional warm summer in the Alps in 2003.

7.2.2 Theory

Electrical Resistivity Tomography (ERT) is based on differences in electrical resistivity of the subsurface over a 2-dimensional or even 3-dimensional grid. The technique allows visualising these spatial differences through indirect measurements at the surface, that is, no direct measurements (e.g., borehole measurements) at the depth of interest are required. Repeating an ERT survey at a later time yields the temporal resistivity changes within the subsurface during the time period between the two measurements. Because the geology of the subsurface will not change over the time scales of interest, the observed resistivity changes can solely be attributed to changes in the frozen and unfrozen water content. A monitoring system based on repeated ERT measurements can thus be used to monitor freeze and thaw processes over long time spans.

In resistivity tomography surveys electrical current is injected into the ground via two current electrodes. The resistance (in Ohm, W) of the ground is then determined by measuring the electric potential between two other electrodes and dividing by the current. By multiplying the resistance with a geometric factor depending on the distance between the electrodes and choosing different electrode spacings and locations, the so-called apparent electrical resistivity (r , given in Wm) is determined on a 2-dimensional grid. By using a tomographic inversion scheme (RES2DINV) these apparent resistivities can be inverted to yield a 2-dimensional specific resistivity model of the ground (Loke and Barker, 1995).

For typical permafrost material a marked increase in resistivity at the freezing point was shown in several field and laboratory studies (e.g., Hoekstra et al., 1975; King et al., 1988). This strong increase in resistivity associated with freezing can be used to relate temporal resistivity changes to freeze and thaw processes within the permafrost (Hauck, 2002). Figure 7.4 shows an example of a laboratory experiment using subsurface material from the Schilthorn monitoring site.

7.2.3 Field site and installation of the geophysical monitoring system

The Schilthorn monitoring site (46°33 'N, 7°50 'E at 2900 m asl) is located in the Bernese Oberland in the Northern Swiss Alps and is included in the PACE21 and PERMOS networks. Permafrost temperatures measured in the boreholes are comparatively warm with a minimum of ca. -0.7 °C at 100 m depth. Consequently, the unfrozen water content is comparatively high leading to low resistivity values (< 10'000 Wm) compared to typical mountain permafrost occurrences. The surface at the monitoring site consists of small to medium size debris originating from weathered bedrock (micaceous shales) with no vegetation cover.

For the ERT monitoring system a set of 30 electrodes with a spacing of 2 m was permanently installed along a 58 m survey line in September 1999 yielding an investigation depth of 10 m. The 30 stainless steel electrodes were buried 1m into the ground and were connected to a manual switchbox via buried cables to ensure accessibility throughout the winter and allow measurements independent of the snow cover thickness (Figure 7.6). Resistivity surveys are made by connecting

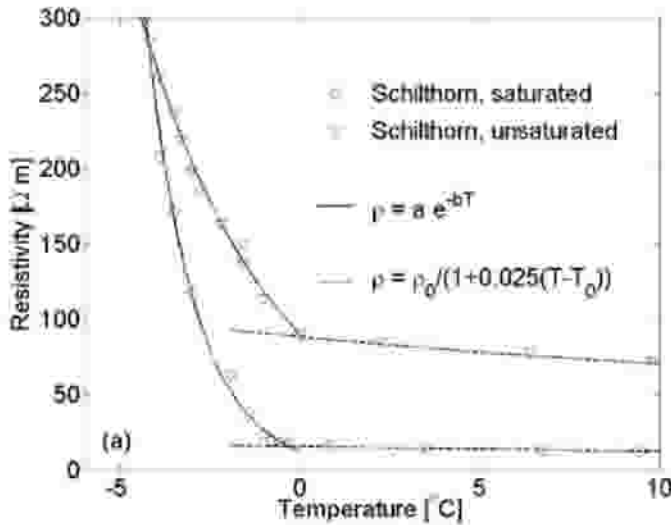


Figure 7.4: Resistivity-temperature relationship determined in the laboratory for saturated and unsaturated Schilthorn samples. The solid and dashed lines relate to equations given in the literature, where ρ and T denote resistivity and temperature, respectively, and a , b , ρ_0 and T_0 are empirically determined constants. For details see Hauck (2001).

a standard resistivity meter to the switchbox for each of the selected electrode configurations (in the so-called Wenner configuration) resulting in 135 single datum points. A commercially available software package (Res2dinv) is used to determine specific resistivities within a finite-element block model from the surface resistance measurements. Ground temperature data from two boreholes along the profile are used to relate resistivity changes to changes in temperature and to estimate the temporal evolution of the unfrozen water content.

The permanency of the electrode array effectively filters resistivity variations due to variable electrode contacts or geological background variations. The installation has proven to be robust to damage by weather and erosion, with only minor maintenance work necessary during the 5-year pilot phase. Besides, the costs of installing and maintenance of the system are low, given that a standard resistivity meter is available. For future long-term monitoring programmes, automation of the monitoring system is recommended.

7.2.4 Results of the permafrost monitoring on the Schilthorn, Bernese Oberland, 1999–2004

Temperature monitoring

Results from ground temperatures measurements in the Schilthorn boreholes are discussed in detail in chapter 2. Figure 7.5 highlights again the impact of the extraordinary warm summer air tempe-

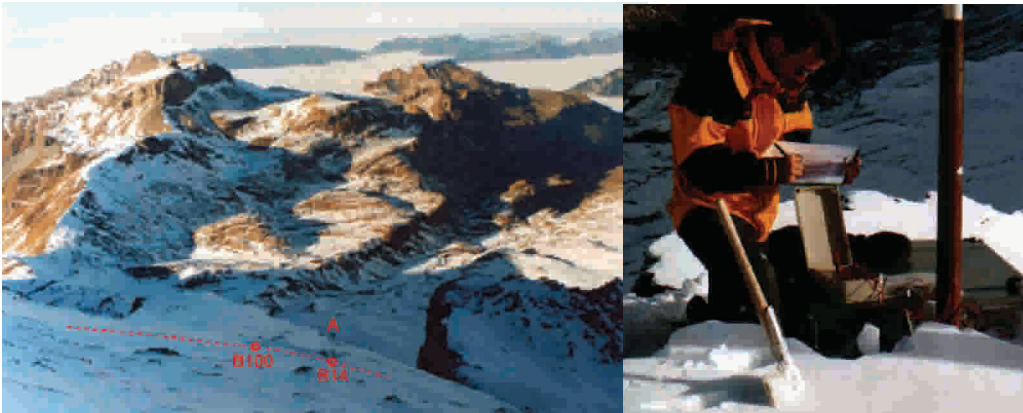


Photo 6: (left) View of the northern slope of Schilthorn and the permafrost monitoring site. The permanent electrode profile is indicated by the dashed line, the location of the two vertical boreholes (100 m and 14 m) and the energy balance station are indicated by the circles and the letter A, respectively (Völksch, 2004). (right) ERT measurement with the manual switchbox in winter (Schudel, 2003).

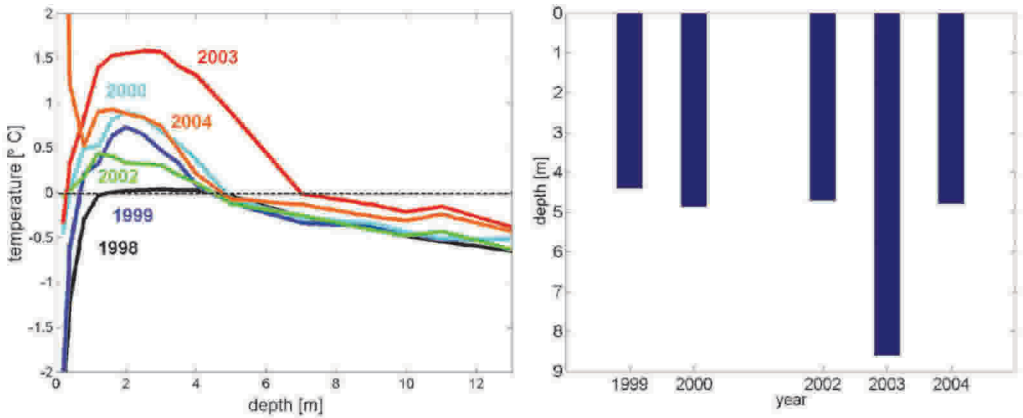


Figure 7.5: (left) Ground temperatures observed in the 14 m borehole between 1998–2004 in October and (right) evolution of the active layer depth during 1999 and 2004. No data from the summer 2001 are available.

ratures in 2003 (red line). The long-term effect of summer 2003 can be seen from the warmer than average ground temperatures in 2004 at depths below 5 m, that is the active layer thickness between 1999 and 2002.

Geophysical monitoring

In a first step the ERT monitoring approach was validated in detail on a seasonal basis during September 1999–August 2000 (Figure 7.6). Key results from this one-year data set included the following:

- Temporal resistivity changes due to freezing and thawing processes can be accurately determined using a fixed electrode array, even in high Alpine environments.
- Maximum seasonal resistivity changes were observed in autumn (September–October), before a permanent snow cover has been established, and in late spring (May–June), when the thawing snow cover and additional water from precipitation greatly decreased the resistivity values in the active layer.
- During winter, the snow cover effectively decouples the ground from atmospheric influences resulting in a gradual downward shift of the freezing front by thermal conduction.
- Resistivity-temperature relationships between the resistivity values at the borehole location and borehole temperatures show good agreement with theory. The increase of resistivity with decreasing temperature is small and linear for temperatures above the freezing point and exponential for temperatures below (cf. Figure 7.4).
- From the resistivity-temperature curves the degree of water saturation at different depths can be estimated suggesting wet conditions around 1.5 m and 4 m depth, and comparatively dry conditions around 0–1 m and 2–3 m depth.
- The calculated temporal evolution of the unfrozen water content shows a strong decrease during the winter months in the active layer and a quasi-sinusoidal behaviour below.

After the successful operation of the system during 1999–2000 a long-term geophysical monitoring at Schilthorn was started in 2002. Figure 7.8 shows the resulting tomograms for the August measurements in the years 1999–2004 (in 2001 no measurements were conducted).

In contrast to Figure 7.6 specific resistivity values of the individual measurements are shown in Figure 7.9. Red colours indicate low resistivities ($<1000 \text{ Wm}$), blue colours high resistivities ($>2500 \text{ Wm}$). Due to the heterogeneous subsurface no straightforward permafrost distribution can be inferred from one tomogram alone. The results for the different years are remarkably similar. However, analysing the resistivity changes from one year to the next a clear indication of a resistivity decrease between 2002 and 2003 can be observed.

The extraordinary resistivity decrease in summer 2003 is highlighted in Figure 7.8, where the resistivity changes of the respective August measurements are shown in percent of the reference measurement in 1999. The typical variability of specific resistivity values is around 15% (except for localised anomalies which may exceed 30%, but represent inherent system noise) and may include regions with decrease and increase within the same year, but in 2003, a strong decrease of 25%

Anomaly Index (ρ_{t+1}/ρ_t)

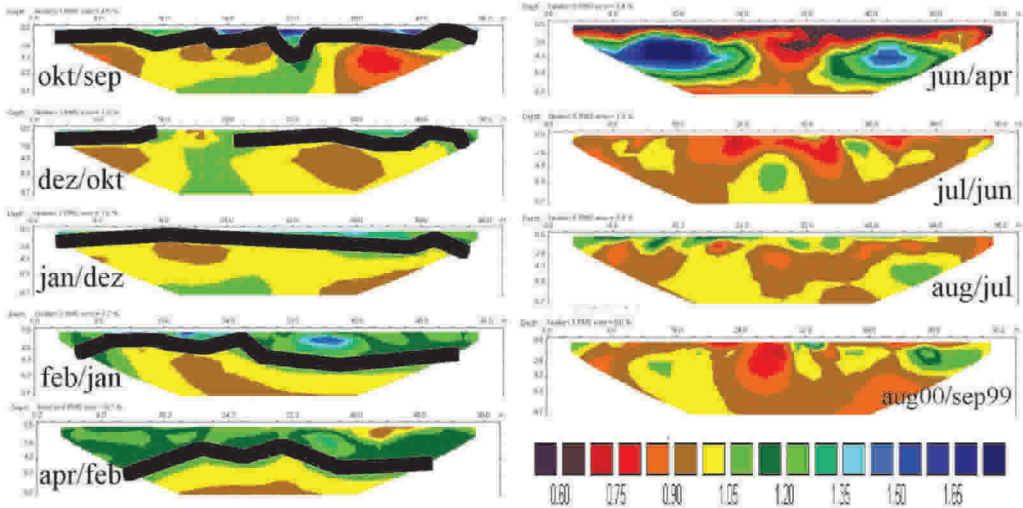


Figure 7.6: Resistivity tomograms shown as anomaly plots between consecutive resistivity measurements (ratio between resistivity r at time instances $t+1$ and t). Blue colours denote a resistivity increase corresponding to freezing, red colours denote a resistivity decrease corresponding to thawing. An anomaly index of 1 (yellow colours) denotes no change between the two measurements. The lowermost panel on the left hand side shows the cumulative change between August 2000 and September 1999 (see Hauck 2002).

on average at larger depths (1.5–8 m) was observed compared to 1999 conditions. This decrease persisted in 2004, although with a slight relative increase compared to 2003, which is shown in detail in Figure 7.9. However, this compensation is strongest in the uppermost 2 m (25% increase compared to 2003) and much smaller at greater depth indicating the strong impact of the warm temperatures on the ice content in 2003.

Figures 7.8 and 7.9 indicate that even though there is a substantial variability in the specific resistivity values from year to year in the uppermost 2 m, the values at greater depths change only slowly (except in 2003) allowing us to monitor permafrost degradation using a resistivity monitoring system. In order to quantify permafrost degradation a relation between resistivity changes and ice content changes has to be found. First approaches based on a well-known geophysical relation called Archie's Law (relating the bulk resistivity of the subsurface to the resistivity of the pore fluid, the porosity and the saturation) yield estimates of around 20% increased saturation due to melting ice (Figure 7.10). Assuming homogeneous conditions, this would result in a 10% decrease in ice content for a mean porosity of 0.5, which could serve as an upper bound for the estimation of per-

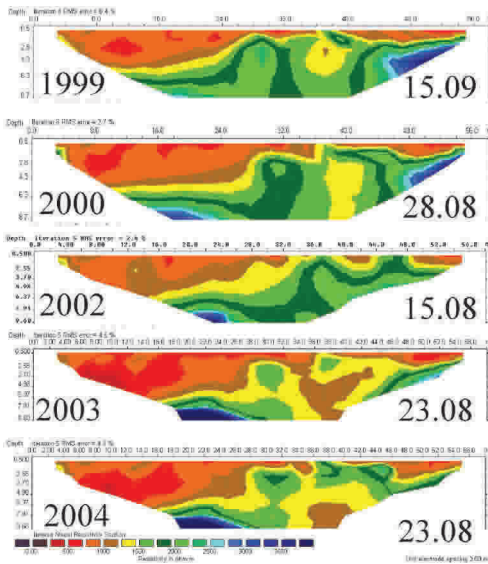


Figure 7.7: Specific resistivities after 2-dimensional inversion of the observed apparent resistivities at the Schilthorn monitoring site for the August measurements 1999–2004. No data from the year 2001 are available.

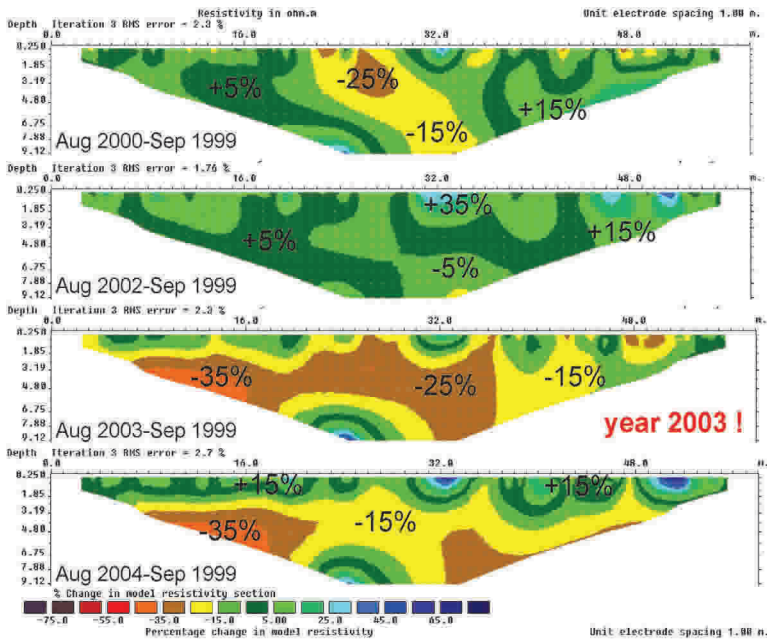


Figure 7.8: Change in specific resistivity of the August measurements compared to the reference measurement in September 1999.

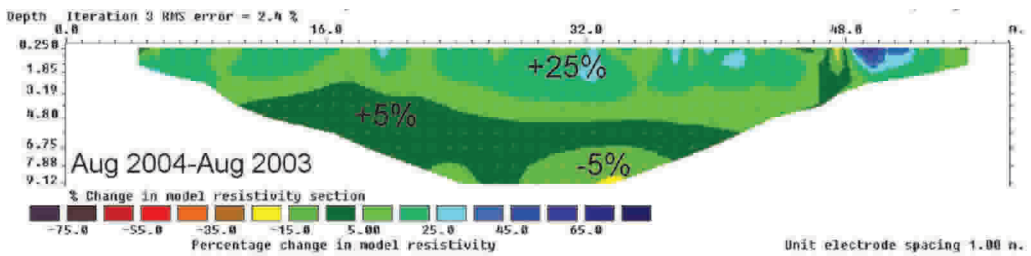


Figure 7.9: Change in specific resistivity between August 2004 and August 2003.

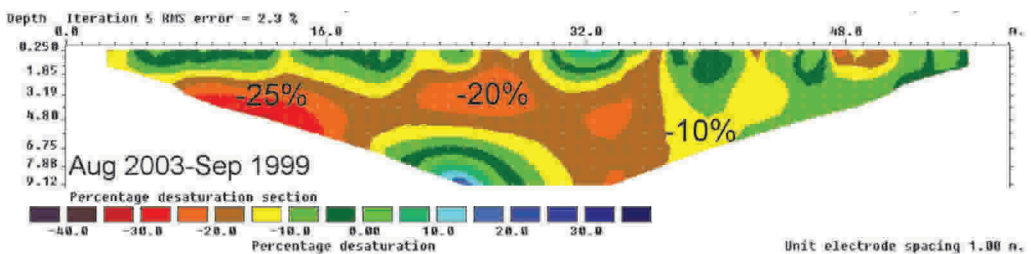


Figure 7.10: Calculated change in desaturation due to decreasing ice content. Red colours indicate an increase in saturation (calculated from Archie's Law).

mafrost degradation due to the summer 2003. However, the many uncertainties in this estimation call for a more sophisticated approach for future permafrost trend analyses.

7.2.5 Conclusion and outlook

Time-lapse resistivity measurements at a mountain permafrost site have been presented as a pilot study for long-term monitoring programmes of the permafrost evolution. Results from this pilot study showed the applicability of the geophysical monitoring system for the monitoring of freeze and thaw processes in the subsurface on time scales from days to several years. The 5-year data set from Schilthorn/Bernese Oberland showed a strong resistivity decrease in 2003 due to the exceptionally warm summer temperatures indicating significant permafrost degradation at depths down to 8 m. This degradation could not be compensated in 2004 even though observed ground temperatures were similar to the values in the years 1999–2002. Thus, resistivity measurements may add a significant parameter to the monitoring strategy of PERMOS, which is closely related to the ground ice content.

Concerning the future PERMOS-network this approach may add two important aspects to the existing monitoring strategy:

- 1 Spatial analysis of freeze and thaw processes around the borehole sites
- 2 Monitoring of the change in ice content

The first point includes the visualisation of the 2- or even 3-dimensional characteristics of the borehole sites. As boreholes represent point information without guaranteeing its representativity for the surrounding region, geophysical monitoring shows whether long-term changes observed in the boreholes are actually characteristic for a larger region. In combination with additional geophysical methods (e.g., seismics) the material composition of the subsurface (in terms of volumetric fractions of ice-, water-, air content within the pore spaces) can be assessed (Hauck et al., 2005). This information may serve as important initial condition for permafrost evolution models and climate change studies.

The second point involves monitoring the most important parameter in the context of slope instability due to climate induced permafrost degradation: the evolution of the ground ice content. The presented data for the years 1999–2004 show the great applicability of the resistivity monitoring approach for detecting changes in the subsurface ice content. Even though an exact calculation of actual ice content values was beyond the scope of this pilot study, the spatially variable change in ice content could be visualised for different years, including a rough estimation of the ice content decrease.

A future joint approach of both aspects including (1) analysing the spatial variability of subsurface characteristics at the PERMOS monitoring sites giving estimates for porosity, saturation and initial ice content and (2) monitoring the evolution of the ice content using a resistivity monitoring approach at the PERMOS sites, would yield valuable additional information to the existing PERMOS monitoring strategy.

Due to the comparatively simple installation and low costs involved we recommend installing the system at 2-5 additional PERMOS sites within the next PERMOS phase. The operational use of the system during the last 5 years showed a very robust performance, both concerning the data quality and its behaviour under severe weather and climatic conditions. Finally, the system is non-invasive (except for the installation of up to 1 m long electrodes into the ground), leading to almost no environmental disturbances at the measurement sites.

7.3 Rock fall from permafrost areas in summer 2003

7.3.1 Introduction

On July 15, 2003 around 1000 m below the Matterhorn summit at an elevation of 3500 m a.s.l. a rock fall of approximately 1000 m³ occurred. This event alerted the local mountain guides as well as public authorities of the canton Valais, which had to transport 90 climbers by helicopter and barricade the main route to the summit for several days. During summer 2003 similar events were observed at many other famous locations, e.g., the Matterhorn South Face, the Eiger North Face, the Dent Blanche, the Mönch NW-Ridge, the Piz Bernina, and the Obergabelhorn. Although rock fall is a common phenomenon in high mountains, the number of rock fall events in this summer was

exceptional throughout the Alps (e.g., Keller et al., 2003). During summer 2003 temperatures were about 3° C above the long time average in Europe (Schaer et al., 2004) and even outside the centre of the heat wave long standing temperature records were beaten (cf. Chapter 1). In the absence of unusually strong precipitation or other plausible transient effects on slope stability, the fast degradation of mountain permafrost has been hypothesized to be the likely cause for the extreme rockfall activity (Gruber et al., 2004a).

The investigation of permafrost in steep rock is still a young field of research and information on the conditions under which such instabilities develop is scarce. Rock falls that have their starting zone located in the periglacial area are inventorized and analyzed by the research group Glaciology, Geomorphodynamics, and Geochronology at the University of Zurich (J. Noetzli and L. Fischer). So far, information on more than 30 events of the summer 2003 has been collected. The thermal conditions of these detachment zones are analyzed using an energy balance model specifically designed for calculating the spatial distribution and evolution of rock temperatures in the Swiss Alps. The model has been validated using rock temperature measurements and calculates energy and heat fluxes in steep rock based on climate time series (Gruber et al., 2004b). By coupling the energy balance model to a heat conduction scheme also subsurface temperature fields in complex topography can be determined (Noetzli et al., 2007).



Photo 7: Rock fall starting zone on the Matterhorn South Face. On the left blank ice is visible below the detached material. Photos: L. Trucco

7.3.2 Permafrost and rock wall instabilities

The stability of ice-bonded discontinuities in perennally frozen rock walls is strongly influenced by the thermal regime and may be reduced due to melting of ice-filled rock joints and subsequent built up of water pressure (Haeberli et al., 1997). Additionally, it has been shown in a series of direct shear box tests that a rise in ground temperature may lead to a reduction in the shear strength of ice-bonded discontinuities and an associated reduction in the factor of safety of the slope, which could result in slope failure even while there is still ice in the joints at temperatures only little below 0 °C (Davies et al., 2001). Therefore, slope stability might be very sensitive to changes in the thermal environment, especially where unfrozen water is present in partially ice-filled bedrock fissures (Haeberli et al., 1997). Instability is expected to concentrate in warm permafrost areas, where many of the starting zones of 20th century periglacial rock fall events are located (Noetzli et al., 2003).

The thermal response of permafrost to atmospheric warming generally takes place at different time and depth scales that correlate strongly with the frequency and magnitude of a possibly resulting rock slope destabilisation (Figure 7.11). Following an increase in mean annual air temperature, with a delay of only months or years, the active layer will thicken (direct response), and thus, new volumes of rock will be subject to critical temperature ranges or thaw. The ice-water-ratio in the mountain is shifted. Since in steep rock walls a debris cover or any thicker snow cover is largely absent, rock walls are directly coupled to the atmosphere through their surface. Their immediate reaction to temperature changes, such as the 2003 summer heat wave in Europe, is confirmed by the exceptional rock fall activity of this summer: mainly near-surface events originating from enlarged active layers are documented. As a delayed response, the temperature field becomes disturbed at greater depth and the permafrost base at a depths of up to hundred metres will rise, both possibly causing large and deep-seated instabilities that are delayed by decades or centuries. For example,

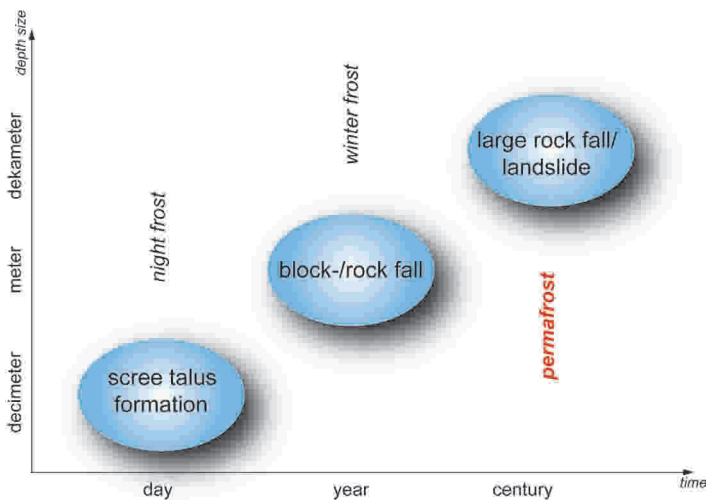


Figure 7.11: Time and depth scales of permafrost-related slope instabilities.

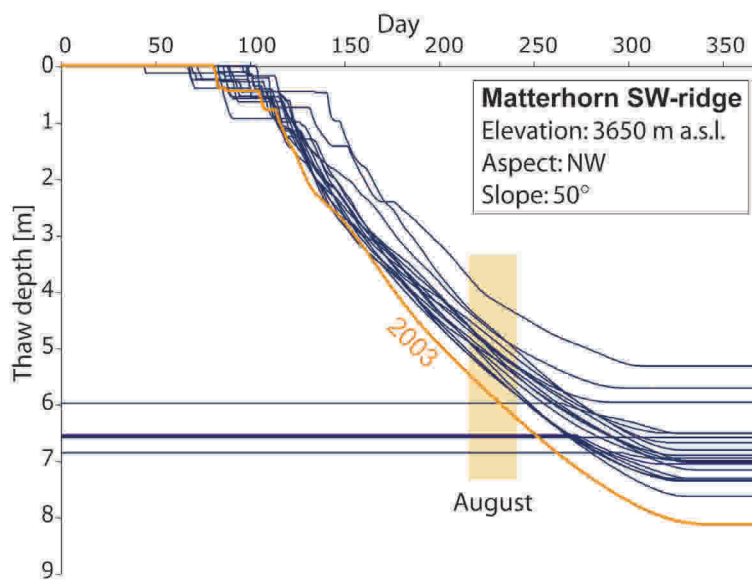


Figure 7.12: Maximum thaw depth in 2003 compared to the 20 previous year for a NW-exposed location at an elevation of 3650 m asl and a slope steepness of 50° (corresponds to the starting zone of a rock fall at the Lion ridge Matterhorn in August 2003).

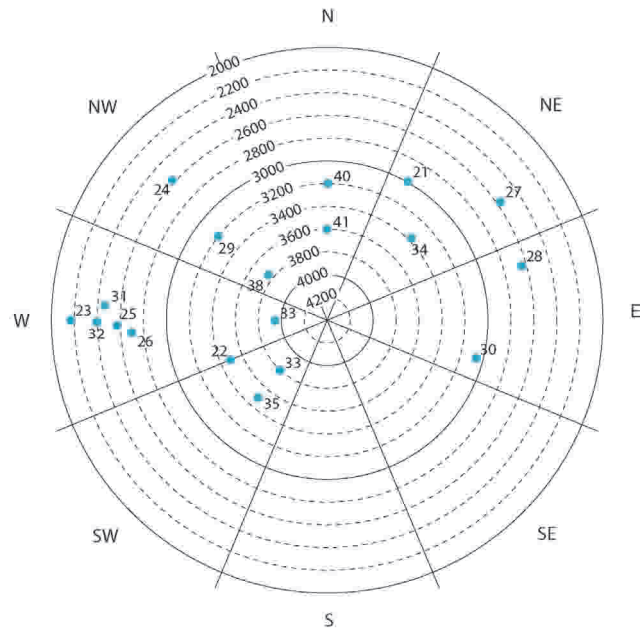


Figure 7.13: Location of around 30 rock fall starting zones of the summer 2003. A concentration in northern aspects is visible. Numbers relate the events to the database.

the Brenva Glacier rock-/ice avalanche 1997 in the Mont Blanc area is seen in relation with a long-term and deep-seated change of the thermal conditions (Deline, 2001).

7.3.3 Detachment zones of the 2003 events

Visible ice in many of the detachment zones and in locations near the lower limit of permafrost occurrence of most of the scarps confirm the relation between destabilisation and warm permafrost conditions, especially the weakness of rock/ice/water mixtures at temperatures close to the melting point. This corroborates the theory of a strong relation between warm permafrost and rock wall instability in high-mountain areas.

Modeled thaw depths of several starting zones markedly exceed maximum values for preceding years. In July and August when most of the rock fall events took place, the active layer had not reached its maximum depth, however, at this time it was about half a metre thicker (with a corresponding stronger heat flux) than in the 21 preceding – and already quite warm – years (Figure 7.12, cf. Gruber et al., 2004).

When looking at the spatial distribution of the starting zones (Figure 7.13), a clear concentration in northern aspects can be seen. Firstly, this can be explained by the greater extent of ice-containing rock faces in northern slopes. Secondly, the anomaly in 2003 is stronger in northerly aspects due to the relatively greater influence of temperature-dependent long-wave radiation on the energy balance at the rock surface compared to southern expositions, where the influence of shortwave solar radiation is more important.

7.3.4 Conclusions

To conclude, it can be stated, that the exceptional rock fall activity in summer 2003 is mainly related to the rapid and direct thermal reaction of steep and snow-free rock walls to changes in the atmosphere as well as to a considerably deeper active layer than in the already warm preceding years (Gruber et al., 2004a). The concentration in warm permafrost is obvious and confirms results from previous studies (Noetzli et al., 2003).

In view of ongoing and projected atmospheric changes and a corresponding rise in surface and subsurface temperatures, rock fall activity as well geotechnical problems in steep rock affecting infrastructure foundations, will likely become more frequent and more widespread. The events of the summer 2003 may be seen as a first sign of such a development and emphasise the importance of improving knowledge on the thermal conditions in rock walls, their changes and consequences.

Acknowledgements

PERMOS is supported financially by the Glaciological Commission of the Swiss Academy of Sciences (SCNAT), the Federal Office for Water and Geology (FOWG) and by the Swiss Agency for Environment, Forests and Landscape (SAEFL). Installation of the various PERMOS sites occurred typically within research projects of the Swiss Federal Institute of Technology (ETH through their institutes IGT and VAW), the Swiss Federal Institute for Snow and Avalanche Research (SLF/WSL), and the Universities of Berne (Geography), Fribourg (Geography), Lausanne (Geography), and Zurich (Geography).

These institutes perform all fieldwork and maintain the PERMOS sites. They therefore contribute significantly to the development of the highly valuable and essential network, which makes the Permafrost Monitoring Switzerland possible. The present report is a compilation from a number of contributors, as can be seen from the front page. In addition, there are numerous field assistants who helped to obtain the PERMOS data. We also thank the Stiftung Wasser (Essen, Germany) for financial support of fieldwork campaigns. The English was edited by C. Harris (Cardiff, UK). The Italian and Romansh summaries were translated by F. Favilli and D. Caduff, respectively. Finally, our thanks go to all who supported PERMOS in any way and enabled this report.

References

- Arenson, L.U. (2002). Unstable Alpine permafrost: a potential important natural hazard – Variations of geotechnical behaviour with time and temperature. PhD thesis, Institute for Geotechnical Engineering, ETH Zurich, 14801.
- Aschwanden, A., Beck, M., Häberli, Ch., Haller, G., Kiene, M., Roesch, A., Sie, R., and Stutz, M. (1996). Bereinigte Zeitreihen – die Ergebnisse des Projekts KLIMA90. MeteoSchweiz, Zürich.
- Barsch, D. and Zick, W. (1991). Die Bewegung des Blockgletschers Macun I von 1965-1988, Unterengadin, Graubünden. Schweizerische Zeitschrift für Geomorphologie 35(1), 1-14.
- Begert, M., Seiz, G., Schlegel, T., Musa, M., Baudraz, G., and Moesch, M. (2003). Homogenisierung von Klimamessreihen der Schweiz und Bestimmung der Normwerte 1961-1990. Schlussbericht des Projekts NORM90. MeteoSchweiz, Zürich.
- Böhm, R., Auer, I., Brunetti, M., Maugeri, M., Nanni, T., and Schöner, W. (2001). Regional temperature variability in the European Alps: 1760-1998 from homogenized instrumental time series. International Journal of Climatology 21(14), 1779-1801.
- Davies, M., Hamza, O., and Harris, C. (2001). The effect of rise in mean annual air temperature on the stability of rock slopes containing ice-filled discontinuities. Permafrost and Periglacial Processes 12, 137-144.
- Delaloye, R. and Lambiel, C. (2005). Evidence of winter ascending air circulation throughout talus slopes and rock glaciers situated in the lower belt of alpine discontinuous permafrost (Swiss Alps). Norwegian Journal of Geography 59(2), 194-203.
- Delaloye, R., Reynard, E., Lambiel, C., Marescot, L., and Monnet, R. (2003). Thermal anomaly in a cold scree slope, Creux du Van, Switzerland. Proceedings of the 8th International Conference on Permafrost, Zurich 2003, Vol. 1, 175-180.
- Deline, P. (2001). Recent Brenva rock avalanches (Valley of Aosta): New chapter in an old story? Suppl. Geografia Fisica e Dinamica Quaternaria V, 55-63.
- Frauenfelder, R. and Kääb, A. (2000). Towards a palaeoclimatic model of rock glacier formation in the Swiss Alps. Annals of Glaciology, 31, 281-286. Hauck, C. (2001). Geophysical methods for detecting permafrost in high mountains. PhD-thesis, ETH Zürich, Mitt. Versuchsanst. Wasserbau, Hydrologie u. Glaziologie der ETH Zürich 171, 204pp.
- Frauenfelder, R., Laustela, M., and Kääb, A. (2004). Velocities and relative surface ages of selected Alpine rockglaciers. In: Bezzola, G. and Semadeni, N., eds., Turbulenzen in der Geomorphologie. Jahrestagung der Schweizerischen Geomorphologischen Gesellschaft, Erstfeld. Mitteilungen der Versuchsanstalt für Wasserbau, Hydrologie und Glaziologie, ETH Zürich 184, 103-118.
- Gruber, S., Hoelzle, M., and Haeberli, W. (2004a). Permafrost thaw and destabilization of Alpine rock walls in the hot summer of 2003, Geophysical Research Letters 31, L13504, doi:10.1029/2004GL020051.
- Gruber, S., Hoelzle, M., and Haeberli, W. (2004b). Rock wall temperatures in the Alps: Modelling their topographic distribution and regional differences, Permafrost Periglacial Processes 15, 299-307.

- Haeberli, W. (1992). Construction, environmental problems and natural hazards in periglacial mountain belts. *Permafrost and Periglacial Processes* 3(2), 111-124.
- Haeberli, W., Wegmann, M., and Vonder Mühll, D. (1997). Slope stability problems related to glacier shrinkage and permafrost degradation in the Alps. *Eclogae Geologicae Helvetiae*, 90, 407-414.
- Hauck, C. (2001). Geophysical methods for detecting permafrost in high mountains. PhD-thesis, ETH Zürich, Mitt. Versuchsanst. Wasserbau, Hydrologie u. Glaziologie der ETH Zürich 171: 204pp.
- Hauck, C. (2002). Frozen ground monitoring using DC resistivity tomography. *Geophysical Research Letters* 29 (21), 2016, doi: 10.1029/2002GL014995.
- Hauck, C., Vonder Mühll, D., and Maurer, H. (2003). Using DC resistivity tomography to detect and characterise mountain permafrost. *Geophysical Prospecting* 51, 273-284.
- Hauck, C., Böttcher, M., and Kottmeier, C. (2005). Modellierung von 4-Phasen Gemischen in gefrorenem Untergrund auf der Basis von Geoelektrik und Seismik. *Proceedings 65. Jahrestagung der Deutschen Geophysikalischen Gesellschaft (DGG)*, Graz, Austria, 47-48.
- Hoekstra P., P.V. Sellmann, and Delaney, A. (1975). Ground and airborne resistivity surveys of permafrost near Fairbanks, Alaska.- *Geophysics* 40, 641-656.
- Kääb, A. (1998). Oberflächenkinematik ausgewählter Blockgletscher des Oberengadins, Beiträge aus der Gebirgs-Geomorphologie. *Jahrestagung 1997 der Schweizerischen Geomorphologischen Gesellschaft. Mitteilungen der Versuchsanstalt für Wasserbau, Hydrologie und Glaziologie der ETH Zürich*, Zürich 158, 121-140.
- Kääb, A. (2000). Photogrammetry for early recognition of high mountain hazards: new techniques and applications. *Physics and Chemistry of the Earth, Part B* 25(9), 765-770.
- Kääb, A. (2005). Remote sensing of mountain glaciers and permafrost creep. *Research perspectives from earth observation technologies and geoinformatics. Schriftenreihe Physische Geographie. Glaziologie und Geomorphodynamik* 48, University of Zurich, 264 pp.
- Kääb, A., Haeberli, W., and Gudmundsson, G.H. (1997). Analysing the creep of mountain permafrost using high precision aerial photogrammetry: 25 years of monitoring Gruben rock glacier, Swiss Alps. *Permafrost and Periglacial Processes* 8(4), 409-426.
- Kääb, A., Kaufmann, V., Ladstädter, R., and Eiken, T. (2003). Rock glacier dynamics: implications from high-resolution measurements of surface velocity fields. *Proceedings, Eighth International Conference on Permafrost 1, Zurich, Balkema*, 501-506.
- Kääb, A., Huggel, C., and Fischer, L. (2005a). Remote sensing of glacier- and permafrost-related hazards in high mountains: an overview. *Natural Hazards and Earth System Sciences* 5, 527-554.
- Kääb, A., Reynolds, J.M., and Haeberli, W. (2005b). Glacier and permafrost hazards in high mountains. In: Huber, U.M., Bugmann, H.K.M. and Reasoner, M.A., eds., *Global Change and Mountain Regions (A State of Knowledge Overview)*. *Advances in Global Change Research*, Springer, Dordrecht, 225-234.
- Kääb, A. and Vollmer, M. (2000). Surface geometry, thickness changes and flow fields on creeping mountain permafrost: automatic extraction by digital image analysis. *Permafrost and Periglacial Processes* 11(4), 315-326.

- Kääb, A., Frauenfelder, R., and Roer, I. (2007). On the response of rockglacier creep to surface temperature increase. *Global and Planetary Change* 56, 172-187.
- Kaufmann, V. (1998). Geomorphometric monitoring of active rock glaciers in the Austrian Alp. *Proceedings, 4th International Symposium on High-Mountain Remote Sensing Cartography*, Karlstadt, Sweden, 97-113.
- Kaufmann, V. and Ladstädter, R. (2002). Spatio-temporal analysis of the dynamic behaviour of the Hohebenkar rock glaciers (Oetzal Alps, Austria) by means of digital photogrammetric methods. *Grazer Schriften der Geographie und Raumforschung* 37, 119-140.
- Keller, F. (2003). Kurzbericht ueber die Steinschlagereignisse im heissen Sommer 2003 im Bergell (Project report on rock fall 2003 to the Kanton Graubunden), report, Institut fuer Tourismus und Landschaft, Academia Engiadina, Samedan, Switzerland, 332-336.
- King M.S., R.W. Zimmerman, and Corwin, R.F. (1988). Seismic and electrical properties of unconsolidated permafrost. *Geophysical Prospecting* 36, 349-364.
- Lambiel, C. (2005). Rock glacier acceleration: a case study in the Mont Gelé area (Swiss Alps). *Proceedings, 2nd European Conference on Permafrost*, Potsdam, Germany, Terra Nostra, GeoUnion Alfred-Wegener-Stiftung, Berlin, 2005/2, 98.
- Lambiel, C. and Delaloye, R. (2004). Contribution of real-time kinematic GPS in the study of creeping mountain permafrost: examples from the Western Swiss Alps. *Permafrost and Periglacial Processes* 15(3), 229-241.
- Loke, M.H. and Barker, R.D. (1995). Least-squares deconvolution of apparent resistivity. *Geophysics* 60, 1682-1690.
- Marescot, L., Loke, M. H., Chapellier, D., Delaloye, R., Lambiel, C., and Reynard, E. (2003). Assessing reliability of 2D resistivity imaging in permafrost and rock glacier studies using the depth of investigation index method. *Near Surface Geophysics* 1(2), 57-67.
- MeteoSwiss (2002). *Witterungsberichte, Jahr 2002*. MeteoSwiss, 69 pp.
- MeteoSwiss (2003). *Witterungsberichte, Jahr 2003*. MeteoSwiss, 71 pp.
- MeteoSwiss (2004). *Witterungsberichte, Jahr 2004*. MeteoSwiss, 69 pp.
- McCarthy, J.J., Canziani, O.F., Leary, N.A., Dokken, D.J., and White, K.S. (Editors), 2001. *Contribution of Working Group II to the Third Assessment Report of the Intergovernmental Panel on Climate Change (IPCC)*. Cambridge University Press, UK, 1000 pp.
- Noetzli, J., Hoelzle, M., and Haeberli, W. (2003). Mountain permafrost and recent Alpine rock-fall events: a GIS-based approach to determine critical factors. In: Phillips M., Springman S. and Arenson L. (eds.), *8th International Conference on Permafrost, Proceedings, 2*, Zurich. Swets & Zeitlinger, Lisse, 827-832.
- Noetzli, J., Gruber, S., Kohl, T., Salzmann, N., and Haeberli, W. 2007. Three-dimensional distribution and evolution of permafrost temperatures in idealized high-mountain topography. *Journal of Geophysical Research* 112, F02S13, doi:10.1029/2006JF000545.
- Perruchoud, E. and Delaloye, R. (2005). Surveying the (seasonal) variations in rock glacier activity using GPS technique (western Swiss Alps). *Proceedings, 2nd European Conference on Permafrost*, Potsdam, Germany, Terra Nostra, GeoUnion Alfred-Wegener-Stiftung, Berlin, 2005/2, 99-100.

- Reynard, E., Delaloye, R., and Lambiel, C. (1999). Prospection géoélectrique du pergélisol alpin dans le massif des Diablerets (VD) et au Mont Gelé (Nendaz, VS), Bull. La Murithienne 117, 89-103.
- Roer, I. (2005). Rockglacier kinematics in a high mountain geosystem. PhD thesis, Department of Geography, Rheinische Friedrich-Wilhelms-Universität Bonn, 217 pp.
- Roer, I., Avian, M., and Delaloye, R. (2005a). Rockglacier «speed-up» throughout European Alps – a climatic signal? Proceedings, 2nd European Conference on Permafrost, Potsdam, Germany, Terra Nostra, GeoUnion Alfred-Wegener-Stiftung, Berlin, 2005/2, 99-100.
- Roer, I., Kääb, A., and Dikau, R. (2005b). Rockglacier acceleration in the Turtmann valley (Swiss Alps) - probable controls. Norwegian Journal of Geography 59(2), 157-163.
- Roer, I., Kääb, A., and Dikau, R. (2005c). Rockglacier kinematics derived from small-scale aerial photography and digital airborne pushbroom imagery. Zeitschrift für Geomorphologie 49(1), 73-87.
- Schaer, C., Vidale, P. L., and Luethi, D. (2004). The role of increasing temperature variability in European summer heatwaves, Nature 427, 332–336.
- Schneider, B. and Schneider, H. (2001). Zur 60-jährigen Messreihe der kurzfristigen Geschwindigkeitsschwankungen am Blockgletscher im Äusseren Hochebenkar, Ötztaler Alpen, Tirol. Zeitschrift für Gletscherkunde und Glazialgeologie 37(1), 1-33.
- Schudel, L. (2003). Permafrost Monitoring auf dem Schilthorn mit geophysikalischen Methoden und meteorologischen Daten. Diplomarbeit Institut für Physische Geographie, Universität Zürich.
- Strozzi, T., Kääb, A., and Frauenfelder, R. (2004). Detecting and quantifying mountain permafrost creep from in-situ, airborne and spaceborne remote sensing methods. International Journal of Remote Sensing 25(15), 2919-2931.
- Völsch, I. (2004). Untersuchung und Modellierung kleinräumiger Unterschiede im Verhalten von Gebirgspermafrost. Diplomarbeit Departement Erdwissenschaften, ETH Zürich.
- WMO (2002). WMO Statement on the status of the global climate in 2002, WMO-no. 949.
- WMO (2003). WMO Statement on the status of the global climate in 2003, WMO-no. 966.
- WMO (2004). WMO Statement on the status of the global climate in 2004, WMO-no. 983.
- Zick, W. (1996). Bewegungsmessungen 1965–1994 am Blockgletscher Macun I (Unterengadin/Schweiz) – neue Ergebnisse. Zeitschrift für Geomorphologie N.F., Supplement-Band 104, 59-71.

Appendix

Boreholes

• Jungfrauoch N/95 and S/95	p. 62
• Schilthorn 51/98, 50/00, and 52/00	p. 66
• Flüela 1/02	p. 70
• Muot da Barba Peider B1/96 and B2/96	p. 72
• Muragl 1/99, 2/99, 3/99, and 4/99	p. 76
• Murtèl-Corvatsch 1/87, 2/87, 1/00, and 2/00	p. 82
• Schafberg-Pontresina 1/90 and 2/90	p. 84
• Arolla, Mt. Dolin B1/96 and B2/96	p. 86
• Emshorn 4/96, 5/96, and 6/96	p. 90
• Gentianes 1/02	p. 92
• Grächen 1/02 and 2/02	p. 94
• Lapires 1/98	p. 96
• Randa Wisse-Schijen 1/98, 2/98, and 3/98	p. 98
• Stockhorn 60/00 and 61/00	p. 102
• Tsaté 1/04	p. 106

Jungfrauoch N/95 and S/95

Site

Description	North/South face of Jungfrau Ostgrat
Coordinates	N: 641000/155120, S: 640990/155050
Elevation [m a.s.l.]	N: 3590, S: 3580
Slope angle [°]	N: ca. 55°, S: ca. 50°
Slope aspect	N: ca. 5° E, S: ca. 135° E
Morphology	Rock wall
Lithology	Gneiss
MAAT	-7.9 °C
Vegetation	No vegetation

Borehole

Drilling date	1995
Depth [m]	N: 21, S: 20
Chain length [m]	N: 21, S: 20
Thermistor depth [m]	N: 2.7, 6.7, 9.7, 10.7, 11.7, 15.7, 16.7, 20.2 S: 1.2, 5.2, 8.2, 11.2, 14.2, 16.2, 17.7, 18.7
Thermistor type	NTC Thermistor, Model 111-103-EAJ-H01 (Fenwal Electronics)
Last calibration	1995

Responsible

SLF, M. Phillips

Other measurements

Deformation measurement (1995-2003)

Comments

Boreholes are not vertical; they are drilled outwards from the inner-tunnel.

Available data

Since 1995

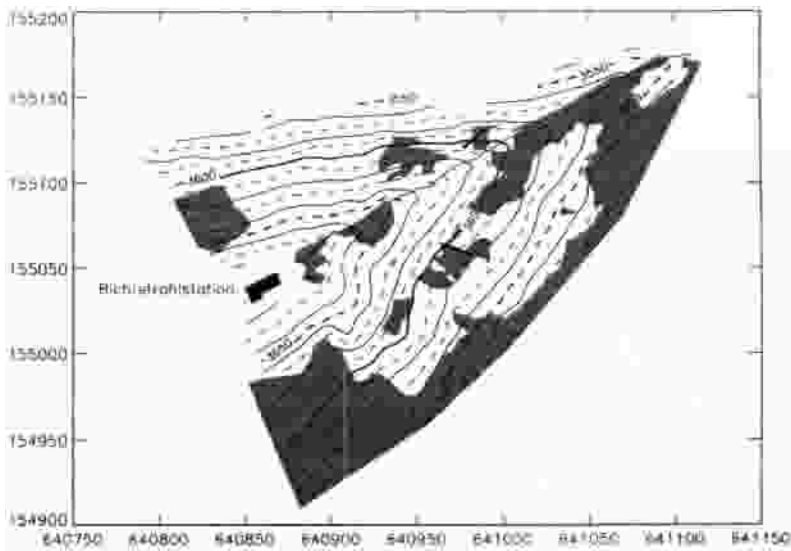


Fig. A.1: Situation at the Jungfrau East ridge. Snowpatches and glacier boundaries are drawn in grey, the ridge, the Richtstrahlstation and the two boreholes are also displayed. From Wegman (1998).

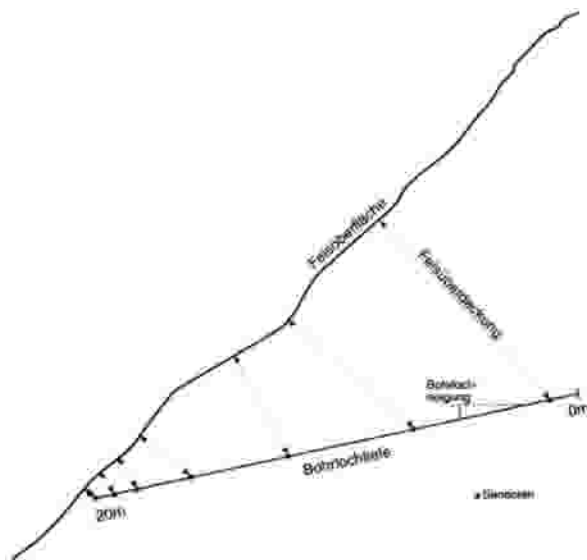


Fig. A.2: The borehole depth is measured from the inside of the Jungfrau East ridge. From Wegmann (1998) .

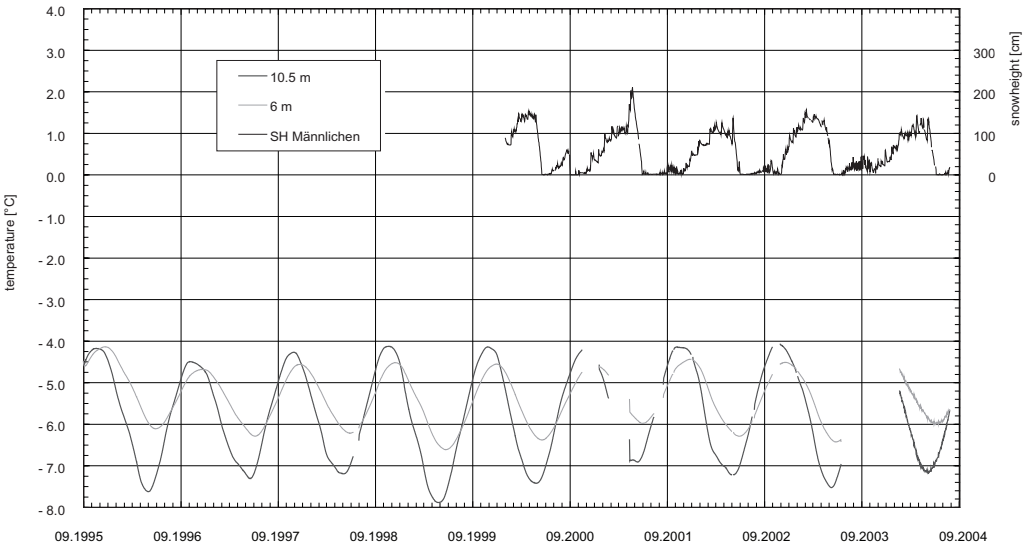


Fig. A.3: Temperature-time-plot of the borehole Jungfrauoch N/95 for the thermistors at 6 and 10.5 m depth. Additionally, the snow height on Männlichen is displayed.

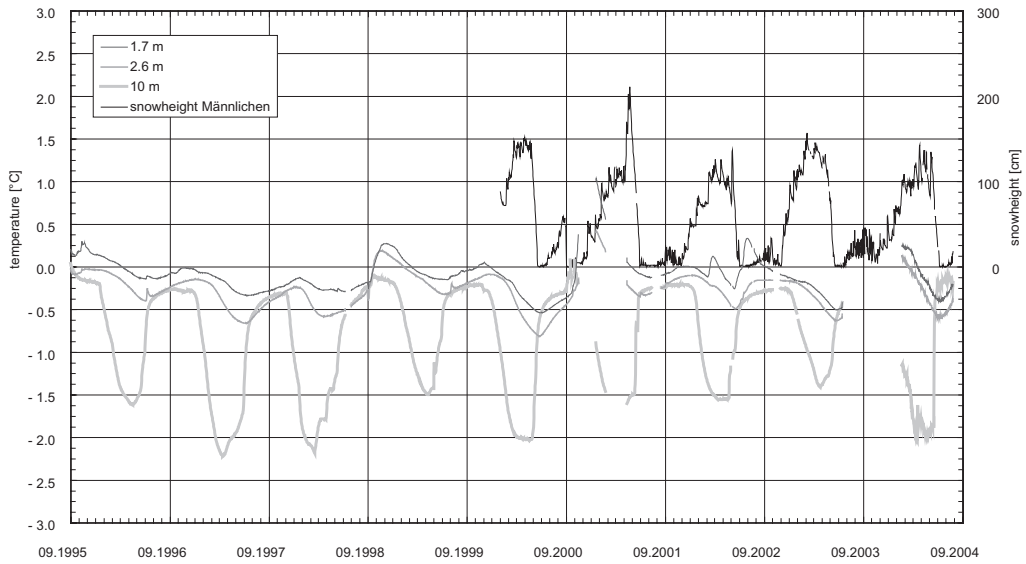


Fig. A.4: Temperature-time-plot of the borehole Jungfrauoch S/95 for the thermistors at 1.7, 2.6, and 10.0 m depth. Additionally, the snow height on Männlichen is displayed.

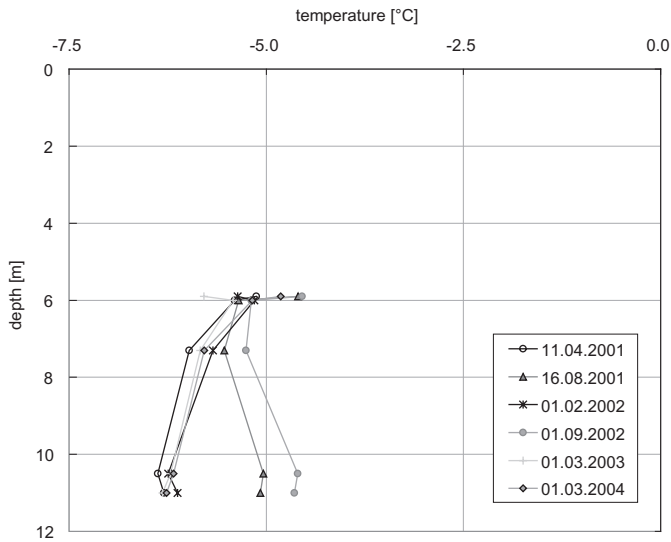


Fig. A.5:

Temperature profile Jungfrau-joch N/95. This borehole was drilled from the tunnel (11 m depth) without reaching the surface (0 m). Two sensors (at 6.3 m and 8.7 m) showed a large drift of about 2 °C between 1996 and 1998 and are therefore omitted in this plot. The increasing temperature amplitude towards depth indicates the influence of the tunnel temperature.

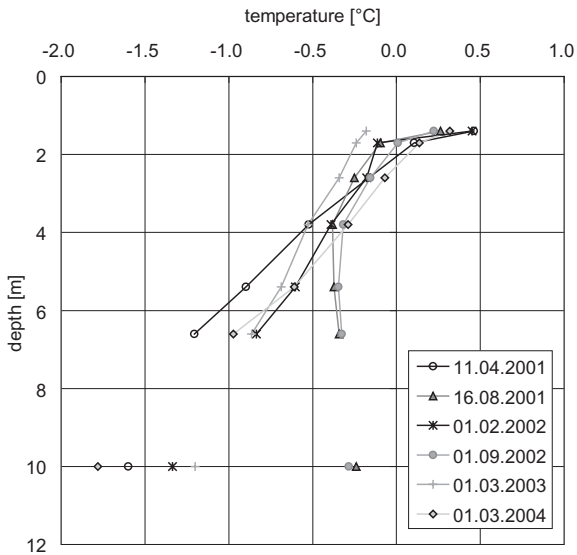


Fig. A.6:

Temperature profile Jungfrau-joch S/95. This borehole was drilled from the tunnel (at 10 m depth) reaching the surface (0 m). Similarly to borehole N/95, temperature amplitude increases towards depth indicating the influence of the tunnel temperature.

Schilthorn 51/98, 50/00, and 52/00

Site

Description	North-east face of Schilthorn, Lauterbrunnental, BE
Coordinates	51/98: 630365/156410, 50/00: 630350/156410, 52/00: 630350/156410
Elevation [m a.s.l.]	51/98: 2909, 50/00: 2910, 52/00: 2910
Slope angle [°]	30
Slope aspect	NE
Morphology	Slope beneath summit
Lithology	Limestone schists
MAAT/Precipitation	-4.3 °C / 2700 mm
Vegetation	No vegetation

Borehole

Drilling date	51/98: 14.10.1998, 50/00 and 52/00: 8.2000
Depth [m]	51/98: 14 m , 50/00: 101.0 m, 52/00: 100.0 m
Chain length [m]	51/98: 13.7 m, 50/00: 100.0 m, 52/00: 100.0 (installed down to 92.0)
Thermistor depth [m]	51/98: 0.2, 0.4, 0.8, 1.2, 1.6, 2.0, 2.5, 3.0, 3.5, 4.0, 5.0, 7.0, 9.0, 10.0, 11.0, 13.0, 13.7 50/00: 0.2, 0.4, 0.8, 1.2, 1.6, 2.0, 2.5, 3.0, 3.5, 4.0, 5.0, 7.0, 9.0, 10.0, 11.0, 13.0, 15.0, 20.0, 25.0, 30.0, 40.0, 50.0, 60.0, 70.0, 80.0, 85.0, 90.0, 95.0, 97.5, 100.0 52/00: 0.0, 1.0, 2.0, 3.0, 5.0, 7.0, 12.0, 17.0, 22.0, 32.0, 42.0, 52.0, 62.0, 72.0, 77.0, 82.0, 87.0, 89.5, 92.0
Thermistor type	NTC-YSI 440006
Last calibration	51/98: 1998, 50/00: 1999, 52/00: 1999

Meteostation

Installation date	10.1998
Sensors	Air temperature, relative humidity, net radiation, snow-depth, wind speed, wind direction

Responsible

GIUZ, M. Hoelzle

Other measurements

BTS/GST, energy balance

Comments

Temperate (warm) permafrost

Available data

Since 1998 (with some gaps)

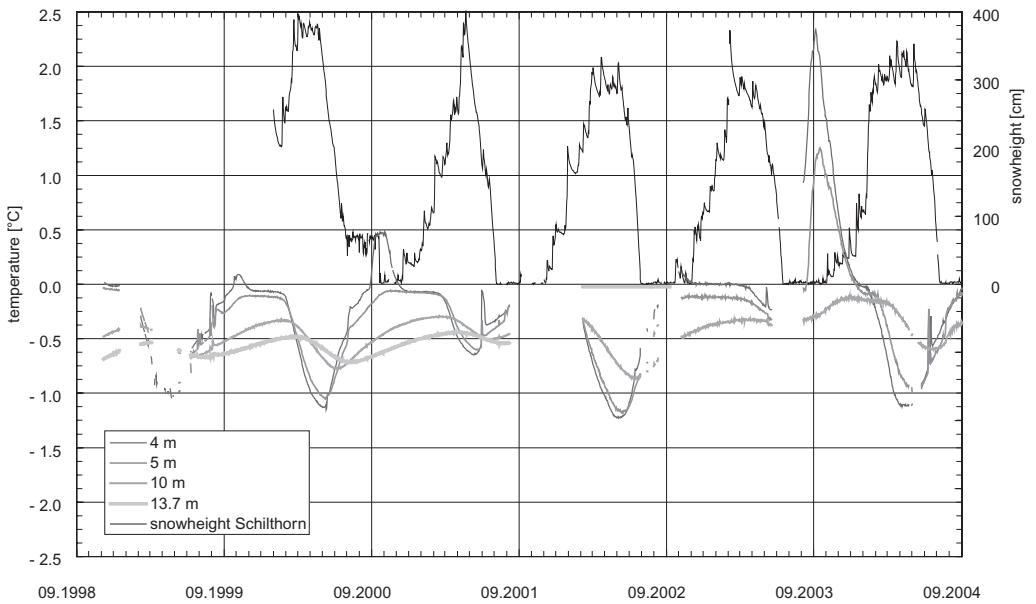


Fig. A.7: Temperature-time-plot of the borehole Schilthorn 51/98 for the thermistors at 4.0, 5.0, 10.0, and 13.7 m depth. Additionally, the snow height on Schilthorn is displayed.

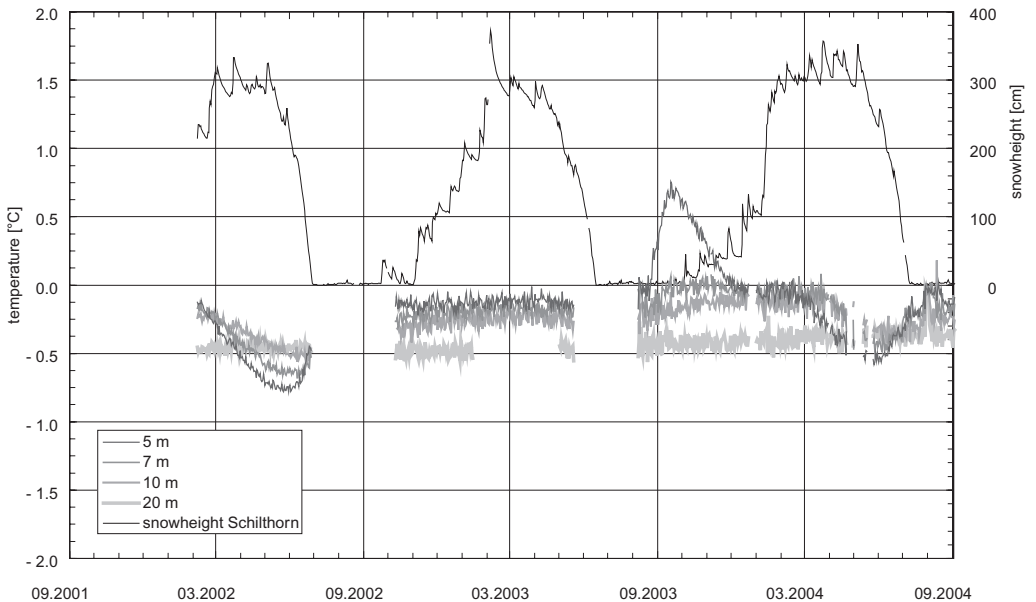


Fig. A.8: Temperature-time-plot of the borehole Schilthorn 50/00 for the thermistors at 5.0, 7.0, 10.0, and 20.0 m depth. Additionally, the snow height on Schilthorn is displayed.

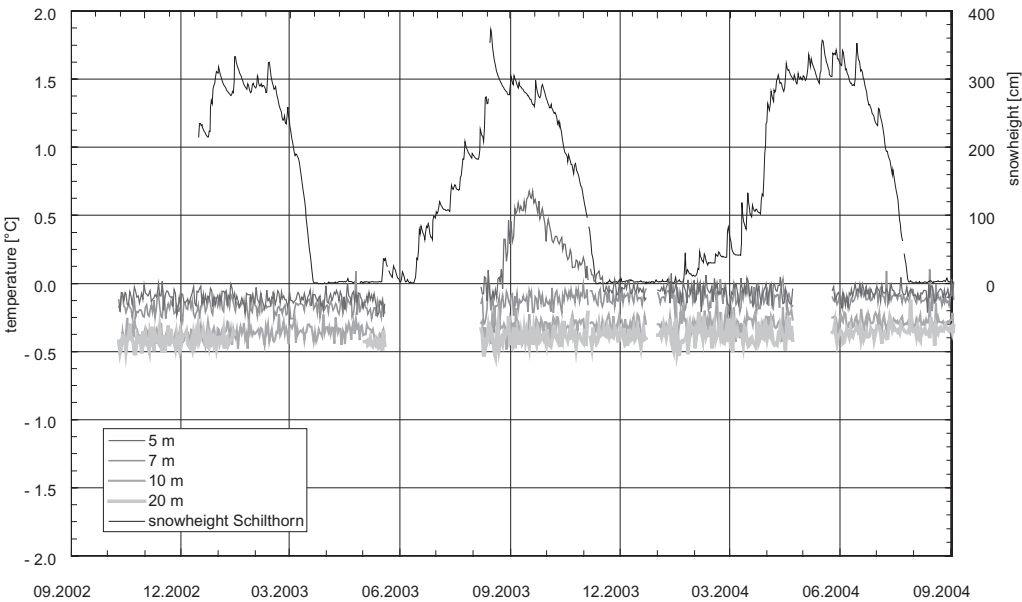


Fig. A.9: Temperature-time-plot of the borehole Schilthorn 52/00 for the thermistors at 5.0, 7.0, 10.0, and 20.0 m depth. Additionally, the snow height on Schilthorn is displayed.

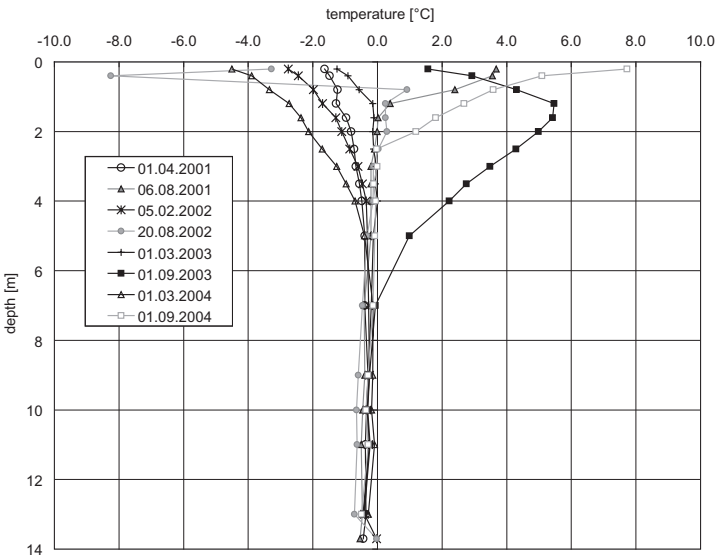


Fig. A.10: Temperature profiles for Schilthorn 51/98.

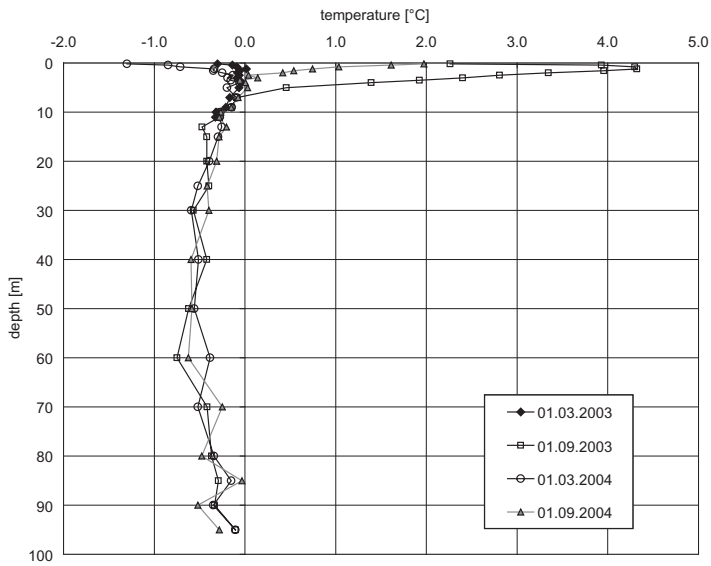


Fig. A.11: Temperature profiles for Schilthorn 50/00.

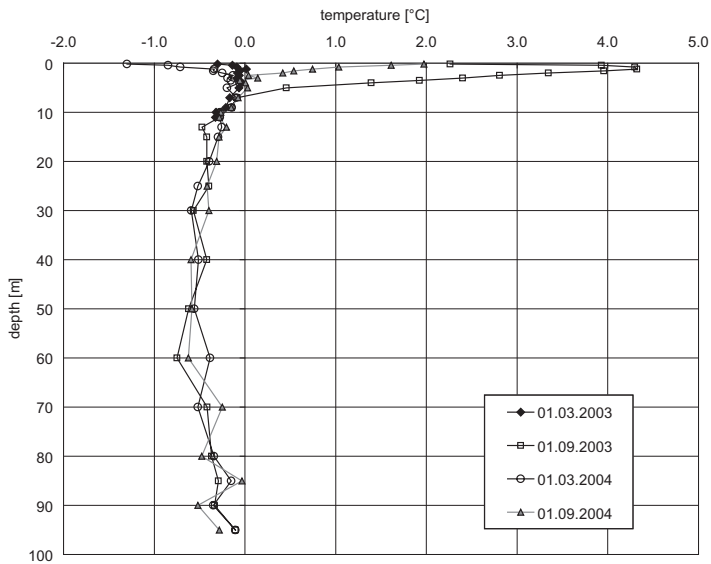


Fig. A.12: Temperature profiles for Schilthorn 52/00.

Flüela 1/02

Site

Description	Flüelapass Schottensee, GR
Coordinates	791375/180575
Elevation [m a.s.l.]	2394
Slope angle [°]	26
Slope aspect	NE
Morphology	Scree slope, slope base
Lithology	Amphibolit, paragneiss
MAAT/Precipitation	–
Vegetation	No vegetation

Borehole

Drilling date	19.8.2002
Depth [m]	23
Chain length [m]	20
Thermistor depths [m]	0.25, 0.5, 1.0, 1.5, 2.0, 3.0, 4.0, 6.0, 8.0, 10.0, 15.0, 20.0
Thermistor type	YSI 46006 + Campbell CR10X
Last calibration	1.10.2002

Responsible SLE, M. Phillips

Other measurements –

Comments –

Available data Since 2002

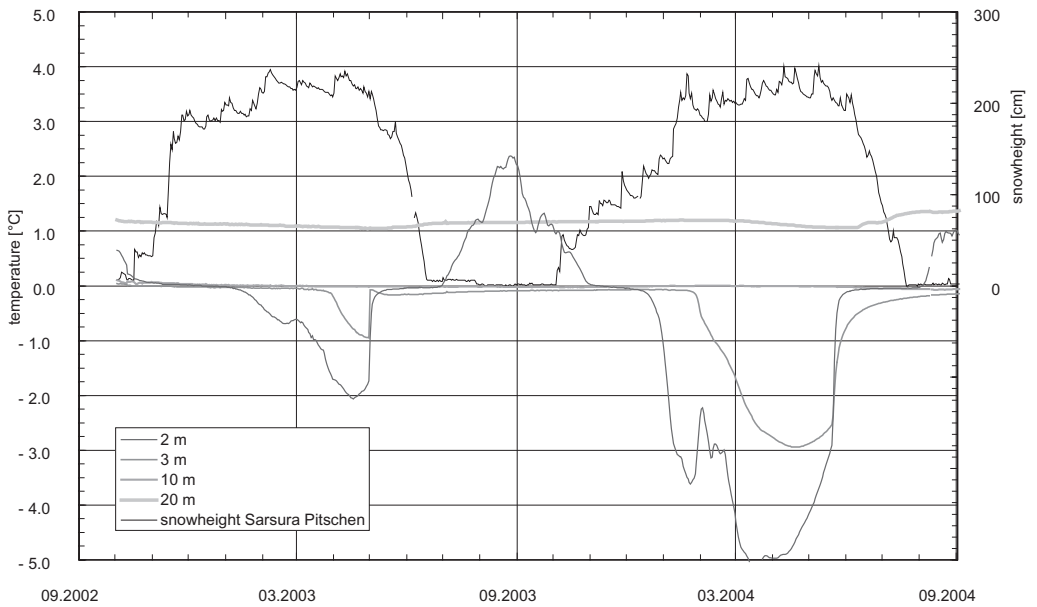


Fig. A.13: Temperature-time-plot of the borehole Flüela 1/02 for the thermistors at 2.0, 3.0, 10.0, and 20.0 m depth. Additionally, the snow height on Sarsura Pitschen is displayed.

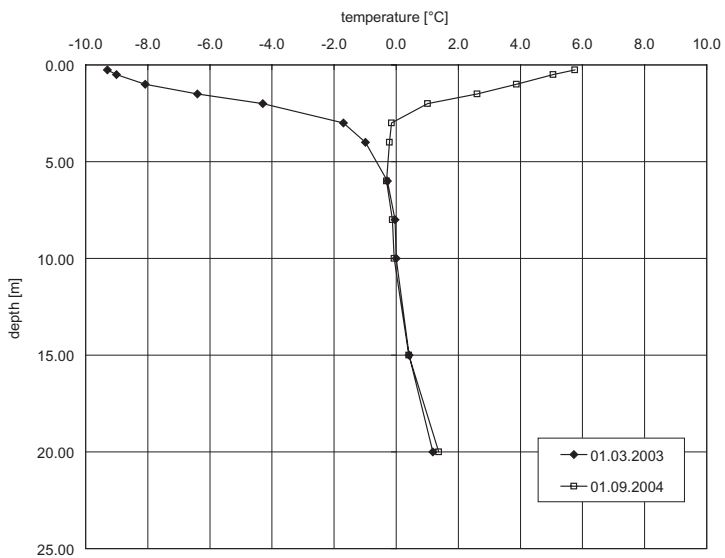


Fig. A.14: Temperature profiles for Flüela 1/02.

Muot da Barba Peider B1/96 and B2/96

Site

Description	Schafberg-Pontresina (Muot da Barba Peider), Upper Engadine, GR
Coordinates	B1/96: 791300/152500; B2/96: 791300/152500
Elevation [m a.s.l.]	B1/96: 2946; B2/96: 2941
Slope angle [°]	38
Slope aspect	NW
Morphology	Scree slope
Lithology	Gneiss
MAAT/Precipitation	-4.5 °C / 2000 mm
Vegetation	No vegetation

Borehole

Drilling date	1996
Depth [m]	18
Chain length [m]	17.5
Thermistor depths [m]	0.5, 1.0, 2.0, 3.0, 4.0, 6.0, 8.0, 10.0, 13.5, 17.5
Thermistor type	YSI 46008 + Campbell CR10X 1996
Last calibration	1996

Meteostation

Installation date	1996
Sensors	Air temperature (UTL), radiation, snow-surface, wind speed/direction

Responsible

SLE, M. Phillips

Other measurements

BTS/GST

Comments

Snow nets at B1/96, no snow nets at B2/96

Available data

Since 1996

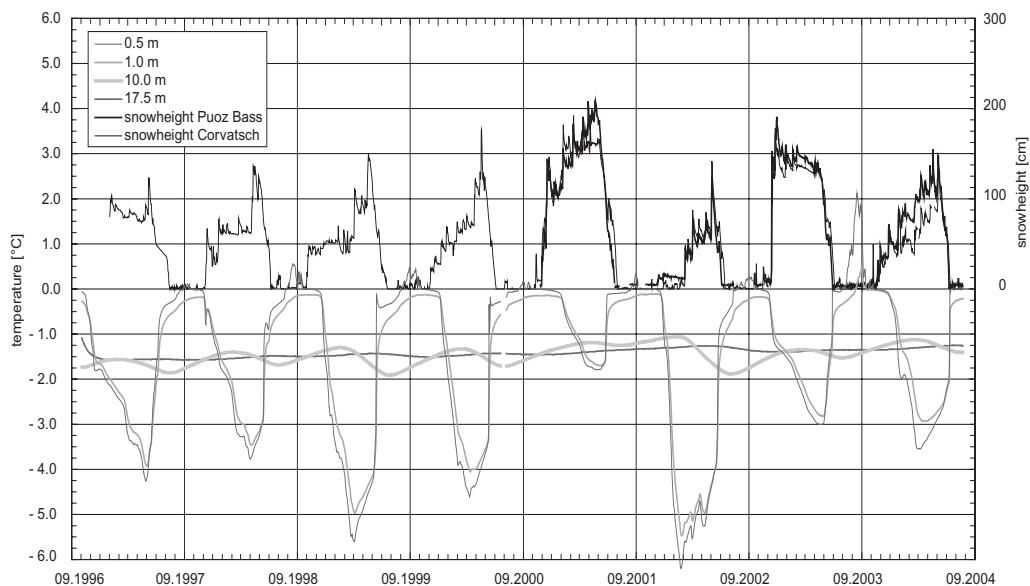


Fig. A.15: *Temperature-time-plot of the borehole Mout da Barba Peider B1/96 for the thermistors at 0.5, 1.0, 10.0, and 17.5 m depth. Additionally, the snow height at Puoz Bass and Corvatsch is displayed.*

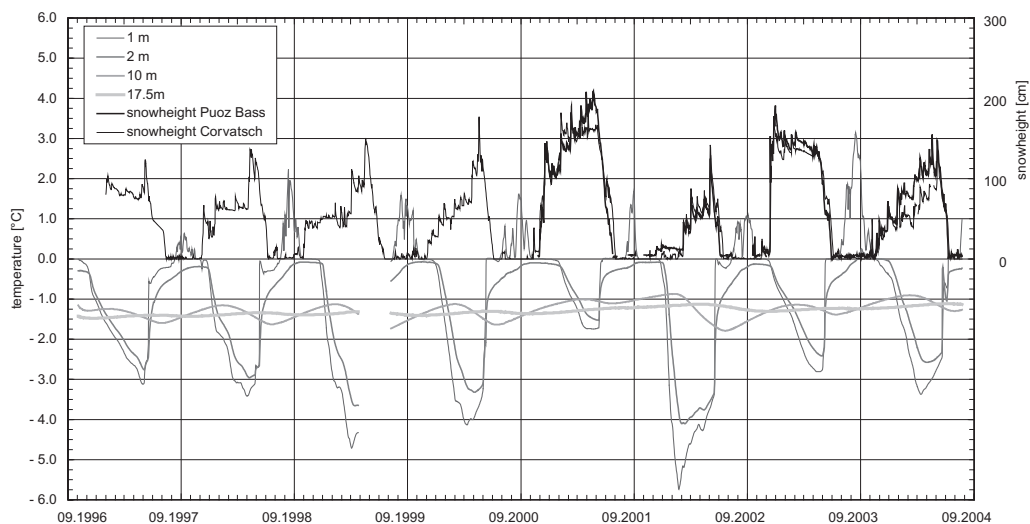


Fig. A.16: *Temperature-time-plot of the borehole Mout da Barba Peider B2/96 for the thermistors at 1.0, 2.0, 10.0, and 13.7 m depth. Additionally, the snow height at Puoz Bass and Corvatsch is displayed.*

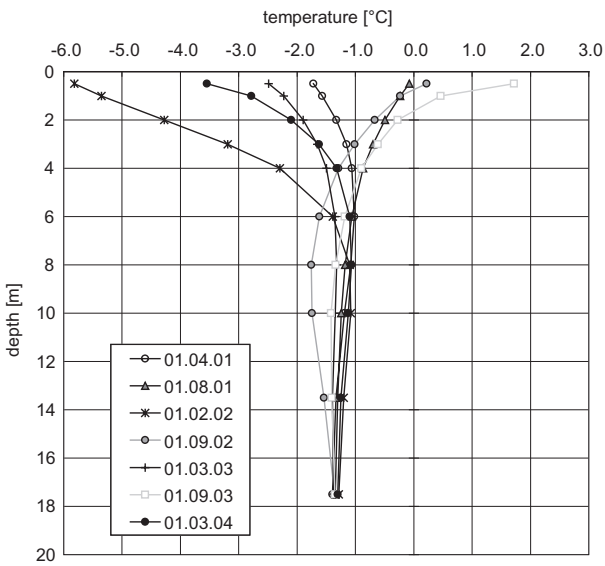


Fig. A.17: Temperature profiles for Muot da Barba Peider B1/96.

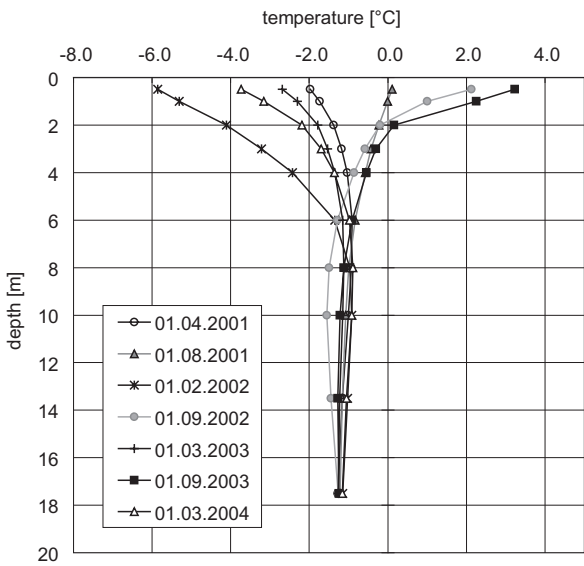


Fig. A.18: Temperature profiles for Muot da Barba Peider B2/96.

Muragl 1/99, 2/99, 3/99, and 4/99

Site

Description	Active rock glacier in the Muragl Valley with a pronounced curvature in the flow. Approx. 45 min from Muottas Muragl.
Coordinates	1/99: 791025/153726, 2/99: 790989/153687 3/99: 791038/153679, 4/99: 791017/153688
Elevation [m a.s.l.]	1/99: 2536.1, 2/99: 2538.5 3/99: 2558.2, 4/99: 2549.2
Slope angle [°]	1/99: 15°, 2/99: 5°, 3/99: 15°, 4/99: 15°
Slope aspect	1/99: W, 3/99: SW, 4/99: SW
Morphology	Active rockglacier
Lithology	Albit-Muskowit schists
MAAT/Precipitation	-2.2 °C / 2000 mm
Vegetation	No vegetation

Borehole

Drilling date	May, June 1999
Depth [m]	1/99: 70.2, 2/99: 64.0 3/99: 72.0, 4/99: 71.0
Chain length [m]	1/99: 69.7, 2/99: 59.7 3/99: 69.6, 4/99: 69.6
Thermistor depths [m]	1/99: 0.0, 0.2, 0.8, 1.4, 2.0, 3.0, 4.0, 5.0, 7.0, 9.0, 11.0, 14.0, 19.0, 24.0, 29.0, 39.0, 54.0, 69.0 2/99: 0.0, 0.1, 0.5, 0.9, 1.3, 1.7, 2.2, 2.7, 3.7, 4.7, 5.7, 7.7, 9.7, 11.7, 13.7, 15.7, 19.7, 24.7, 29.7, 34.7, 39.7, 59.7, 59.7 3/99: 0.0, 0.4, 0.8, 1.2, 1.6, 2.1, 2.6, 3.6, 4.6, 5.6, 7.6, 9.6, 11.6, 13.6, 15.6, 17.6, 19.6, 24.6, 29.6, 34.6, 39.6, 49.6, 59.6, 69.6 4/99: 0.0, 0.4, 0.8, 1.2, 1.6, 2.1, 2.6, 3.6, 4.6, 5.6, 7.6, 9.6, 11.6, 13.6, 15.6, 19.6, 24.6, 29.6, 34.6, 39.6, 59.6, 69.6
Thermistor type	YSI 44006
Last calibration	05.999

Responsible IGT-ETH, L. Arenson, S.M. Springman

Other measurements BTS/GST

Comments –

Available data 1/99: 10.99–04.00, 09.02–, 2/99: 11.00–
3/99: 10.99–04.00, 09.02–, 4/99: 10.99–04.00, 09.02–

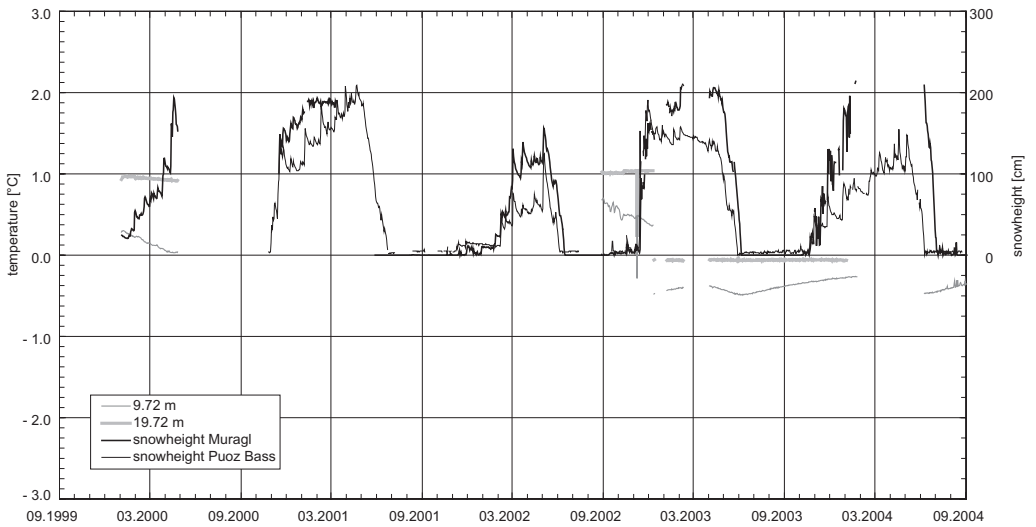


Fig. A.19: Temperature-time-plot of the borehole Muragl 1/99 for the thermistors at 9.72 and 19.72 m depth. Additionally, the snow height at Puoz Bass and Muragl is displayed.

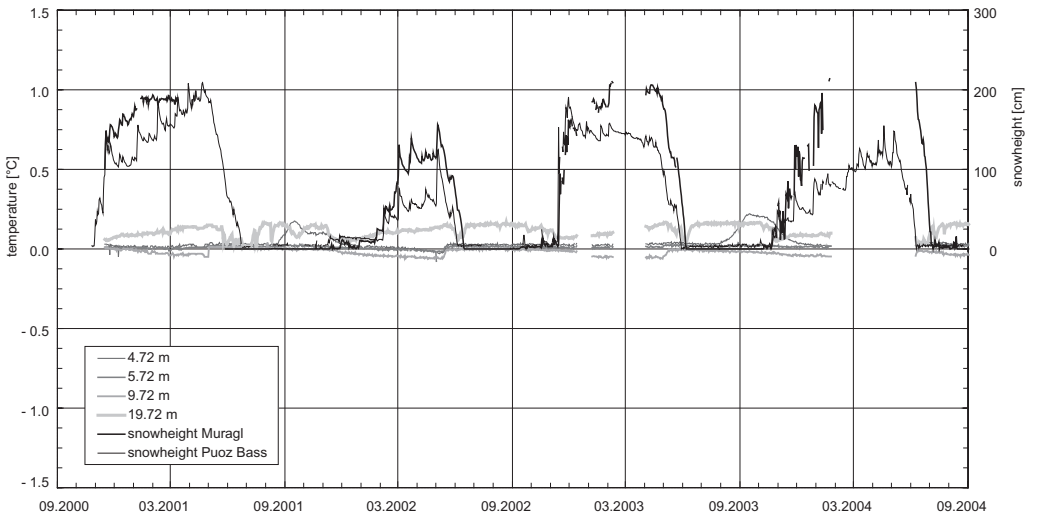


Fig. A.20: Temperature-time-plot of the borehole Muragl 2/99 for the thermistors at 4.72, 5.72, 9.72, and 19.72 m depth. Additionally, the snow height at Puoz Bass and Muragl is displayed.

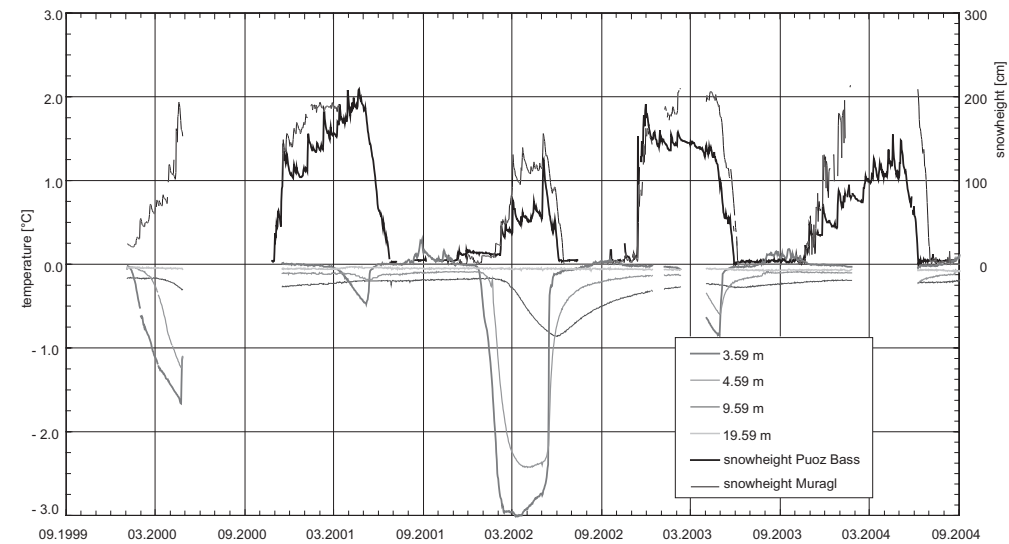


Fig. A.21: Temperature-time-plot of the borehole Muragl 3/99 for the thermistors at 3.59, 4.59, 9.59, and 19.59 m depth. Additionally, the snow height at Puoz Bass and Muragl is displayed.

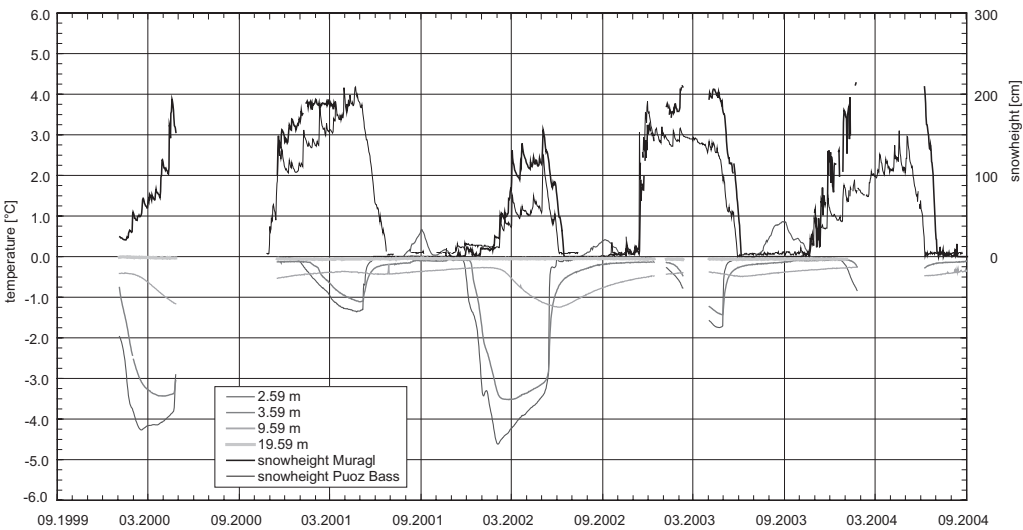


Fig. A.22: Temperature-time-plot of the borehole Muragl 4/99 for the thermistors at 2.59, 3.59, 9.59, and 19.59 m depth. Additionally, the snow height at Puoz Bass and Muragl is displayed.

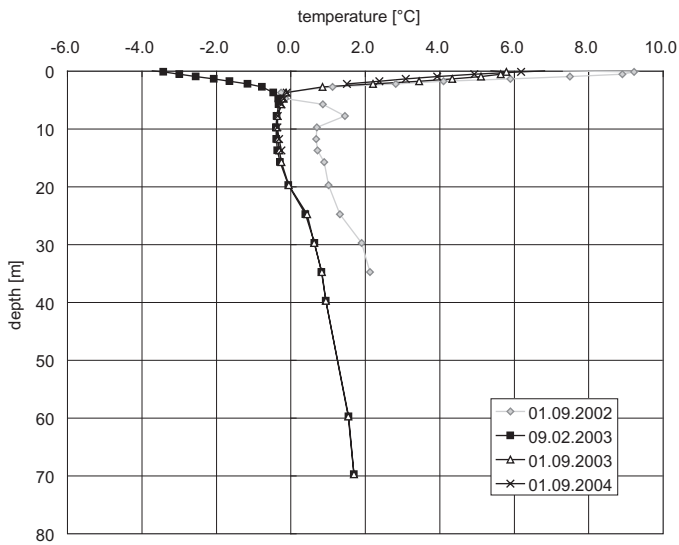


Fig. A.23: Temperature profiles for Muragl 1/99.

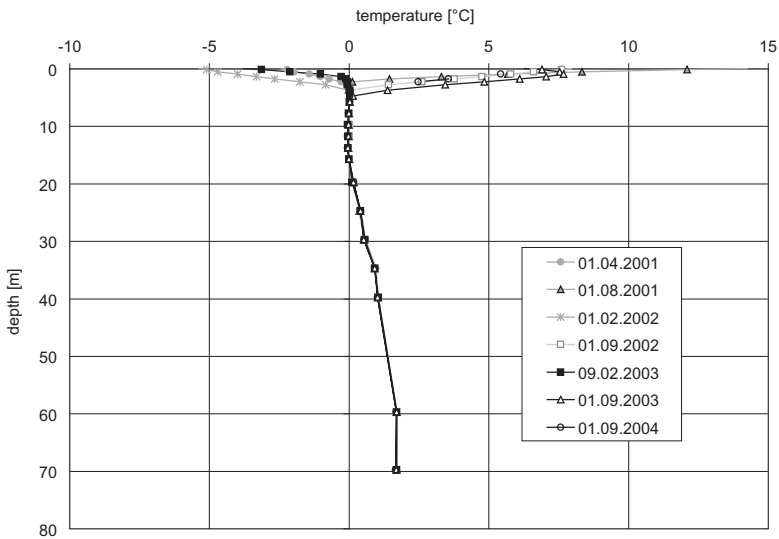


Fig. A.24: Temperature profiles for Muragl 2/99.

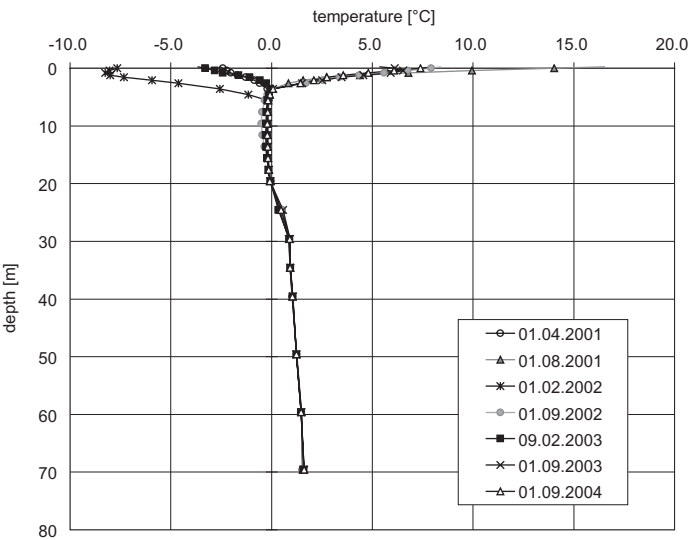


Fig. A.25: Temperature profiles for Muragl 3/99.

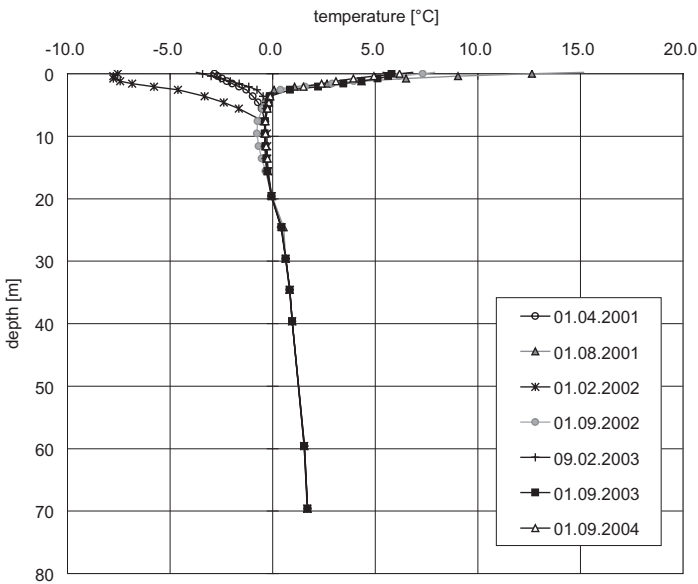


Fig. A.26: Temperature profiles for Muragl 4/99.

Murtèl-Corvatsch 1/87, 2/87, 1/00, and 2/00

Site

Description	Active rock glacier south-west of the cable car station Murtèl
Coordinates	1/87: 783158/144720, 2/87: 783160/144720 1/00: 783168/144703, 2/00: 783175/144692
Elevation [m a.s.l.]	1/87: 2670, 2/87: 2670, 1/00: 2673, 2/00: 2672
Slope angle [°]	10°
Slope aspect	NNW
Morphology	Rockglacier
Lithology	Crystalline rock of the Corvatsch nappe: granodiorit, schists
MAAT/Precipitation	-3 °C / 2000 mm
Vegetation	No vegetation

Borehole

Drilling date	1/87: 05.1987, 2/87: 06.87, 1/00: 05.2000, 2/00: 06.2000
Depth [m]	1/87: 32.0, 2/87: 62.0, 1/00: 51.9, 2/00: 63.2
Chain length [m]	1/87: 21.0, 2/87: 58.0, 1/00: no temperature sensors installed, 2/00: 62.0
Thermistor depths [m]	1/87: 0.8, 1.8, 2.8, 3.8, 4.8, 5.8, 6.8, 7.8, 8.8, 9.8, 10.8, 11.8, 12.8, 13.8, 14.8, 15.8, 16.8, 17.8, 18.8, 19.8, 20.8 2/87: 0.6, 1.6, 2.6, 3.6, 4.6, 5.6, 6.6, 7.6, 8.6, 9.6, 10.6, 11.6, 12.6, 13.6, 14.6, 15.6, 16.6, 17.6, 18.6, 19.6, 20.6, 21.6, 23.6, 24.6, 25.6, 26.6, 27.6, 30.0, 33.0, 36.0, 39.0, 42.0, 45.0, 46.0, 47.0, 48.0, 49.0, 50.0, 51.0, 52.0, 53.0, 53.9, 54.9, 55.9, 56.9, 58.0 2/00: 0.5, 1.0, 1.5, 2.0, 2.5, 3.0, 3.5, 4.0, 5.0, 7.5, 10.0, 15.0, 20.0, 25.0, 30.0, 40.0, 42.0, 44.0, 46.0, 48.0, 50.0, 52.0, 54.0, 56.0, 57.0, 58.0, 60.0, 61.0, 62.0
Thermistor type	1/87 and 2/87: YSI 44006, Fernwall UUA 41J1, 2/00: YSI 44006 (Stump String #21)
Last calibration	1/87: and 2/87: 1987 (fix installed), 2/00: July 2000

Meteostation

Installation date	1.1997
Sensors	Air and surface temperature, relative humidity, net radiation, snow-depth, wind speed/direction

Responsible

1/87 and 2/87: GIUZ, M. Hoelzle
1/00 and 2/00: IGT-ETH, L. Arenson, S.M. Springman

Other measurements

BTS/GST

Comments

Air circulation through talus slope

Available data

2/87: since 1987 (with some gaps); 2/00: since 2000.

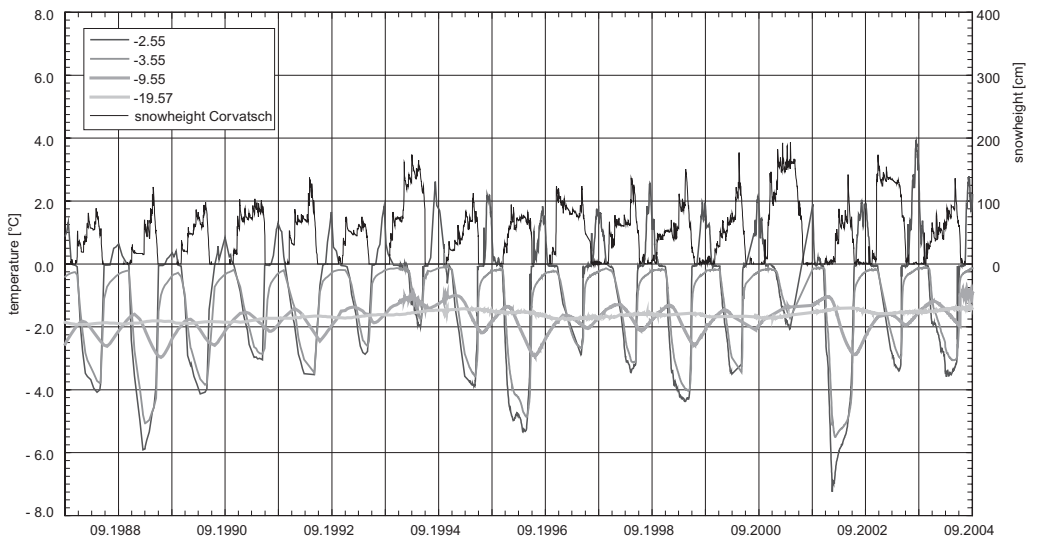


Fig. A.27: Temperature-time-plot of the borehole Corvatsch 2/87 for the thermistors at 2.55, 3.55, 9.55, and 19.57 depth. Additionally, the snow height at Corvatsch is displayed.

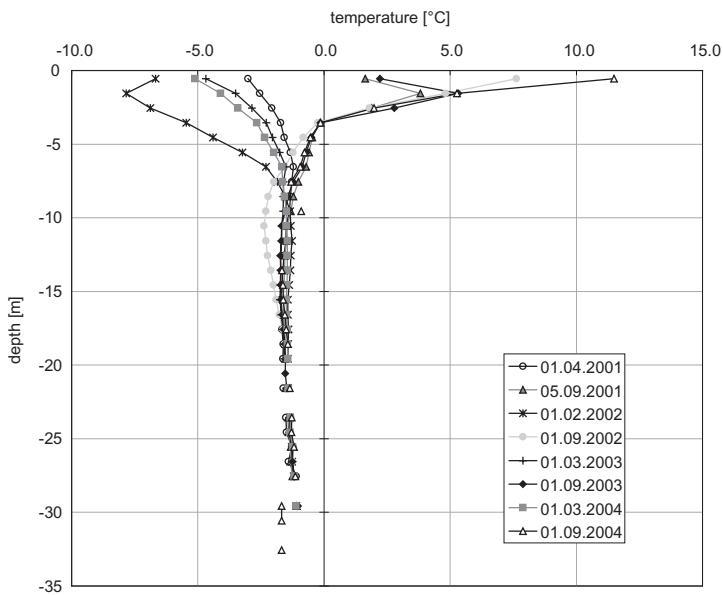


Fig. A.28: Temperature profiles for Corvatsch 2/87.

Schafberg-Pontresina 1/90 and 2/90

Site

Description	Schafberg-Pontresina (Muot da Barba Peider), Upper Engadine, GR
Coordinates	1/90: 791000/152500, 2/90: 790750/152775
Elevation [m a.s.l.]	1/90: 2755, 2/90: 2735
Slope angle [°]	Flat
Slope aspect	Flat
Morphology	Rockglacier
Lithology	Gneiss
MAAT/Precipitation	-3.5 °C / 2000 mm
Vegetation	No vegetation

Borehole

Drilling date	1990
Depth [m]	1/90: 67.0, 2/90: 37.0
Chain length [m]	1/90: 18.0, 2/90: 25.2
Thermistor depths [m]	2/90: 0.0, 1.2, 3.2, 5.2, 7.2, 9.2, 13.2, 17.2, 21.2, 25.2
Thermistor type	2/90: YSI 46006 + Campbell CR10X
Last calibration	2/90: 1997

Meteostation

Installation date	Planned for summer 2004
Sensors	Air temperature, relative humidity, net radiation, snow depth/surface/temperature, wind speed/direction

Responsible 1/90: VAW, 2/90: SLF, M. Phillips

Other measurements BTS/GST

Comments Borehole 2/90 sheared off in 2000 at 28 m

Available data 2/90: Since 1997

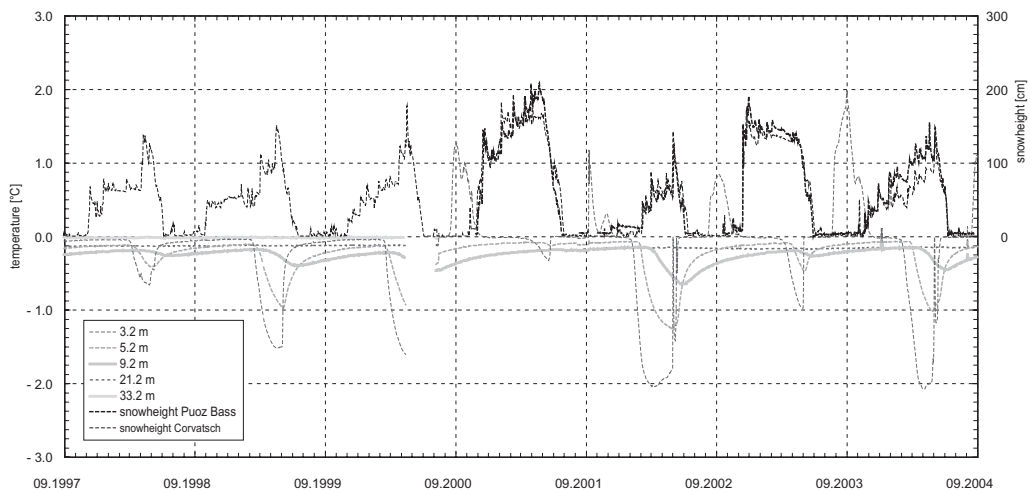


Fig. A.29: Temperature-time-plot of the borehole Schafberg-Pontresina 2/90 for the thermistors at 3.2, 5.2, 9.2, 21.2 and 33.2 m depth. Additionally, the snow height at Puoz Bass and on Corvatsch is displayed.

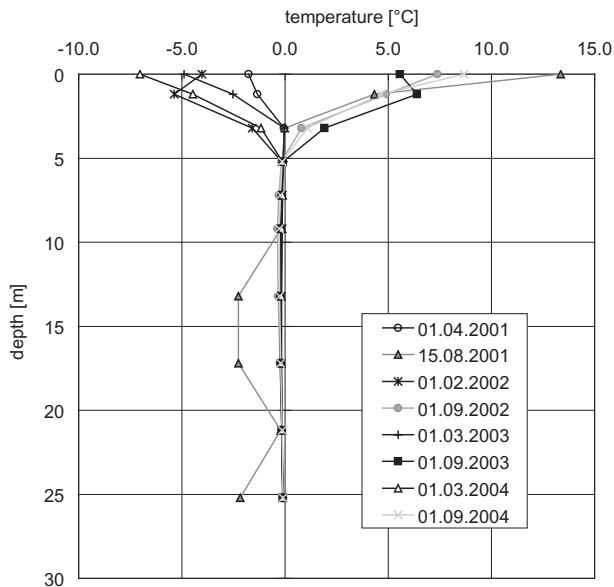


Fig. A.30: Temperature profiles for Schafberg-Pontresina 2/90.

Arolla, Mt. Dolin B1/96 and B2/96

Site

Description	Arolla, Mt. Dolin, VS
Coordinates	B1/96: 601246/97232, B2/96: 601257/97248
Elevation [m a.s.l.]	B1/96: 2840, B2/96 2820
Slope angle [°]	38-40
Slope aspect	NE
Morphology	Scree slope
Lithology	Dolomite
Vegetation	No vegetation

Borehole

Drilling date	1996
Depth [m]	10
Chain length [m]	5.5
Thermistor depths [m]	0.5, 1.5, 2.5, 3.5, 5.5
Thermistor type	YSI 46008 + Campbell CR10X
Last calibration	1996

Responsible SLE, M. Phillips

Other measurements BTS/GST

Comments Snow nets

Available data Since 1996

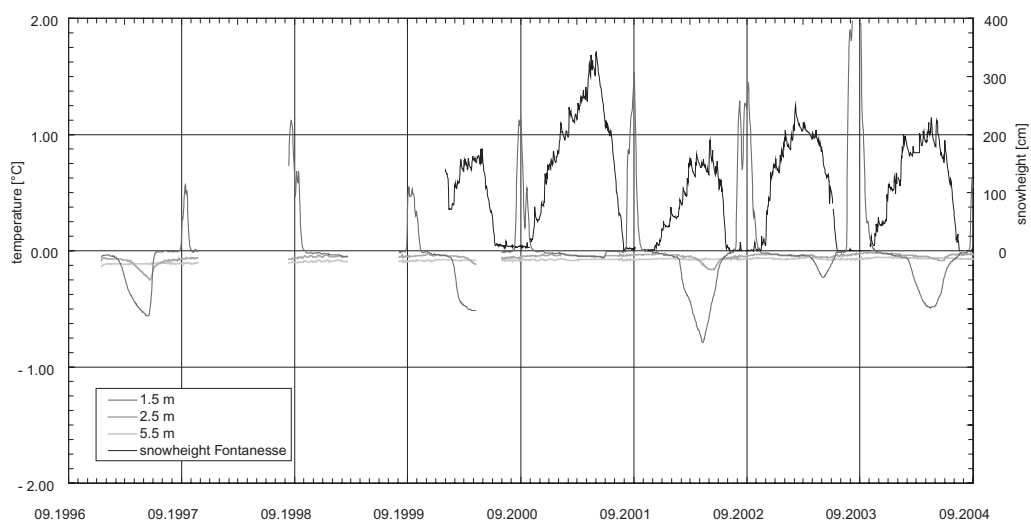


Fig. A.31: Temperature-time-plot of the borehole Arolla B1/96 for the thermistors at 1.5, 2.5, and 5.5 m depth. Additionally, the snow height at Fontanesse is displayed.

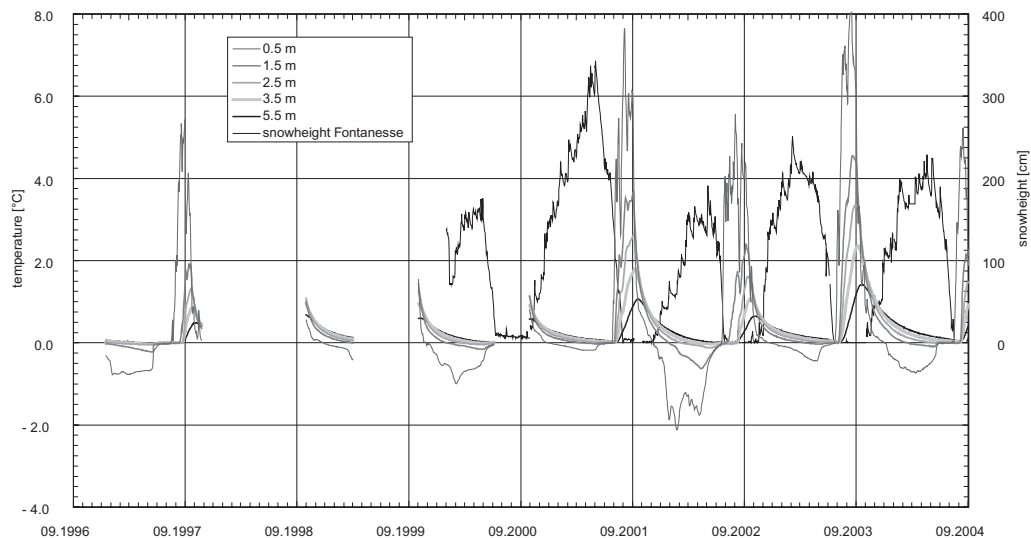


Fig. A.32: Temperature-time-plot of the borehole Arolla B2/96 for the thermistors at 0.5, 1.5, 2.5, 3.5, and 5.5 m depth. Additionally, the snow height at Fontanesse is displayed.

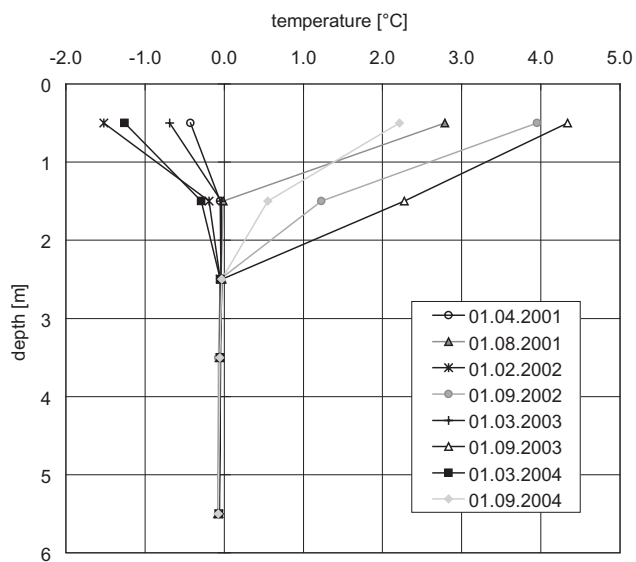


Fig. A.33: Temperature profiles for Arolla B1/96.

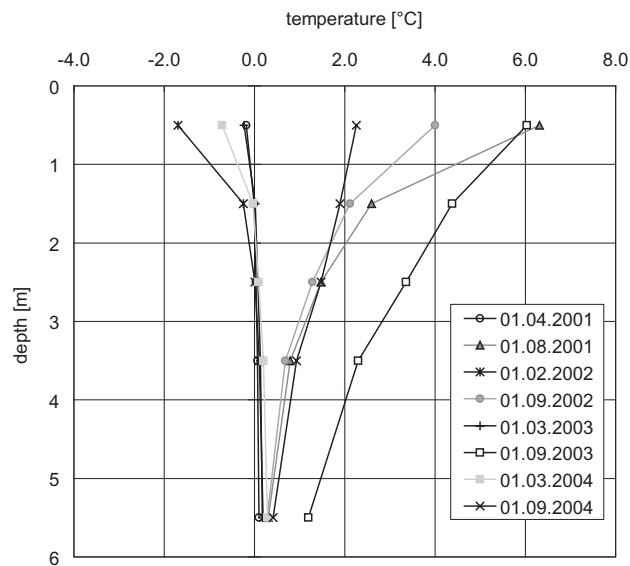


Fig. A.34: Temperature profiles for Arolla B2/96.

Emshorn 4/96, 5/96, and 6/96

Site

Description	Emshorn, Central Valais, VS
Coordinates	618500/124100
Elevation [m a.s.l.]	2470-2500
Slope angle [°]	35
Slope aspect	NE
Morphology	Steep grassy ridge
Lithology	Shale
Vegetation	Alpine grass

Borehole

Drilling date	1996
Depth [m]	6-8
Chain length [m]	—
Thermistor depths [m]	—
Thermistor type	—
Last calibration	—

Responsible SLE, M. Phillips; GIUZ, D. Vonder Mühl

Other measurements —

Comments Manual measurements

Available data Since 1996

Gentianes 1/02

Site

Description	Moraine
Coordinates	589450/103650
Elevation [m a.s.l.]	2890
Slope angle [°]	Flat
Slope aspect	–
Morphology	Lateral moraine
Lithology	Gneiss
MAAT/Precipitation	-1.5 °C / 1700 mm
Vegetation	No vegetation

Borehole

Drilling date	10.2002
Depth [m]	20
Chain length [m]	20
Thermistor depths [m]	0.5, 1.0, 1.5, 2.3, 3.6, 5.09, 7.08, 9.57, 12.56, 20.04
Thermistor type	MADD-T30E
Last calibration	10.2002

Responsible

IGUL, C. Lambiel

Other measurements

DC resistivity soundings, movements (GPS)

Comments

–

Available data

Since 2002

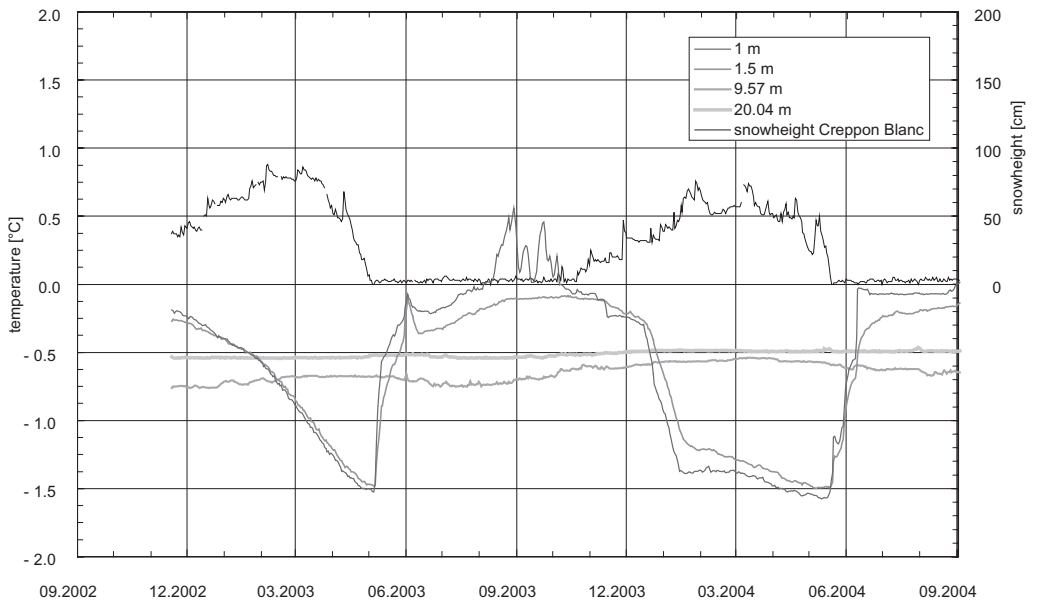


Fig. A.35: Temperature-time-plot of the borehole Gentianes 1/02 for the thermistors at 1.0, 1.5, 9.57, and 20.04 m depth. Additionally, the snow height at Creppon Blanc is displayed.

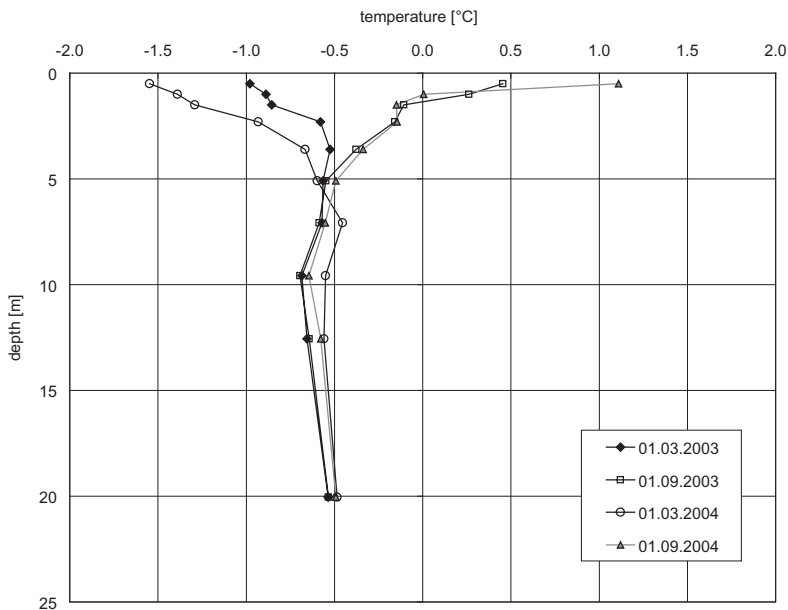


Fig. A.36: Temperature profiles for Gentianes 1/02.

Grächen 1/02 and 2/02

Site

Description	Midway station Seetalhorn chairlift
Coordinates	6235490/112120
Elevation [m a.s.l.]	2450
Slope angle [°]	Flat
Slope aspect	NW
Morphology	Moraine, artificially modified
Lithology	Moraine
Vegetation	No vegetation

Borehole

Drilling date	09.2002
Depth [m]	25
Chain length [m]	24
Thermistor depths [m]	0.25, 0.5, 1.0, 1.5, 2.0, 3.0, 4.0, 6.0, 8.0, 10.0, 15.0, 24.0
Thermistor type	YSI 46006 + Campbell CR10X
Last calibration	2002

Responsible SLE, M. Phillips

Other measurements –

Comments One borehole has a 20 m thick talik, the other an active layer of ca. 6 m

Available data Since 2002

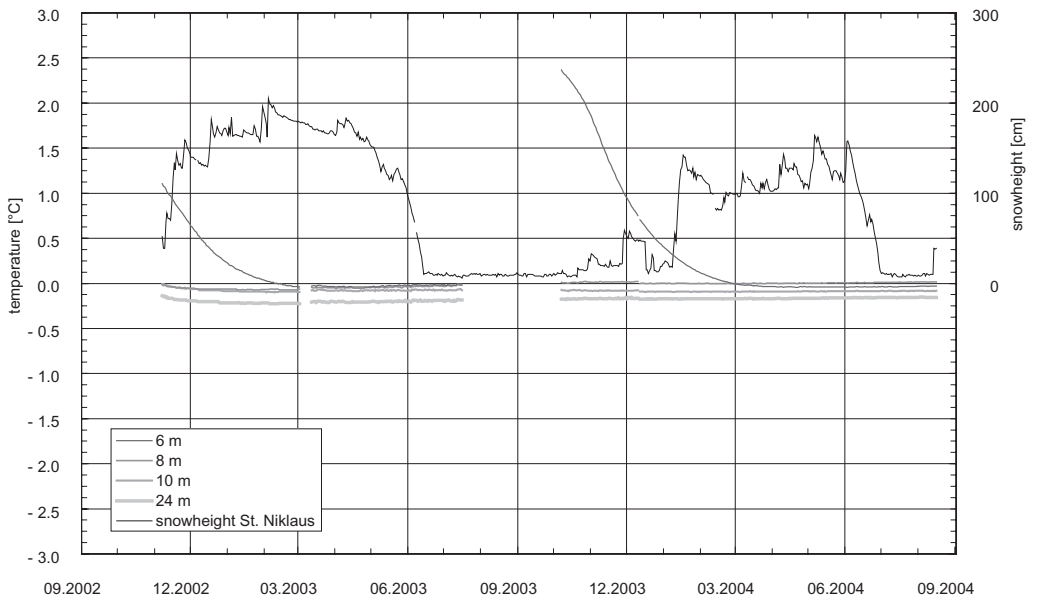


Fig. A.37: Temperature-time-plot of the borehole Grächen 1/02 for the thermistors at 6.0, 8.0, 10.0, and 24.0 m depth. Additionally, the snow height at St. Niklaus is displayed.

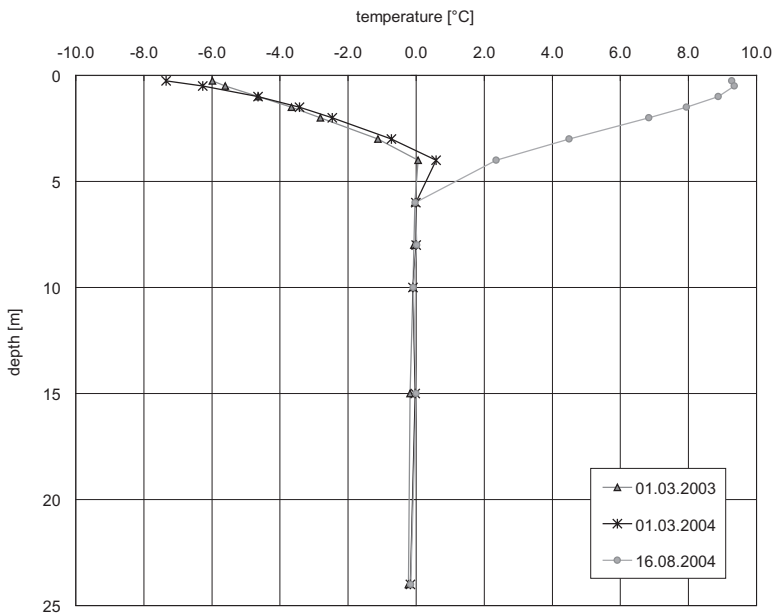


Fig. A.38: Temperature profiles for Grächen 1/02.

Lapires 1/98

Site

Description	Val de Nendaz, VS
Coordinates	588070/106080
Elevation [m a.s.l.]	2500
Slope angle [°]	25
Slope aspect	NE
Morphology	Talus slope
Lithology	Gneiss (mainly)
MAAT	0.5 °C
Vegetation	No vegetation

Borehole

Drilling date	10.1998
Depth [m]	19.6
Chain length [m]	19.6
Thermistor depths [m]	0.7, 1.7, 2.45, 2.8, 3.15, 3.61, 4.03, 4.51, 5.01, 6.7, 11.1, 19.6
Thermistor type	Pt 100
Last calibration	11.1998

Meteostation

Installation date	11.1998
Sensors	Air temperature, shortwave radiation, reflected shortwave radiation

Responsible IGUF, R. Delaloye

Other measurements BTS/GST

Comments Temperate (warm) permafrost, air circulation through the talus slope.

Available data Since 1998 (with some gaps)

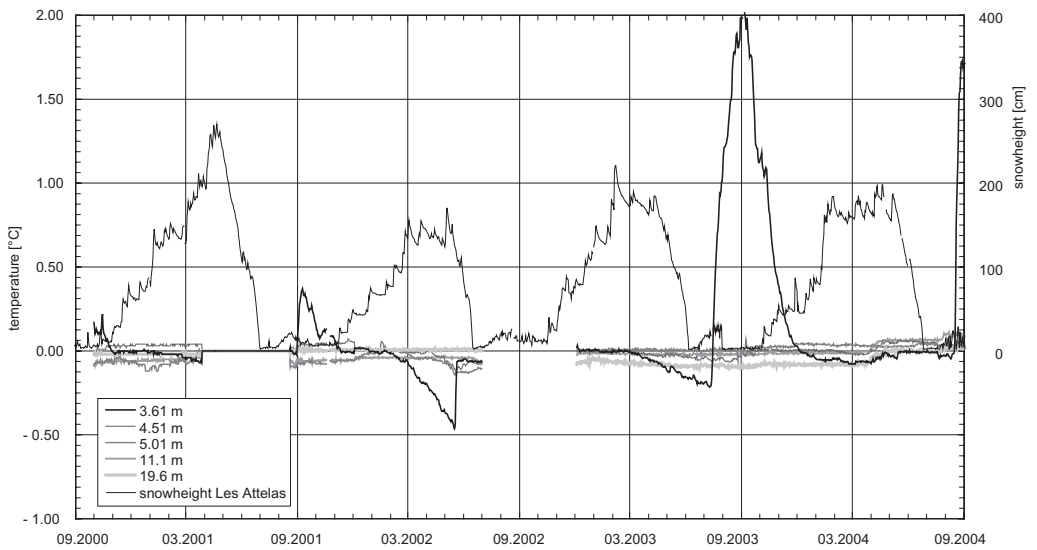


Fig. A.39: Temperature-time-plot of the borehole Lapires 1/98 for the thermistors at 3.61, 4.51, 5.01, 11.10, and 19.60 m depth. Additionally, the snow height at Les Attelas is displayed.

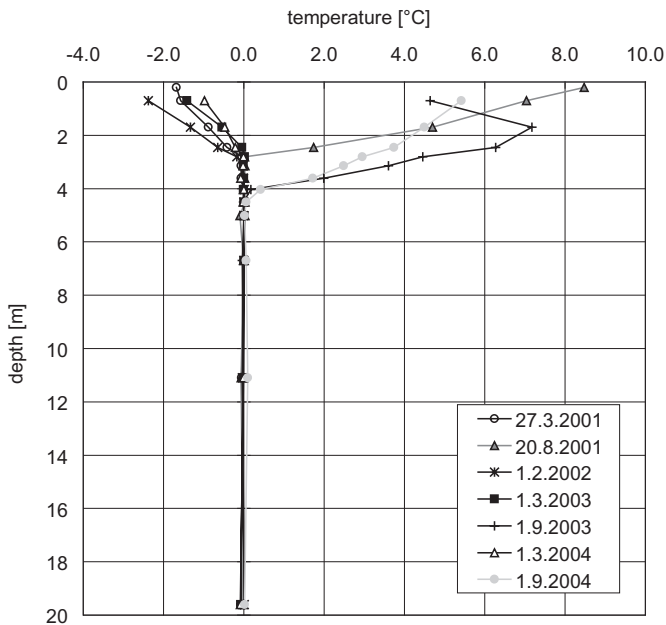


Fig. A.40: Temperature profiles for Lapires 1/98.

Randa Wisse-Schijen 1/98, 2/98, and 3/98

Site

Description	Matter Valley, VS
Coordinates	1/00: 624032/105064, 2/00: 624050/105080, 3/00: 624140/105100
Elevation [m a.s.l.]	1/00: 3070, 2/00: 3045, 3/00: 2950
Slope angle [°]	40
Slope aspect	ENE
Morphology	Scree slope
Lithology	Gneiss, quartzite, marble
MAAT/Precipitation	–
Vegetation	No vegetation

Borehole

Drilling date	1998
Depth [m]	4
Chain length [m]	2.8
Thermistor depths [m]	0.3, 0.8, 1.8, 2.8
Thermistor type	UTL
Last calibration	–

Responsible

SLE, M. Phillips

Other measurements

BTS/GST

Comments

Snow nets, boreholes deeper, but filled with salt

Available data

Since 2001

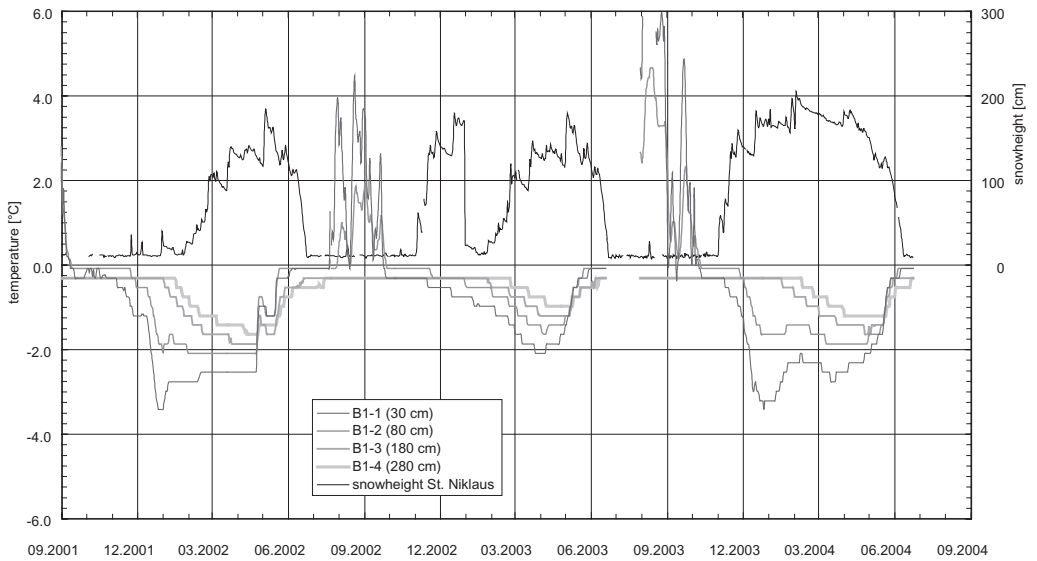


Fig. A.41: Temperature-time-plot of the borehole Randa 1/98 for the thermistors at 0.3, 0.8, 1.8, and 2.8 m depth. Additionally, the snow height at St. Niklaus is displayed.

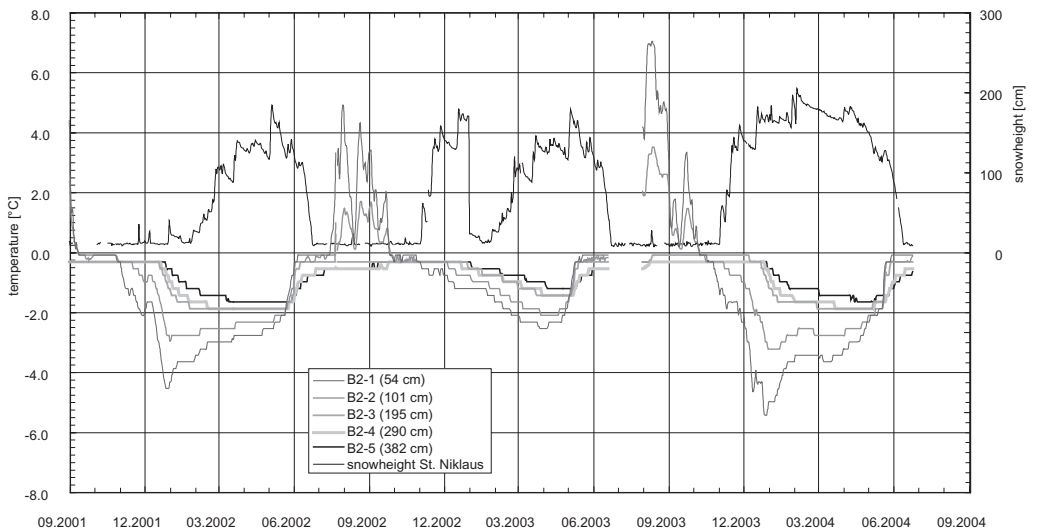


Fig. A.42: Temperature-time-plot of the borehole Randa 2/98 for the thermistors at 0.54, 1.01, 1.95, 2.90, and 3.82 m depth. Additionally, the snow height at St. Niklaus is displayed.

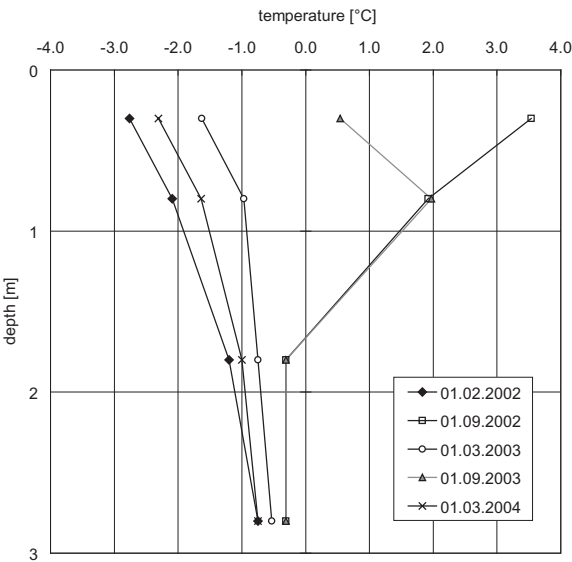


Fig. A.43: Temperature profiles for Randa Wisse-Schijen 1/98.

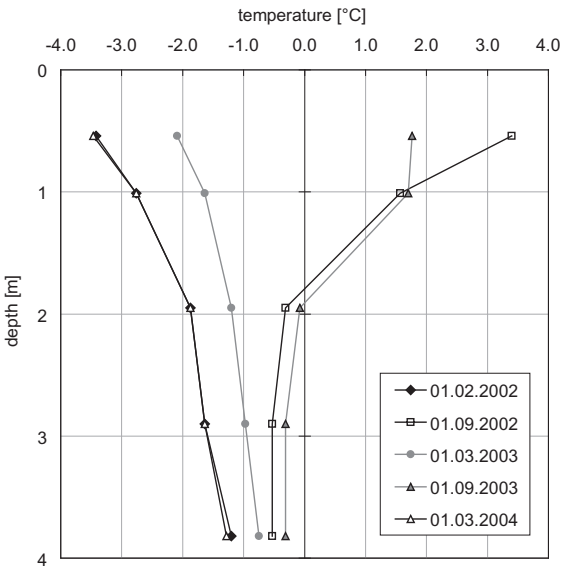


Fig. A.44: Temperature profiles for Randa Wisse-Schijen 2/98.

Stockhorn 60/00 and 61/00

Site

Description	Stockhorn Plateau, Gornergrat, Matter Valley, VS
Coordinates	60/00: 629878/92876; 61/00: 629867/92850
Elevation [m a.s.l.]	3410
Slope angle [°]	8
Slope aspect	S
Morphology	Plateau on crest
Lithology	Albit-Muskowit schists
MAAT/Precipitation	-5.5 °C / 1500 mm
Vegetation	No vegetation

Borehole

Drilling date	August 2000
Depth [m]	60/00: 100; 61/00: 31
Chain length [m]	60/00: 100; 61/00: 17
Thermistor depths [m]	PACE standard
Thermistor type	NTC-YSI 440006
Last calibration	August 2000

Meteostation

Installation date	6.2002
Sensors	Air temperature, relative humidity, net radiation, snow-depth, wind speed/direction

Responsible GIUZ, M. Hoelze and S. Gruber; Univ. Giessen, L. King

Other measurements BTS/GST

Comments –

Available data Since 2000

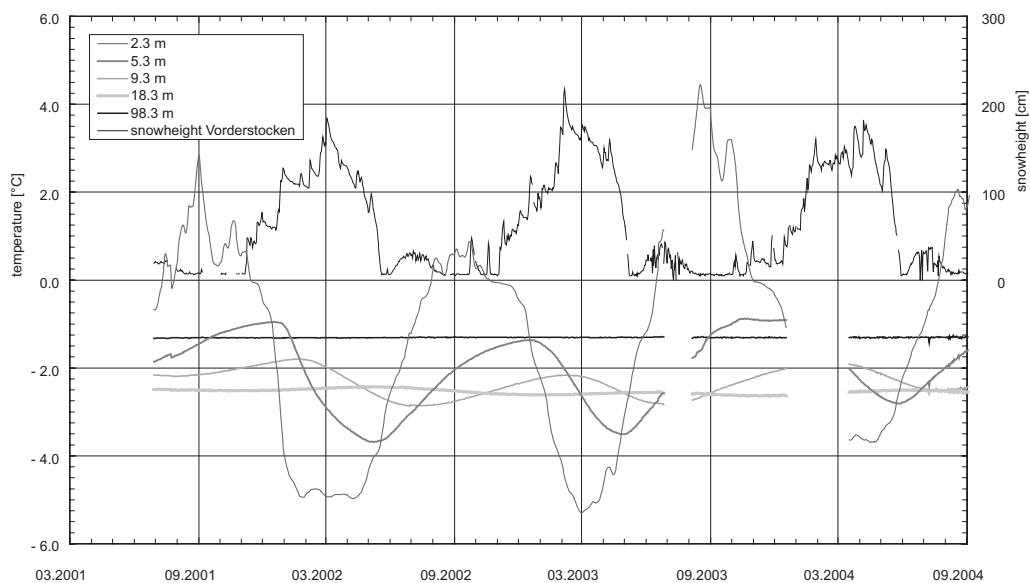


Fig. A.45: Temperature-time-plot of the borehole Stockhorn 60/00 for the thermistors at 2.3, 5.3, 9.3, 18.3, and 98.3 m depth. Additionally, the snow height at Vorderstocken is displayed.

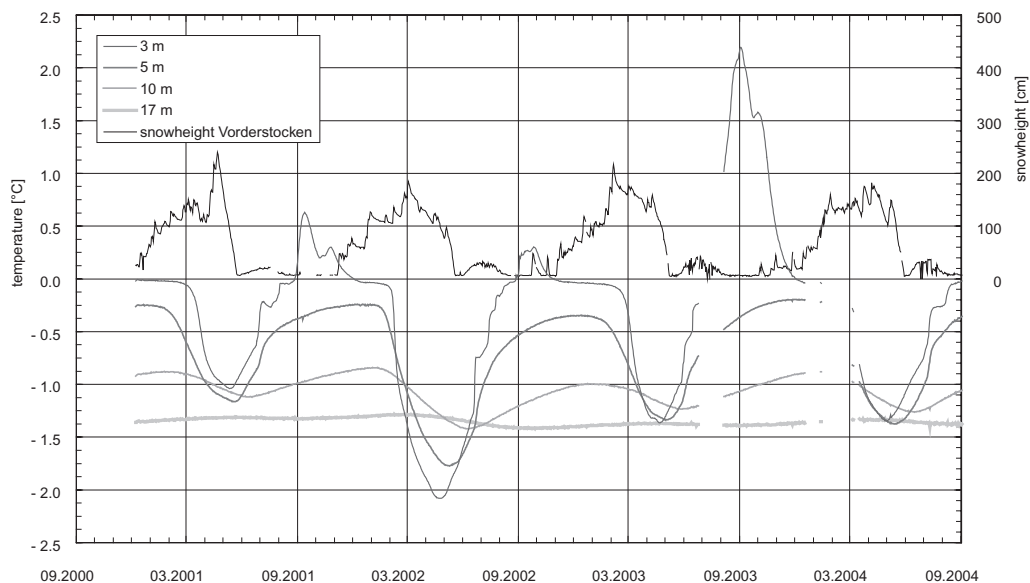


Fig. A.46: Temperature-time-plot of the borehole Stockhorn 61/00 for the thermistors at 3.0, 5.0, 10.0, and 17.0 m depth. Additionally, the snow height at Vorderstocken is displayed.

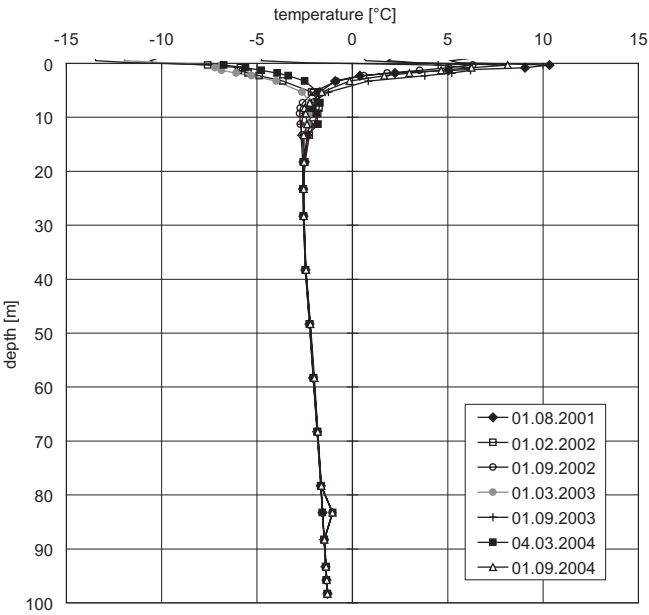


Fig. A.47: Temperature profiles for Stockhorn 60/00.

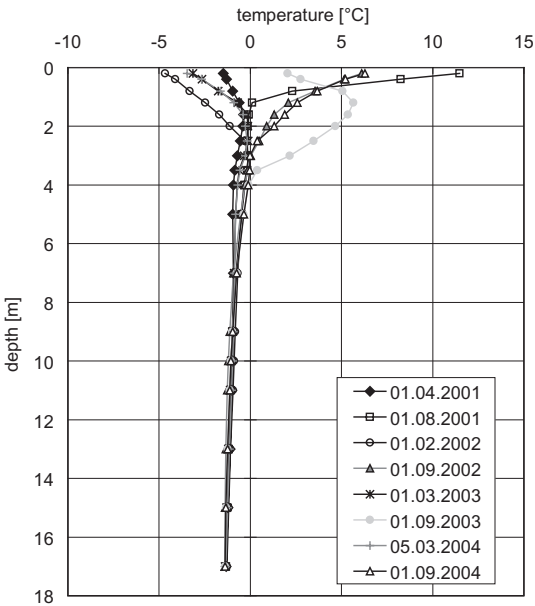


Fig. A.48: Temperature profiles for Stockhorn 61/00.

Tsaté 1/04

Site

Description	Bedrock
Coordinates	608500/106400
Elevation [m a.s.l.]	3040
Slope angle [°]	35
Slope aspect	W
Morphology	Rock slope
Lithology	Calc-schist
MAAT/Precipitation	-1.5 °C / 1700 mm

Vegetation	No vegetation
------------	---------------

Borehole

Drilling date	08.2004
Depth [m]	20
Chain length [m]	19.5
Thermistor depths [m]	0.5, 1.0, 1.5, 2.3, 3.5, 5.0, 7.0, 9.5, 13.0, 19.5
Thermistor type	MADD-T30E
Last calibration	—

Responsible	IGUL, C. Lambiel
--------------------	------------------

Other measurements	—
---------------------------	---

Comments	—
-----------------	---

Available data	Since 2004
-----------------------	------------

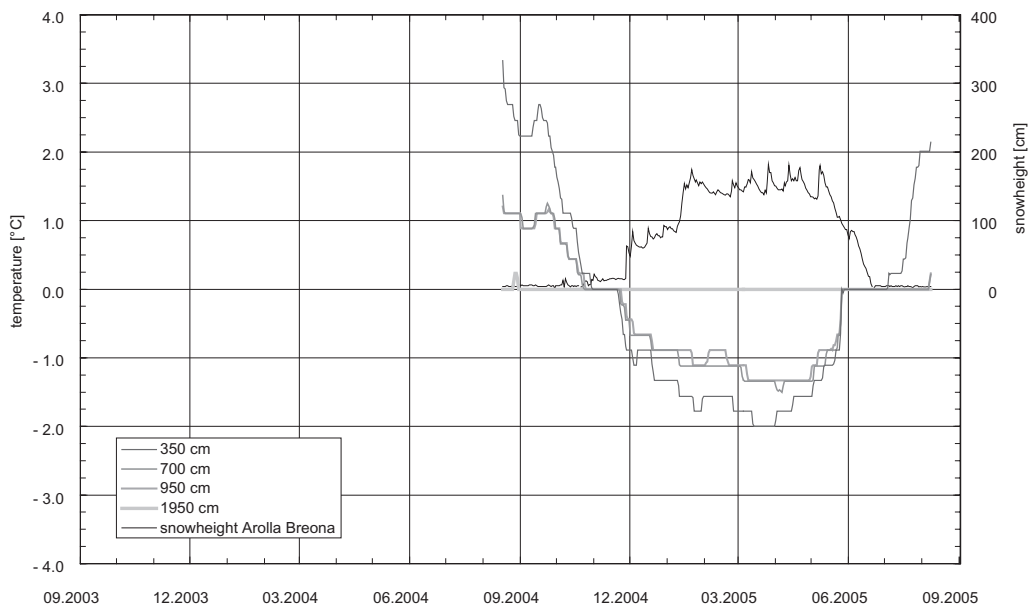


Fig. A.49: Temperature-time-plot of the borehole Tsaté 1/04 for the thermistors at 3.5, 7.0, 9.5, and 19.5 m depth. Additionally, the snow height at Arolla Breona is displayed.

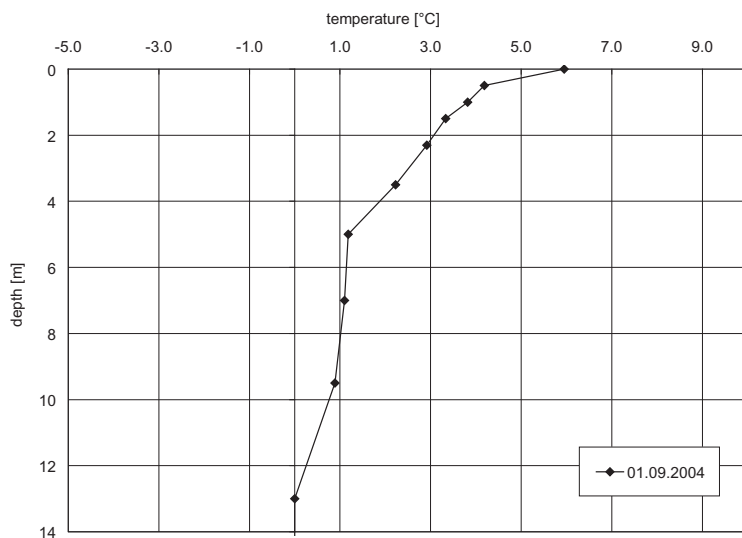


Fig. A.50: Temperature profile for Tsaté 1/04.

